Design of the insect respiratory system: a test case for symmorphosis

Edward Snelling

Presented for the degree of Doctor of Philosophy

School of Earth and Environmental Sciences
University of Adelaide, South Australia, AUSTRALIA

August 2011

CONTENTS

Abstract iv

Acknowledgements vi

Chapter One: Introduction 1

Chapter Two: Scaling of resting and maximum hopping metabolic rate throughout the lifecycle of the locust *Locusta migratoria*. 6

Preamble 6

1. Abstract 7

2. Introduction 8

3. Methods 10

4. Results 15

5. Discussion 20

6. Acknowledgements 24

Chapter Three: Resting and maximum metabolic rate during tethered-flight in the adult locust *Locusta migratoria* 25

1. Abstract 25

2. Introduction 26

3. Methods 28

4. Results 35

5. Discussion 39

6. Acknowledgements 44

Chapter Four: Symmorphosis and the insect respiratory system: allometric variation 45

Preamble 45

1. Abstract 46

2. Introduction 47

3. Methods 50

4. Results 61

5. Discussion 75

6. Acknowledgements 82

Chapter Five: Symmorphosis and the insect respiratory system: a comparison between flight and hopping muscle 83

1. Abstract 83

2. Introduction 84

3. Methods 86

4. Results 91
5. Discussion 104
6. Acknowledgements 110
Chapter Six: Discussion 111
Appendix: Moulting of insect tracheae captured by light and electron-microscopy in the metathoracic femur of a third instar locust *Locusta migratoria* 118
Preamble 118
1. Abstract 119
2. Introduction 120
3. Methods 122
4. Results and discussion 124
5. Acknowledgements 138
References 139

Abstract

The idea that animals are designed economically follows the line of reasoning that building and maintaining superfluous structure is energetically expensive, and should therefore be selected against. It was on these foundations that Taylor and Weibel introduced the theory of symmorphosis, which posits no more structure should exist in an animal than is necessary for the structure to fulfil its maximum functional task. In support of the theory, the volume of mitochondria in mammalian muscle appears perfectly matched to the muscle's aerobic capacity. But contrary to the predictions of symmorphosis, the mammalian lung is capable of oxygen delivery rates that exceed the maximum needs of the mitochondria. The purpose of this dissertation is to examine whether the insect respiratory system conforms to the economic principles of symmorphosis, such that the capacity of the tracheal system to deliver oxygen is matched to the aerobic capacity of the mitochondrial sink. The insect respiratory system conveys a number of attributes that make it well suited for such a task. Perhaps the most important of these is the fact that insects achieve the highest mass-specific aerobic metabolic rates of all animals, and in theory, the strong selective forces acting on such a system should push it towards an optimal design. The insect used for this purpose is the migratory locust *Locusta migratoria* where the delivery and consumption of oxygen increases significantly throughout development and also once adults take to the wing.

I, Edward Snelling, certify that this work contains no material which has been accepted for the award of any other degree or diploma in any university or other tertiary institution and, to the best of my knowledge, contains no material previously published or written by another person, except where due reference has been made in the text.

I give consent to this copy of my thesis when deposited in the University Library, being made available for loan and photocopying, subject to the provisions of the Copyright Act 1968. I also give permission for the digital version of my thesis to be made available on the web, via the University's digital research repository, the Library catalogue, and through web search engines, unless permission has been granted by the University to restrict access for a period of time. I acknowledge that copyright of published works contained within this thesis (as listed below*) resides with the copyright holder(s) of those works.

*Snelling EP, Seymour RS, Matthews PGD, Runciman S, White CR (2011) Scaling of resting and maximum hopping metabolic rate throughout the lifecycle of the locust *Locusta migratoria*. *Journal of Experimental Biology* **214**, 3218-3224.

*Snelling EP, Seymour RS, Runciman S, Matthews PGD, White CR (2011) Symmorphosis and the insect respiratory system: allometric variation. *Journal of Experimental Biology* **214**, 3225-3237.

*Snelling EP, Seymour RS, Runciman S (2011) Moulting of insect tracheae captured by light and electron-microscopy in the metathoracic femur of a third instar locust *Locusta migratoria*. *Journal of Insect Physiology* **57**, 1312-1316.

Edward Snelling
August 2011

Acknowledgements

I am indebted to my principal supervisor, Professor Roger Seymour. Thank you for the advice, support, critique, and mentoring. I am excited at the possibility of working with you in the near future as there are still many aspects of comparative physiology to learn from you. The attention and time you give to each of your students is well beyond the expectations of a regular supervisor – and we all appreciate that. I am also extremely grateful to Dr Sue Runciman who handed down her knowledge and experience in all things stereological, and was always available when I required her expert advice. I am also grateful for the support given to me by my lab mates, Dr Phil Matthews, Caragh Heenan, Dr Casey Mueller, Imogen Munro, Nina James, Manoli Photakis, Sarah Smith, Dr Brett Goodman, Tari Pawlyk and Cassandra So. I also express gratitude to Dr Craig White, who has provided very valuable input over the years. I must also thank Dr Nick Payne – without your friendship and colleagueship over the years this thesis would have been finalised months earlier. Kerry Gascoigne and Dr Mike Teo of Flinders Microscopy and Ruth Williams and Lyn Waterhouse of Adelaide microscopy shared their expertise in the field of light and electron microscopy. Professor Stephen Simpson and Tim Dodgson of the University of Sydney provided technical advice on rearing a lab colony of locusts. Finally, thank you to my family – Mum, Dad, Jack, Lucia, Tom, Nada, Caroline, the other Jack, Margie, Molly, Helena, Frank, Joe, Peter, Thomas Edward, Ruthie, Edith, Jovan, and Ana Smiljana.

Chapter One: Introduction

Economical design and symmorphosis

The idea that animals are designed economically follows logic that building and maintaining superfluous structure is a waste of resources, places unnecessary loads on the body, and should therefore be selected against. Examples of economical design in animals seem pervasive. For instance, the digestive system of animals appears well matched to their diet, such that herbivores with hard to process cellulose diets have large and complex digestive tracts, whereas carnivores with easy to process protein diets have comparatively reduced digestive tracts. Likewise, animals that require acute eyesight often have well developed visual systems, whereas animals that have little requirement for sight, such as many cave-dwelling organisms, tend to have reduced visual systems. And ontogenetically, muscle mass can increase with regular use, and skeletal mass can increase when subject to sustained heavy loads. Conversely, the opposite occurs when muscles are not regularly used, and bones are subject to reduced loads. However, such observations are only suggestive of economical design. It was not until 1981 that the idea was turned into a testable hypothesis, when Taylor and Weibel introduced the theory of symmorphosis, which they defined as the 'state of structural design commensurate to functional needs resulting from regulated morphogenesis, whereby the formation of structural elements is regulated to satisfy but not exceed the requirements of the functional system' (Taylor and Weibel 1981b).

Symmorphosis and the effect of body mass on respiratory design

In a seminal series of papers, Taylor and Weibel predicted that if the mammalian respiratory system conforms to symmorphosis, then the functional capacity of each of the steps in the oxygen cascade should be matched to one another, such that no single component limits the maximum flow of oxygen through the system (Taylor and Weibel 1981a). To test this theory, an allometric comparative analysis was performed on mammals over a wide range of body mass, because changes in body size are associated with changes in maximum oxygen consumption rate, and the morphology of the oxygen supply pathway could be quantified to assess if the changes were proportional. They found that the aerobic capacity of mammals scales with body mass in parallel with the volume of mitochondria in the diaphragm and locomotory muscles (Mathieu et al., 1981; Seeherman et al., 1981). Likewise, the total length of capillaries in selected muscles was also found to scale roughly in parallel with aerobic capacity (Hoppeler et al., 1981b; Weibel et al., 1981b). However, the anatomical diffusing capacity of the lung was shown to increase with body mass faster than maximum oxygen

consumption rate, which suggests that larger mammals have more lung structure than they require (Gehr et al., 1981). Potentially, the over-supply of lung could function to counter a lower alveolar pressure head for diffusion, allowing larger mammals to transfer oxygen from the lungs to the blood at the same rate as smaller mammals (Gehr et al., 1981).

Symmorphosis and the effect of aerobic ability on respiratory design

Six years following the allometric study, Taylor and Weibel published another series of papers in which they quantified the aerobic capacity and morphometry of the respiratory system in the 'athletic' dog and pony, and compared it to the 'nonathletic' goat and calf (Weibel et al., 1987b). They showed that the 2.5-fold higher maximum oxygen consumption rate of athletic mammals is matched by a 2.5-fold higher mitochondrial volume, as predicted by symmorphosis (Hoppeler et al., 1987; Taylor et al., 1987a). Similarly, the higher aerobic capacity of athletic mammals is achieved through a combined, but proportional, increase in muscle capillary supply, blood oxygen carrying capacity, and heart size (Conley et al., 1987; Karas et al., 1987b). However, the study also found that the higher aerobic capacity of athletic mammals is only partly met by an increase in pulmonary diffusing capacity (Weibel et al., 1987a), and that all mammals appear to have more lung structure than they require to saturate the blood with oxygen, even during heavy exercise (Karas et al., 1987a). It was reasoned that the over-supply of lung tissue might represent a safety factor that enables mammals to tolerate hypoxia, as would occur at high altitudes (Taylor et al., 1987b). Taylor and Weibel concluded that symmorphosis holds for the internal compartments of the mammalian respiratory system (blood, heart, muscle capillaries, and mitochondria), whereas it must be rejected for the lungs (Weibel et al., 1992; Weibel et al., 1991). Interestingly, it has since been demonstrated that the avian lung is in fact symmorphotic, both phylogenetically and ontogenetically (Canals et al., 2011; Seymour et al., 2008; Runciman et al., 2005; Seymour et al., 2004). It would therefore seem that any potential adaptive advantage afforded by an over-supply of lung does not apply to birds.

Symmorphotic breakdowns and built-in safety factors

Despite being a highly influential theory of biological design, symmorphosis has been heavily criticised by evolutionary biologists who argue that natural selection leads to adequate or sufficient design, but not optimal or symmorphotic design (Garland 1998; Dudley and Gans 1991; Garland and Huey 1987; Smith 1978). They suggest symmorphosis is not an inevitable outcome because environmental unpredictability means that evolutionary selective forces vary

too much in space and time to produce a structure or organism that is functionally optimal (Dudley and Gans 1991). Apparently, symmorphotic-like matching between structure and function could only ever be realised when selective forces influencing design have either been static for a long time (Dudley and Gans 1991) or when selective pressures have been directed towards extreme performance (Jones and Lindstedt 1993). In support, critics refer to a number of instances in which animals appear to be in possession of unnecessary structure. For example, bird and mammal bones exhibit irreversible deformation only when peak stress exceeds natural loads by 2- to 5-fold; the functional capacity of the cat intestine's arginine transporter exceeds arginine ingestion by 7- to10-fold; and the enzymatic output of the human pancreas is around 10-fold higher than that required, which is evident by the fact that individuals lacking a functioning pancreas escape malabsorption if enzymes are supplied exogenously at one-tenth the rate normally secreted by the pancreas (as summarised by Diamond 1998). However, it is also plausible that the excess capacity of many of these structures could represent a built-in safety factor, analogous to the safety factor engineers build in to bridges, buildings, and elevators. In circumstances where breakage might lead to a serious fitness reduction for the animal, the built-in safety margin could be considerable. For example, the greater than 7-fold excess capacity of the cat intestine's arginine transporter might help maximise arginine absorption along the gut, which is critical if carnivores are to adequately eliminate large quantities of toxic nitrogenous waste (Diamond and Hammond 1992). In addition, it is also reasonable to expect large excess capacities in structures that do not incur a significant energy cost for the animal, whereas structures that are energetically expensive to maintain, such as flight muscle, might be subject to stronger selective pressures driving them towards an optimal, or at least reasonable, design.

Symmorphosis and the insect respiratory system

The theory of symmorphosis does not really apply to single structures like those just mentioned, but rather it predicts functional matching of structures along entire physiological systems. However, many physiological systems are less than ideal models on which to base studies of symmorphosis. One problem with testing for symmorphosis in the mammalian respiratory system is that the cardiovascular component performs a range of tasks, and so it is difficult to establish whether its design is geared towards oxygen delivery, and not some other function, such as substrate delivery, lactate removal, carbon dioxide removal, pH regulation, or heat dispersal (Dudley and Gans 1991; Garland and Huey 1987). As an alternative, the insect respiratory system has a number of characteristics that make it more appealing. For

instance, unlike the cardiovascular system, the primary function of the insect tracheal system is oxygen delivery (Schmitz and Perry 1999; Wigglesworth 1965), and so any analysis need not account for other variables influencing design. Furthermore, mass-specific oxygen consumption rates in insects surpass all other animals (Suarez 2000; Bartholomew and Casey 1978; Sacktor 1976), and it has been suggested that symmorphosis is most likely to occur in systems selected for extreme performance (Jones and Lindstedt 1993). Finally, the insect respiratory system displays a considerable range of aerobic capabilities, owing to the wide body mass range of insects, and also due to the different energy requirements for flight compared to terrestrial locomotion.

Thesis and chapter objectives

The aim of this dissertation is to detail investigations made into the design and functional capacity of the insect respiratory system. Specifically, the question is asked: does the insect respiratory system conform to the economic principles of symmorphosis? To answer this question, the study exploits significant variation that exists in the maximum oxygen uptake rate of the migratory locust *Locusta migratoria* during hopping exercise at selected developmental stages, and also during flight in the adult locust. The following chapter summaries briefly detail the approach used.

Chapter Two: The allometric scaling of resting and maximum oxygen consumption rate during hopping exercise is determined in locusts throughout development. To encourage maximum exertion a technique is introduced whereby locusts are forced to perform strenuous jumping exercise while carrying a weight attached to the pronotum. The derived metabolic scaling exponents also provide an empirical test for the popular fractal network model of West, Brown and Enquist (West et al., 1997), which claims that metabolic scaling is a consequence of the way in which nutrients are taken up and transported throughout the body.

Chapter Three: The resting and maximum oxygen consumption rate of adult locusts during tethered-flight is determined. Previous estimates of locust flight energetics are relatively low compared to other insects of similar size, and to ensure this is not an artefact of tethering, weights are affixed to the wings of flying locusts and measurements of lift and wing-stroke frequency are also recorded. The low metabolic cost of flight in locusts is discussed in light of the fact that their flight motor is small compared to other insects.

Chapter Four: The allometric scaling of selected respiratory structures associated with the oxygen cascade in locust hopping muscle is determined throughout juvenile development. Tracheole volume, surface area, and anatomical diffusing capacity, as well as mitochondrial

volume and mitochondrial inner membrane surface area, are all found to scale congruently with the maximum oxygen consumption rate of the hopping muscle. This allometric examination suggests that the insect respiratory system conforms to the economic design principles of symmorphosis.

Chapter Five: The amount of respiratory structure associated with the flight and hopping muscle in adult locusts is quantified. The difference in tracheole volume, surface area, and diffusing capacity, between the flight and hopping muscle, closely matches the difference in the maximum oxygen consumption rate of the two muscles. However, the difference in mitochondrial volume between the two muscles is not matched to the difference in aerobic capacity. In fact, the flight muscle appears to be over-supplied with mitochondria by a factor of 3-fold. Symmorphosis is therefore upheld with respect to the design of the tracheal system, but not in relation to the amount of mitochondria. Processes operating on the molecular level, which differ between the hopping and flight muscle, could explain this apparent economical breakdown.

Chapter Two: Scaling of resting and maximum hopping metabolic rate throughout the lifecycle of the locust *Locusta migratoria*.

Preamble

The following chapter forms the basis of a published co-authored manuscript* and is reproduced with permission from the *Journal of Experimental Biology*. Snelling conducted the experiments, collected and analysed the data, and wrote the manuscript. Seymour and Matthews provided assistance with open-flow respirometry design and techniques, and Runciman and White provided valuable input and assistance over the course of the entire study. They each give permission** for the inclusion of the manuscript in the thesis.

*Snelling EP, Seymour RS, Matthews PGD, Runciman S, White CR (2011) Scaling of resting and maximum hopping metabolic rate throughout the lifecycle of the locust *Locusta migratoria*. *Journal of Experimental Biology* **214**, 3218-3224.

**Signatures of co-authors:

Roger Seymour

Philip Matthews

Sue Runciman

Craig White

1. Abstract

The hemimetabolous migratory locust *Locusta migratoria* progresses through five instars to the adult, increasing in mass from 0.02 to 0.95 g, a 45-fold change. Hopping locomotion occurs at all life stages and is supported by aerobic metabolism and provision of oxygen through the tracheal system. This allometric study investigates the effect of body size (M_b) on oxygen consumption rate (μmol h^{-1}) to establish resting metabolic rate (RMR), maximum metabolic rate during hopping (MMR), and the maximum metabolic rate of the hopping muscles ($MMR_{hop\ muscle}$) in first, third, fifth instar, and adult locusts. Oxygen consumption rates increase throughout development according to the allometric equations, RMR = $30.1M_b^{0.83 \pm 0.02\ (95\%\ CI)}$, MMR = $155M_b^{1.01 \pm 0.02}$, $MMR_{hop\ muscle} = 120M_b^{1.07 \pm 0.02}$, and if adults are excluded, $MMR_{juvenile} = 136M_b^{0.97 \pm 0.02}$ and $MMR_{juvenile\ hop\ muscle} = 103M_b^{1.02 \pm 0.02}$. Increasing body mass by 20-45% with attached weights does not increase MMR significantly at any life stage, although mean hopping metabolic rate is slightly higher (ca. 8%) when juvenile data are pooled. The allometric exponents for all measures of metabolic rate are much greater than 0.75, and therefore do not support West, Brown and Enquist's optimised fractal network model, which predicts that metabolism scales with a ¾-power exponent owing to limitations in the rate at which resources can be transported within the body.

2. Introduction

Metabolic rate generally follows an allometric relationship with body mass, such that small animals consume more energy per unit body mass than large animals over a given period of time (White et al., 2006; Savage et al., 2004). In recent years a range of mechanistic theories have been put forward to explain the allometric scaling of metabolism (Banavar et al., 2010; Price et al., 2007; Barbosa et al., 2006; Kozlowski and Konarzewski 2004; Banavar et al., 2002; Darveau et al., 2002; West et al., 1997). The fractal network model proposed by West, Brown and Enquist has received the most attention because it purports to explain the metabolic rate of all living organisms (West et al., 2003; West et al., 1999; West et al., 1997). The model is based on the theory that metabolism is matched to the rate at which resources are most efficiently transported within fractal distribution networks of the body. Their original optimised model predicts that metabolic rate scales allometrically with an exponent of 0.75 (West et al., 1997). Three key assumptions are central to the model: the delivery network is a space-filling fractal-like branching pattern that supplies all cells with oxygen, the final branch of the network is a size-invariant unit, and the energy required to distribute resources is minimised (West et al., 1997). These assumptions are met by the fractal-like branches of the insect tracheal system, where terminal tracheoles represent the final size-invariant unit of the network (West et al., 1997). Therefore, the model predicts that the standard metabolic rate (SMR) of insects should scale with a ¾-power exponent. However, there is little consensus as to whether or not this actually occurs. On the one hand, the results of a global meta-analysis show that insect SMR scales with an exponent close to 0.75 (Addo-Bediako et al., 2002). On the other hand, a number of studies report significant variation in the derived exponents for insect SMR, particularly at lower taxonomic levels where allometric slopes range from 0.67 to 1 (Strauss and Reinhold 2010; Chown et al., 2007; Terblanche et al., 2004).

In theory, variation in the metabolic scaling exponents can be accommodated in the network model, and recent presentations that relax some assumptions of the model by incorporating a range of branching patterns, predict allometric slopes from 0.5 to 1 (e.g. Banavar et al., 2010; Price et al., 2007). Nonetheless, the ¾-power exponent predicted by the model of West et al. (1997) remains a valid prediction against which the scaling of insect metabolic rate can be compared for two reasons. Firstly, West, Brown and Enquist explicitly state that their original model "...predicts structural and functional properties of ... insect tracheal tubes" (West et al., 1997; p122), although they later state that West et al. (1997) "...do not present a model for insect tracheal systems", but suggest that if insect metabolic rate

does scale with an exponent of ¾, then the principles of fractal-like design should apply to the structure and function of the tracheal system, and that this represents a testable hypothesis (Brown et al., 2005; p737). Thus, there is some confusion in the literature about the extent to which the optimised fractal model applies to insects. Secondly, a recent comparative analysis concludes that insect metabolic rate does scale with a ¾-power exponent (Riveros and Enquist 2011), and the authors use this as evidence to provide broad support for the core predictions of the West et al. (1997) model, but suggest that more work is required.

To add further complexity, some researchers believe that the fractal network model is in fact more relevant to the scaling of maximum metabolic rate (MMR), than it is to SMR. They argue that because the model is based on the theory that metabolic rate arises due to scaling of resource delivery, it is under conditions of maximum activity that this is most likely to apply (Suarez and Darveau 2005). Very few insect studies have scaled MMR with body mass. A recent study on Mormon crickets *Anabrus simplex* reports that overall MMR at ambient temperatures spanning 10-40°C scales with an exponent of 0.62, but only over a four-fold range in adult body mass (Chappell et al., 2009). Interspecific insect flight studies spanning a 100-fold range in mass, on the other hand, suggest that the scaling exponent for flight MR could trend towards 0.82-0.87 (Niven and Scharlemann 2005; Bartholomew and Casey 1978), which is similar to the exponent of MMR for birds and mammals (Weibel and Hoppeler 2005; White and Seymour 2005; Savage et al., 2004; Weibel et al., 2004; Bishop 1999). Clearly, the lack of insect MMR scaling data preclude researchers from assessing whether or not theoretical metabolic scaling theories, such as the fractal network model, are supported empirically.

The lack of research undertaken on the aerobic capacity of insects could be partly due to the difficulty in obtaining maximum aerobic activity levels from these animals. Insects appear so adept at meeting the challenges of oxygen supply that even the most energetically demanding of tasks, such as flight, are thought to be almost entirely aerobic (Komai 1998; Beenakkers et al., 1984; Worm and Beenakkers 1980; Kammer and Heinrich 1978). This makes the accurate determination of maximum aerobic metabolic rate particularly difficult. One option available to researchers is to force insects to exercise while carrying a load. A number of studies have already calculated the metabolic cost of ants carrying pupae (Bartholomew et al., 1988), and the transport costs of ants and beetles carrying artificial weights (Kram 1996; Lighton et al., 1993; Lighton et al., 1987). This technique could be adapted to insects that are then forced to undertake strenuous exercise. Potentially, the

energetic burden of carrying a load during heavy exercise could increase aerobic metabolism and reveal an untapped metabolic reserve that would have otherwise gone undetected.

The aim of the present study is to determine the resting and maximum metabolic rate of the migratory locust *Locusta migratoria* throughout ontogeny, during which body mass increases 45-fold. Weights are attached to exercising locusts in an attempt to increase oxygen consumption rates during terrestrial locomotion. The allometric exponents derived for resting and maximum metabolic rate are then used to assess whether there is empirical support for the hypothesis that insect metabolism conforms to the ¾-power exponent predicted by the optimised fractal network model.

3. Methods

3.1. Animals

Gregarious-phase locusts *Locusta migratoria* were sourced from a breeding colony at the University of Sydney, Australia, and then reared under crowded conditions at the University of Adelaide, Australia. They were kept in a large breeding container at 33 ± 1°C, at a relative humidity of ~30%, under a 12:12 h light-dark cycle, and had *ad libitum* access to seedling wheatgrass and wheat germ.

The developmental stage of each locust was determined based on instar-specific differences in wing morphology. Newly moulted individuals were transferred into separate plastic terraria with other locusts of the same age. Measurements of resting and hopping metabolic rate were conducted on first, third, and fifth instar locusts, as well as adults. Insects were measured three to four days post-moult to provide sufficient time for the exoskeleton to stiffen while minimising compression of the tracheal system due to growth (Greenlee and Harrison 2004b; Queathem 1991). All locusts were fasted 6-10 h prior to experiments to minimise elevation in oxygen consumption due to the heat increment of feeding (Nespolo et al., 2005; Gouveia et al., 2000).

3.2. Respirometry system

Flow-through respirometry was carried out using a dual-channel oxygen analyser (FC-2 Sable Systems, Las Vegas, NV, USA). First, outside air was pumped into an air pressure buffer cylinder using an air compressor (Sparmax, AT-250A, Taipei, Taiwan) before being scrubbed of H_2O vapour and CO_2 using a series of Drierite (W. A. Hammond Drierite Co. Ltd, Xenia, OH, USA), soda lime, and Drierite columns. This dry, CO_2-free air was then split into an experimental and reference line, both of which were directed through mass flow controllers

(Sierra Instruments Inc. Mass-Trak, Monterey, CA, USA, Model 810C, 0-100 ml min^{-1} and 0-1000 ml min^{-1} used depending on insect chamber volume; calibrated with a bubble flow meter, Gilibrator, Sensidyne, Clearwater, FL, USA) where their flow rates were matched. Both lines then entered a temperature cabinet set to 35 ± 2°C, where the experimental line was connected to a metabolic chamber that contained the insect. Upon exiting the temperature cabinet, the reference line was directed straight into the oxygen analyser, whereas the experimental line was first scrubbed of H_2O vapour and CO_2 using a small Drierite, Ascarite (A. H. Thomas Co., Philadelphia, PA, USA), Drierite column. The experimental line also had a bypass around the metabolic chamber which was controlled with two 3-way valves and allowed for baseline measurements of oxygen concentration before and after measurements with insects.

The differential mode of the oxygen analyser was used to measure the difference in oxygen level between the reference and experimental line at 1 s intervals. The analog outputs from the oxygen analyser and both mass flow controllers were recorded to a computer with a PowerLab data acquisition system and LabChart software (ADInstruments, Bella Vista, NSW, Australia). Baseline measurements of ambient oxygen concentration taken before and after insect measurements were used to correct experimental data for drift. Oxygen consumption rates were then calculated as:

$$(1) \qquad MR_{non-inst.} = M_I \cdot \left(F_{I_{O_2}} - F_{E_{O_2}}\right) / \left(1 - F_{E_{O_2}}\right)$$

where $MR_{non-inst.}$ is the oxygen consumption rate (μmol O_2 h^{-1}) of the locust prior to instantaneous correction, M_I is the flow rate (μmol h^{-1}) of the dry CO_2-free air prior to entering the metabolic chamber, F_{IO_2} is the fractional O_2 concentration of the dry CO_2-free air (i.e. 0.2095) prior to entering the metabolic chamber, and F_{EO_2} is the fractional O_2 concentration in air that has exited the metabolic chamber following the removal of CO_2 and H_2O vapour. This calculation for the rate of oxygen consumption is appropriate for respirometry set-ups where both H_2O vapour and CO_2 are removed prior to measurement of M_I and F_{EO_2} (Withers 2001).

Oxygen consumption rates were then instantaneously corrected as:

$$(2) \qquad MR = \left(MR_{non-inst.\ 1} - MR_{non-inst.\ 2} \cdot e^{k(t_2 - t_1)}\right) / (1 - e^{k(t_2 - t_1)})$$

where MR is the instantaneous oxygen consumption rate of the locust, $MR_{non-inst.\ 1}$ and $MR_{non-inst.\ 2}$ are the oxygen consumption rates of the locust at time t_1 and t_2, respectively, and k is the

washout constant determined for each chamber at the appropriate flow rate (Seymour et al., 1998).

Instantaneous oxygen consumption rates (MR) were then used for all analyses. Resting oxygen consumption rates (RMR) were calculated for each individual by averaging the lowest oxygen consumption rate over 2 min during an initial period of rest. In a number of experiments, individuals exhibited cyclic gas exchange and in such cases RMR was calculated by averaging over two or more successive ventilation cycles. Maximum oxygen consumption rates during exercise (MMR) were calculated for each individual by averaging the highest oxygen consumption rate over a 30 s period (consistent with Kirkton et al., 2005). The maximum metabolic rate of the hopping muscle ($MMR_{hop\ muscle}$) was calculated by subtracting RMR from MMR in each locust. This ignores the metabolic contribution made by the hopping muscle to overall RMR; however, the error in this approach is likely to be small given that the metathoracic hopping femurs represent just 5-10% of locust body mass (Chapter Four; Kirkton et al., 2005).

3.3. Respirometry during rest and hopping

Rest and hopping oxygen consumption rates were measured in locusts using metabolic hopping chambers constructed specifically for each developmental stage. Briefly, cylindrical hopping chambers were fashioned from either polymethyl methacrylate or polyethylene tube and sealed at the top and bottom with rubber stoppers. Incurrent and excurrent air-flow ports were located in the top and bottom stoppers, respectively, and wire mesh was fastened over the inner surface of the bottom stopper to provide insects with a coarse horizontal platform on which to jump.

Chamber volumes and flow rates varied to account for the large size range of insects tested. For first instar experiments (N=37 individuals), the chamber volume was 8 ml through which dry CO_2-free air was pushed at a rate of 20 ml min^{-1} STPD. Third instar (N=32), fifth instar (N=21) and adult (N=12) hopping chambers had volumes of 50, 120, and 500 ml respectively, with flow rates of 90, 150, and 410 ml min^{-1} STPD, respectively.

Each insect was given 30 min to acclimate to the hopping chamber, during which time a starting baseline oxygen level was recorded. Using the 3-way valves, incurrent air was then directed from the bypass line into the chamber so that the insect's resting oxygen consumption rate could be recorded for 10 min (up to 30 min if cyclic gas exchange was evident). During this time, locusts were monitored for movement, although most locusts settled within minutes of the initial acclimation period.

Next, hopping was induced for 5 min by persistently harassing the locust with five plastic beads located in the chamber while oxygen consumption was recorded (Fig. 1A). The external diameter of the beads ranged from 3 mm for first instar experiments, 5 mm for third instars, 10 mm for fifth instars, and 12 mm for adults. This technique elicited high and continual hopping activity from locusts. After the hopping period, oxygen consumption rate during recovery was recorded for a further 8 min, after which time the chamber was bypassed and baseline values were measured for the final 10 min of the trial. Immediately following the experiment the insect was weighed to 0.1 mg on an analytical balance (AE163, Mettler, Greifensee, Switzerland). No locusts were reused within a given life stage, however it is possible that some individuals were reused at a later life stage.

3.4. Respirometry with weight attachments

In an attempt to elicit maximum oxygen consumption rate, a second cohort of locusts were exercised exactly as previously described but with a weight attached to their body (Fig. 1B). For first instars (N=18 individuals), the weight was a bead of depilatory wax (Klorane, Boulogne, France) that was attached while warm to the pronotum of the insect and allowed to set. Careful attention was paid to ensure the wax was not excessively hot upon application. For larger third instars (N=21), fifth instars (N=16), and adults (N=11) the same procedure was employed except that a small steel plate was affixed to the wax before it set. The mass of the attached weight varied depending on the insect's developmental stage, ranging between 20-45% (including wax mass) of body mass for all locusts. Insects at all life stages behaved normally following the attachment of the weight. Oxygen consumption rates from individuals with a weight attached to their body, MR_{weight}, RMR_{weight}, and MMR_{weight}, were calculated exactly as described for individuals without a weight attached.

All mean values and allometric exponents include 95% confidence intervals (CI). Statistical significance between means was tested using paired and unpaired T-tests for equal or unequal variance, as appropriate. When three or more means were compared, an ANOVA was performed followed by a Tukey's or Dunnett's post-hoc test, as appropriate. Allometric data were transformed into $\log_{10}$ base before statistical analysis using ordinary least squares regressions. ANCOVA comparisons of regressions (Zar 1998), ANOVAs and T-tests were carried out with GraphPad Prism 5 statistical software (GraphPad Software, La Jolla, CA, USA).

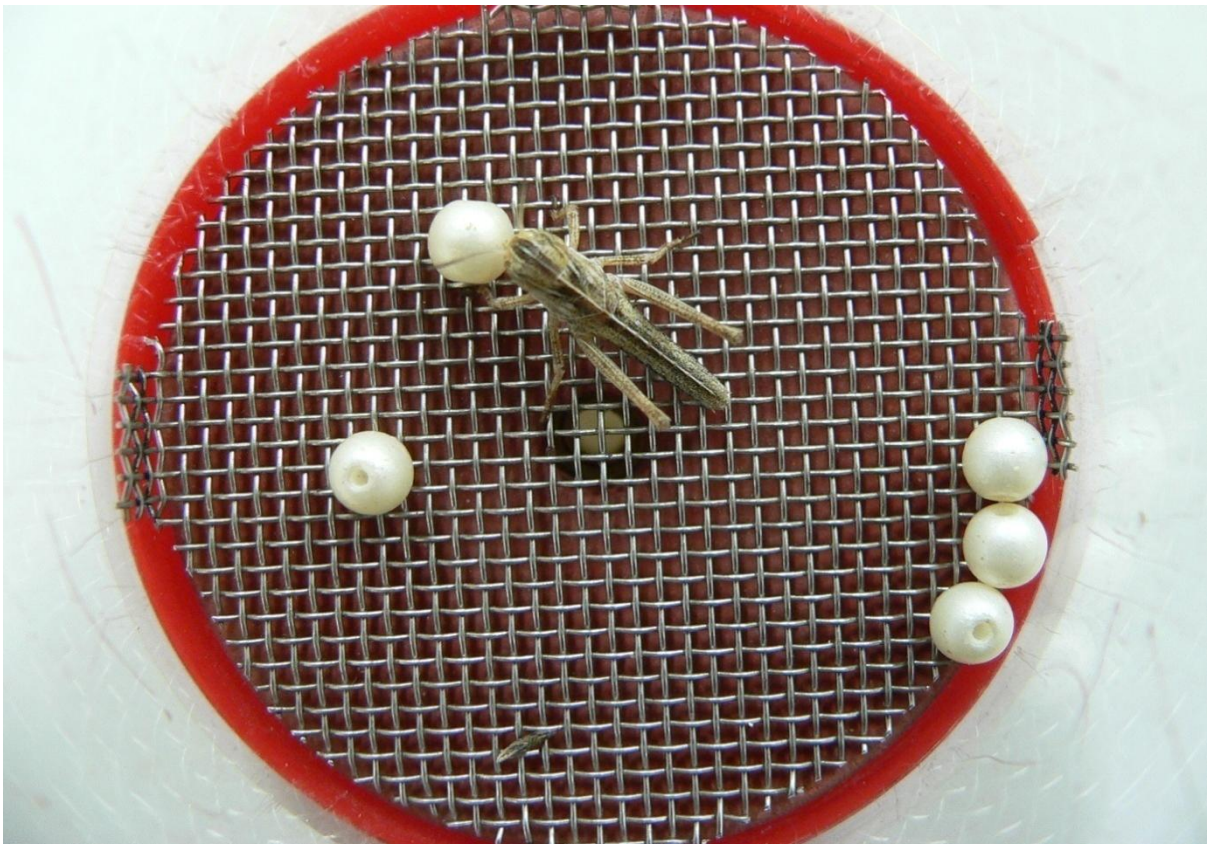


Fig. 1A. Third instar locust inside a metabolic hopping chamber with five plastic exercising beads.



Fig. 1B. Adult locust with a steel plate weight attached with depilatory wax to the pronotum.

4. Results

4.1. Body mass

Body mass increased 45-fold from hatching to early adulthood. First instars had a mean body mass of 0.022 ± 0.001 g, which increased to 0.131 ± 0.007 g by the third instar stage, and by the fifth instar stage mean body mass was 0.666 ± 0.052 g. Male and female adults 3-4 days post-moult had a mean mass of 0.945 ± 0.096 g.

4.2. Allometry

RMR and RMR_{weight} values were pooled because they had statistically indistinguishable allometric slopes (ANCOVA, $F_{1, 190}$=0.07; P=0.79) and elevations (ANCOVA, $F_{1, 191}$=0.07; P=0.79). The pooled data shows that throughout ontogeny resting metabolic rate increases with body mass according to the allometric equation $RMR = 30.1M_b^{0.83 \pm 0.02 (95\% CI)}$ μmol O_2 h^{-1} at 35°C (r^2=0.97, N=194) (Fig. 2). If adults are excluded from the regression, the resting metabolic rate of first, third and fifth instar juveniles scales as, $RMR_{juvenile} = 32.3M_b^{0.86 \pm 0.02}$ μmol O_2 h^{-1} at 35°C (r^2=0.97, N=145). The exponents for RMR and $RMR_{juvenile}$ are statistically indistinguishable (ANCOVA, $F_{1, 335}$=2.1; P=0.15).

There was no significant difference in the slope (ANCOVA, $F_{1, 163}$=0.07; P=0.79) or elevation (ANCOVA, $F_{1, 164}$=3.26; P=0.07) between MMR and MMR_{weight}. Pooled hopping data shows that maximum hopping metabolic rate increases with body mass according to $MMR = 155M_b^{1.01 \pm 0.02}$ μmol O_2 h^{-1} at 35°C (r^2=0.99, N=168). However, adults have a disproportionately high MMR and if they are excluded from the regression, juvenile maximum oxygen consumption rate scales as, $MMR_{juvenile} = 136M_b^{0.97 \pm 0.02}$ μmol O_2 h^{-1} at 35°C (r^2=0.99, N=145) (Fig. 2). The exponent for $MMR_{juvenile}$ is significantly lower than when adults are included in the analysis (ANCOVA, $F_{1, 308}$=10.9; P<0.01). There is also a significant difference between the exponent derived for RMR and MMR (ANCOVA, $F_{1, 357}$=182; P<0.0001) and between $RMR_{juvenile}$ and $MMR_{juvenile}$ (ANCOVA, $F_{1, 286}$=66; P<0.0001).

The maximum oxygen consumption rate of the hopping muscle increases with body mass according to the allometric equation, $MMR_{hop\ muscle} = 120M_b^{1.07 \pm 0.02}$ μmol O_2 h^{-1} at 35°C (r^2=0.98, N=168). If adults are excluded, the juvenile maximum oxygen consumption rate of the hopping muscle scales as, $MMR_{juvenile\ hop\ muscle} = 103M_b^{1.02 \pm 0.02}$ μmol O_2 h^{-1} at 35°C (r^2=0.98, N=145) (Fig. 3). The exponent for $MMR_{juvenile\ hop\ muscle}$ is significantly lower than when adults are included in the analysis (ANCOVA, $F_{1, 307}$=8.1; P<0.01).

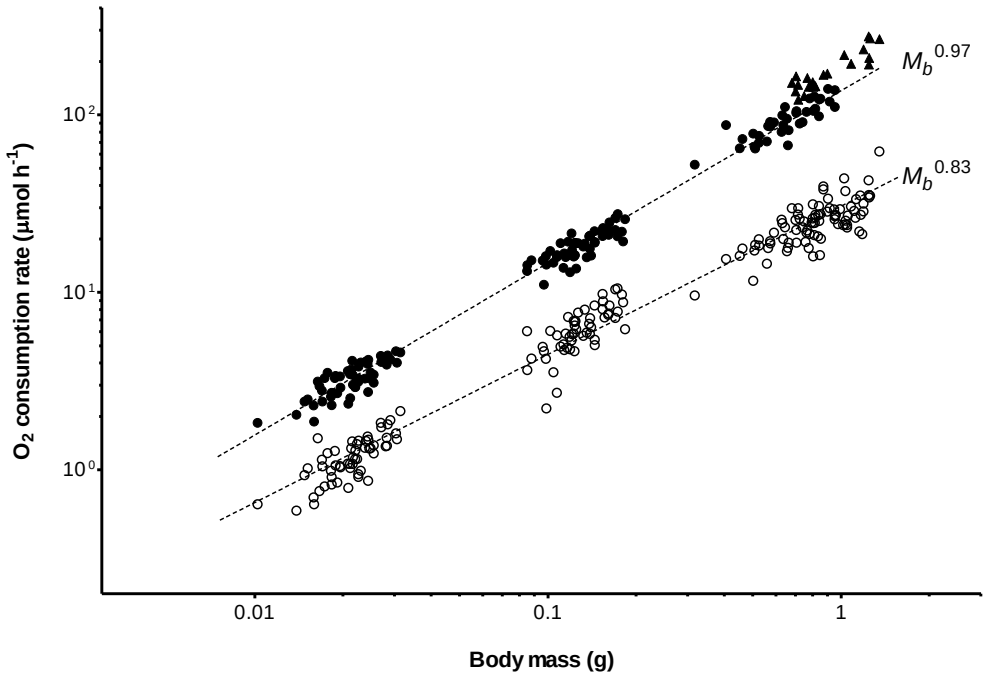


Fig. 2. Relationship between body mass (M_b) and resting metabolic rate (RMR) in first (N=55), third (N=53), fifth instar (N=37), and adult locusts (N=49) (unfilled circles). Also shown is the relationship between body mass and juvenile maximum metabolic rate during hopping ($MMR_{juvenile}$) in first (N=55), third (N=53), and fifth instar locusts (N=37) (filled circles). The maximum hopping metabolic rate of adult locusts is also presented (N=23) (filled triangles), but excluded from the regression due to their disproportionately high MMR.

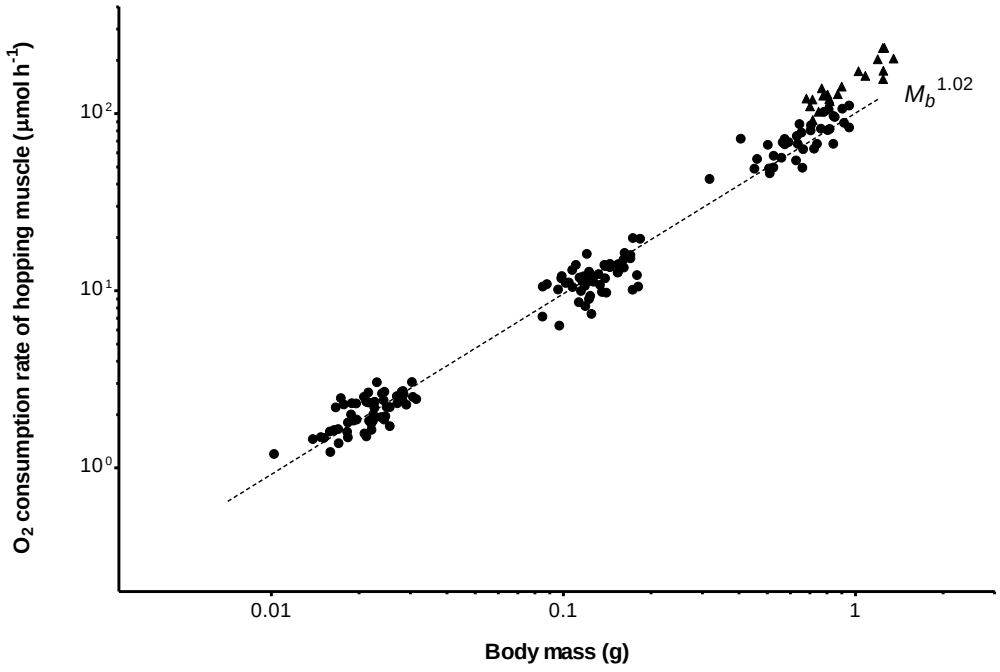


Fig. 3. Relationship between body mass (M_b) and the maximum metabolic rate of the juvenile hopping muscle ($MMR_{juvenile\ hop\ muscle}$) in first ($N$=55), third ($N$=53), and fifth instar locusts (N=37) (filled circles). The maximum metabolic rate of the adult hopping muscle is also presented (N=23) (filled triangles), but excluded from the regression due to their disproportionately high $MMR_{hop\ muscle}$.

4.3. Resting oxygen consumption

During the initial rest period, locusts at all developmental stages regularly exhibited cyclic gas exchange, which is indicative of inactivity (Chown et al., 2006). RMR increased nearly 25-fold throughout development from 1.2 ± 0.1 μmol O_2 h^{-1} in first instars to approximately 28 ± 3 μmol O_2 h^{-1} in adults. However, mass-specific RMR was highest in first instars at around 55 ± 3 μmol O_2 g^{-1} h^{-1}, and declined steadily with age to 48 ± 3 μmol O_2 g^{-1} h^{-1} in third instars, 33 ± 2 μmol O_2 g^{-1} h^{-1} in fifth instars, and 29 ± 2 μmol O_2 g^{-1} h^{-1} in adults (ANOVA, $P<0.0001$) (Fig. 4). Post-hoc analysis reveals that a significant difference in mass-specific RMR exists between all life stages (Tukey's, $P<0.05$) except between fifth instars and adults (Tukey's, $P>0.05$).

The attachment of weights had no effect on mass-specific RMR at any developmental stage (first instars, Mann-Whitney U-test, $P=0.99$; third instars, T-test, $P=0.96$; fifth instars, T-test, $P=0.51$; adults, T-test, $P=0.48$) (Fig. 4).

4.4. Maximum oxygen consumption

MMR during hopping exercise increased nearly 55-fold throughout development from 3.3 ± 0.2 μmol O_2 h^{-1} in first instars to 176 ± 24 μmol O_2 h^{-1} in adults. However, mass-specific MMR was similar amongst the juvenile instars in that first instars consumed a maximum of 150 ± 6 μmol O_2 g^{-1} h^{-1}, third instars consumed a maximum of 139 ± 6 μmol O_2 g^{-1} h^{-1}, and fifth instars consumed a maximum of 141 ± 10 μmol O_2 g^{-1} h^{-1} (Fig. 4). Adults had a slightly higher mass-specific MMR of 195 ± 13 μmol O_2 g^{-1} h^{-1}. Statistical analysis confirms that the mean value of adults is significantly greater than each of the juvenile stages (ANOVA, $P<0.0001$; and Tukey's post-hoc, $P<0.05$), but that juvenile values are all similar to one another (Tukey's post-hoc, $P>0.05$).

The attachment of weights had no effect on mass-specific MMR at any of the developmental stages (first instars, T-test, $P=0.15$; third instars, T-test, $P=0.14$; fifth instars, T-test, $P=0.56$; adults, T-test, $P=0.59$) (Fig. 4).

4.5. Difference between sexes

It was possible to determine the sex of adult locusts. Mean mass-specific RMR was 31 ± 1 μmol O_2 g^{-1} h^{-1} in males ($N=14$) and 32 ± 3 μmol O_2 g^{-1} h^{-1} in females ($N=9$) with no significant difference between sexes (T-test, $P=0.84$). Mean mass-specific MMR was 193 ± 5 μmol O_2 g^{-1} h^{-1} in males ($N=14$) and 191 ± 8 μmol O_2 g^{-1} h^{-1} in females ($N=9$) and once again there was no significant difference between sexes (T-test, $P=0.84$).

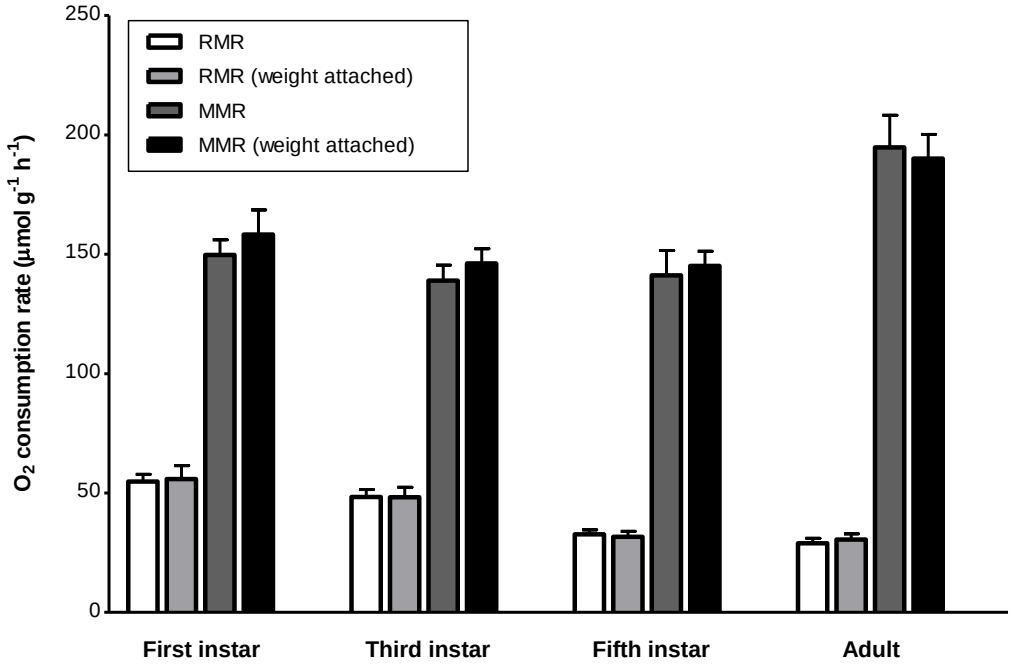


Fig. 4. Mass-specific resting metabolic rate (RMR) and maximum metabolic rate (MMR) (mean ± CI) in first instars with (N=18) and without weights (N=37), in third instars with (N=21) and without weights (N=32), and in fifth instars with (N=16) and without weights (N=21). Also shown is RMR in adults with (N=11) and without weights (N=38) and MMR in adults with (N=11) and without weights (N=12).

4.6. Oxygen consumption during rest, hopping and recovery

The pattern of change in mass-specific MR during hopping experiments in first, third and fifth instar locusts were very similar and so combined juvenile data are presented (Fig. 5). From initial low resting levels, juvenile MR increased significantly at the commencement of hopping with the highest rates occurring 2-3 min into exercise when mean hopping MR ranged from 124-133 μmol O_2 g^{-1} h^{-1}. In a similar pattern, adult MR also increased quickly during forced hopping, and after 1 min of exercise mean MR was matched with that of juveniles at the same time (T-test, P=0.44) (Fig. 5). However, for the remainder of the exercise period mean MR in adults remained significantly above juvenile hopping MR (T-tests and Mann-Whitney U-test, P<0.05) reaching 180 μmol O_2 g^{-1} h^{-1} before a final decline.

The attachment of weights to the juvenile locust body did not produce a substantial increase in hopping MR, although a slight but significant increase (6-9%) in mean mass-specific MR was observed 2 and 3 min into the exercise period (T-test, P<0.05) (Fig. 5). In adults, there was no detectable effect of weights on mean hopping MR (T-tests and Mann-Whitney U-test, P>0.05).

Following exercise, recovery was quick with mean mass-specific MR returning back to resting levels within 2 min in juveniles and 4 min in adults (Fig. 5). The attachment of weights did not have a significant effect on mean MR during recovery in either juveniles or adults (T-tests and Mann-Whitney U-test, $P>0.05$).

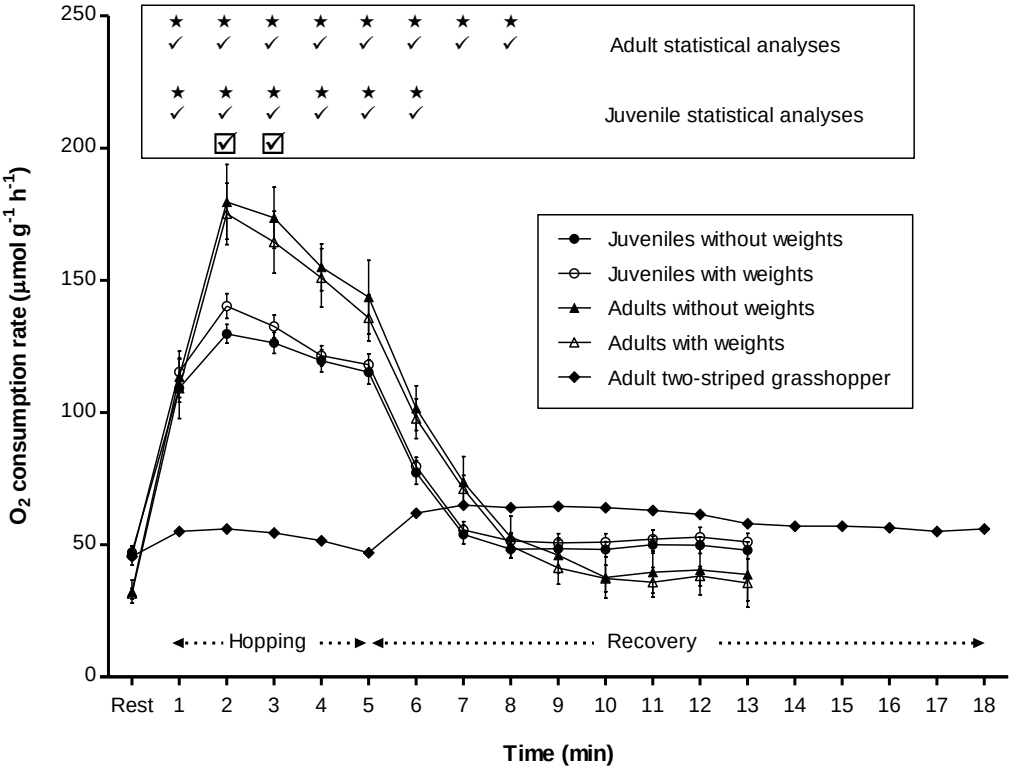


Fig. 5. Mass-specific metabolic rate (mean ± CI) during rest, 5 min hopping, and 8 min recovery for combined juvenile data with (*N=55*) and without weights (*N=90*), and adults with (*N=11*) and without weights (*N=12*). ★ Indicates that the individual mean MR is significantly greater than the initial resting metabolic rate in locusts without weights (ANOVA with Dunnett's, $P<0.05$). ✓ Indicates that the individual mean MR is significantly greater than the initial resting metabolic rate in locusts with weights (ANOVA with Dunnett's, $P<0.05$). ☑ Indicates a significant difference between individual mean MR for locusts with weights and without weights at a given time (T-tests $P<0.05$). Also shown is the mean mass-specific MR during rest, 5 min hopping, and 13 min recovery in adult two-striped grasshoppers *Melanoplus bivittatus* (*N=8*) measured by Harrison and co-workers (Harrison et al., 1991).

5. Discussion

5.1. Allometry

Resting oxygen consumption rate in locusts increases with body mass throughout development with an exponent of 0.83 ± 0.02 (Fig. 2). This accords well with the exponents of 0.77 and 0.80 derived in two separate studies on resting American locusts *Schistocerca americana* (Harrison et al., 2005; Greenlee and Harrison 2004a), and also the exponent of 0.84 determined for resting *Encoptolophus sordidus* grasshoppers (Bailey and Riegert 1973). Maximum oxygen consumption rate of locusts undertaking hopping exercise increases with body mass in a near-isometric relationship, scaling with an exponent of 1.01 ± 0.02 when adults are included in the regression, or 0.97 ± 0.02 when adults are excluded (Fig. 2). Regardless of whether adults are included in the analysis, MMR scales with an exponent that is significantly steeper than RMR. In birds and mammals a similar pattern emerges in that MMR tends to scale with a steeper exponent than basal metabolic rate (Weibel and Hoppeler 2005; White and Seymour 2005; Savage et al., 2004; Weibel et al., 2004; Bishop 1999). This might suggest that the factors that drive the scaling of MMR are different from those that drive basal or resting rates, and that this could be a feature of metabolic scaling in animal groups other than just birds and mammals.

5.2. Scaling exponents do not support an optimised fractal network model

The scaling exponents for RMR, MMR, $MMR_{juvenile}$, $MMR_{hop\ muscle}$, and $MMR_{juvenile\ hop\ muscle}$ are all significantly greater than 0.75 (Figs 2, 3). Therefore, the current study does not provide empirical support for the hypothesis that insect metabolism conforms to the original optimised presentation of the fractal network model (West et al., 1997). The same conclusion has emerged from a number of recent interspecific (Chown et al., 2007) and intraspecific allometric analyses of insect metabolic rate (Strauss and Reinhold 2010; Chappell et al., 2009; Chown et al., 2007). Perhaps a potential problem with applying the fractal network model to insects is that it assumes metabolic rate is set by the delivery of oxygen along the tracheal system. However, limited oxygen supply seems inconsistent with the fact that many insect species engage in intermittent gas exchange, during which the spiracles are occluded, sometimes for hours between breaths (Contreras and Bradley 2009; Quinlan and Gibbs 2006; Lighton 1996). In fact, it has been suggested that this respiratory pattern could have evolved to prevent oxidative damage as a result of excess oxygen supply (Hetz and Bradley 2005). Even during flight, and to some extent hopping, the supply of oxygen appears to exceed, or at least match the requirements of the locomotory muscle owing to the lack of anaerobic

metabolites produced (Kirkton et al., 2005; Harrison et al., 1991; Beenakkers et al., 1984; Worm and Beenakkers 1980; Kammer and Heinrich 1978).

The lack of agreement between the metabolic scaling exponents derived in the present study and the ¾-power exponent predicted by the fractal network model might also arise if the model is not an appropriate description of oxygen transport in these animals. The apparent interspecific scaling exponent of ¾ determined for insect SMR could simply be a coincidence (e.g. Addo-Bediako et al., 2002). Certainly insects appear to violate at least one core assumption of even the most recent iterations of the model (Banavar et al., 2010): the insect tracheal system is not a network in which resources (oxygen) are distributed from a single source. Instead, atmospheric oxygen enters the tracheal system through multiple valve-like spiracles, with each spiracle typically interconnected by a longitudinal tracheal trunk, anastomosing with a series of transverse trunks that are then often interconnected with a number of medial longitudinal trunks (Harrison et al., 2005). It is only at a relatively fine scale that a fractal-like branching pattern emerges, and multiple parallel branching networks serve to deliver oxygen throughout the animal. Perhaps, therefore, the near-isometric scaling of MMR observed in the present study arises because the total maximum delivery capacity of the parallel branching system scales as M_b^{1} rather than $M_b^{3/4}$.

5.3. Addition of weights

The addition of weights did not increase the maximum or mean hopping MR of adult locusts (Figs 4, 5). However, weights did induce a slight, but insignificant increase in the MMR of first, third and fifth instar locusts (Fig. 4), and when juvenile instar data are combined the mean hopping MR of weighted juveniles is significantly higher than their unweighted counterparts at 2 and 3 min into exercise (Fig. 5). However, the increase in juvenile hopping MR is only around 8%, which might be considered modest given that weighted locusts were forced to carry a load equivalent to 20-45% of their body mass. On balance, it would seem that the hopping muscles of both weighted and unweighted individuals were probably operating at or near their aerobic limits during exercise, and if weights did induce an increase in overall energy expenditure, then this was likely met by anaerobic means.

Any number of factors could set the upper functional metabolic limit of the jumping muscles, including the capacity to deliver and utilise oxygen and metabolic substrate, or even the mechanical limits of the myofibril machinery or associated nervous system could set the muscle's aerobic capacity. If a single factor is responsible for limiting hopping metabolic rate, then it would follow that all other components that make up the jumping system are

present in excess. Alternatively, a well known but controversial hypothesis is that all structures involved in hopping should be quantitatively matched to the functional capacity of the entire system, such that no single component limits maximum oxygen consumption rate (symmorphosis, Chapter Four; Weibel et al., 1998; Weibel et al., 1991).

5.4. High hopping metabolic rate in adults

Another finding from this study is that adults have a 1.3-fold higher mass-specific hopping MR than juvenile conspecifics (Figs 4, 5). This is not dissimilar to the American locust, where mass-specific hopping metabolic rates are 2-fold higher in adults compared to juveniles (Kirkton et al., 2005). The high aerobic capacity of the adult hopping muscle is puzzling because it is inconsistent with the observation that its primary function is to perform single powerful jumps required to initiate flight (Kirkton and Harrison 2006; Katz and Gosline 1993): such short-term energy needs are more likely to be met by local ATP supplies that are temporarily maintained by arginine phosphate (Schneider et al., 1989; Newsholme et al., 1978). In light of this, it is possible that the high hopping metabolic rate of adult locusts could be due to the inadvertent stimulation of flight muscles during jumping exercise. The flight muscles only develop during adulthood (Mizisin and Ready 1986), and although there was no evidence of obvious wing movements during adult hopping, smaller wing movements could have easily gone undetected. Potentially, the larger 2-fold difference between adult and juvenile hopping metabolic rates in the Kirkton et al. (2005) study might be due to their use of more mature adults (up to 21 days post-moult), which compared to the young adults used in the present study (3-4 days post-moult), would likely have better developed flight muscles (Mizisin and Ready 1986).

5.5. Comparison with the two-striped grasshopper

The hopping metabolic rate of migratory locusts in the current study differs greatly from previous measurements taken from adult two-striped grasshoppers *Melanoplus bivittatus* (Harrison et al., 1991). In contrast to the rapid increase in oxygen consumption that occurs during hopping in migratory locusts, two-striped grasshoppers increase oxygen consumption rates barely above resting levels (Fig. 5). In fact, in *M. bivittatus* the highest rates of oxygen consumption occur after exercise, and then they remain elevated above resting levels for the entire recovery period. Harrison and colleagues suggested that there might be an intrinsic constraint on ventilation during hopping in this insect which limits oxygen delivery. In contrast, gas exchange during hopping exercise in migratory locusts does not appear to be

compromised, and so the results of the current study probably provide a better indication of typical terrestrial locomotion energetics for the Orthoptera.

5.6. Summary

This study quantifies the allometric scaling of RMR and MMR in the migratory locust throughout ontogenetic development. Similar to the pattern in birds and mammals, MMR scales with an exponent that is significantly steeper than RMR. This study also demonstrates that neither RMR, MMR, $MMR_{juvenile}$, $MMR_{hop\ muscle}$, nor $MMR_{juvenile\ hop\ muscle}$ scales in a manner consistent with the optimised fractal network model (West et al., 1997). This might be due to the effectiveness at which oxygen is delivered along the tracheal system, or because the tracheal system is not well described by a model designed for networks that deliver resources from a single source. Finally, this study shows that the addition of weights to hopping locusts does not increase their maximum aerobic metabolic rate, implying that the functional aerobic limits of the jumping muscles were reached during exercise.

6. Acknowledgements

This research was supported by the Australian Research Council, project no. DP0879605. The author thanks Professor Stephen Simpson and Mr Tim Dodgson from the University of Sydney for technical advice and providing the founding locust colony. I also thank Dr John Terblanche and one anonymous reviewer who provided comments that improved an earlier version of this manuscript.

Chapter Three: Resting and maximum metabolic rate during tethered-flight in the adult locust *Locusta migratoria*

1. Abstract

Insects during flight achieve the highest mass-specific aerobic metabolic rates of all animals, and some insects reveal additional metabolic potential when added demands are placed on the flight system or when the constraints of tethering are removed. Because locust flight respirometry typically involves some form of tethering, and no steps have been taken to make flight more energetically taxing for the insect, estimates of locust flight metabolism could be sub-maximal. To address this, oxygen consumption was measured during tethered-flight in adult locusts *Locusta migratoria* some of which had small weights attached to each wing (totalling 30-45% of body mass). Metabolic rates increased from 28 ± 2 μmol O_2 g^{-1} h^{-1} at rest, to 896 ± 101 during flight in weighted locusts, and 1032 ± 69 in unweighted locusts. Allometrically, locust flight metabolic rate follows the equation, $MR_{locust\ flight} = 1018 M_b^{0.77 \pm 0.18}$ μmol O_2 h^{-1}, whereas flight metabolic rate in other insects is around 2.6-fold higher according to the equation, $MR_{other\ insect\ flight} = 2631 M_b^{0.85 \pm 0.07}$. The lower flight metabolic rate of locusts is unlikely an artefact of individuals failing to exert themselves during exercise because mean maximum lift was sufficient to support 90 ± 14% of body mass, and mean wing-stroke frequency was 23.9 ± 0.8 Hz, which are close to free-flight values. Instead, the modest flight metabolic rate of locusts could reflect the limits of their relatively small flight motor, which likely affords the insect considerable energy savings.

2. Introduction

Insects sustain the highest mass-specific aerobic metabolic rates of all animals (Suarez 2000; Casey et al., 1985; Sacktor 1976; Weis-Fogh 1964b). The high oxygen demand of insect tissue is met by the tracheal system, which delivers oxygen from the atmosphere along a branching network of internal tubes that terminate in close proximity to mitochondria. Because oxygen delivery occurs almost entirely in the gas-phase, even the most strenuous forms of exercise, such as flight, are almost entirely aerobic (Harrison and Lighton 1998; Komai 1998; Beenakkers et al., 1984; Beenakkers et al., 1981; Worm and Beenakkers 1980; Kammer and Heinrich 1978; Kammer and Heinrich 1974). Based on this observation, it is reasonable to suspect that the absolute aerobic potential of insects is not limited by the capacity of the tracheal system to deliver oxygen, but by the ability of the muscle to convert chemical energy into mechanical work.

Measuring maximum oxygen consumption rate is generally more difficult than measuring resting rates because it usually requires the construction of apparatus in which to exercise insects. Despite the challenges, data exist on the energetics of running in ants, beetles and cockroaches (Rogowitz and Chappell 2000; Lighton et al., 1993; Bartholomew et al., 1985; Herreid and Full 1984). But for the purpose of testing the limits of insect respiration, flight studies are of greater interest. The high metabolic cost of flight has been demonstrated in a diversity of insect groups including bees, dragonflies, locusts and moths (Rascon and Harrison 2005; Harrison and Lighton 1998; Armstrong and Mordue 1985; Casey et al., 1985; Bartholomew and Casey 1978; Kammer and Heinrich 1974; Weis-Fogh 1967). However, there is evidence to suggest that many metabolic flight estimates are sub-maximal, given few studies take additional steps to increase the energetic cost of flying.

The potential to underestimate metabolic capacity is demonstrated in a novel study in which the flight metabolic rate of carpenter bees *Xylocopa varipuncta* was shown to increase by as much as 35% in low-density heliox atmospheres (Roberts et al., 2004). Presumably, this metabolic reserve would go undetected in normal air. Other studies have increased the energetic cost of flight by adding either natural or artificial weights to free-flying insects, which effectively increases their wing-loading. However, the results of these experiments are conflicting. One study found there was no ‘clear-cut’ dependence between metabolic rate and weight load in foraging honeybees *Apis mellifera* carrying either a lead weight or a crop load (Balderrama et al., 1992), while another study showed that honeybees carrying a nectar load have metabolic rates around 35% higher than unloaded bees (Wolf et al., 1989). The latter

study is in line with results from bumblebees *Bombus edwardsii* in which energy expenditure during flight is correlated with body mass, as affected by stomach contents (Heinrich 1975).

Given that the energetics of insect flight can increase when additional demands are placed on the system, it is reasonable to suspect that sub-maximal metabolic rates could occur when no effort is made by researchers to increase the cost of flight. Studies involving locusts should come under particular scrutiny because this insect needs to be tethered for flight respirometry since it appears incapable of hovering in a metabolic chamber long enough for gas exchange measurements (Rascon and Harrison 2005; Armstrong and Mordue 1985; Weis-Fogh 1967). The problem with tethering is that it interrupts sensory feedback loops, which can lead to unnatural flight behaviour and sub-maximal flight efforts (Kutsch et al., 1999; Preiss and Gewecke 1991; Dudley and Ellington 1990; Zarnack and Wortmann 1989). Studies have shown that tethered locusts have lower wing-stroke frequencies than free-flying locusts (Kutsch et al., 1999; Baker et al., 1981; Kutsch and Stevenson 1981). There is also evidence that tethered locusts do not always produce enough lift to support body mass (Gee and Robertson 1998; Robertson and Johnson 1993; Wolf 1993; Kutsch and Gewecke 1979; Gewecke 1975), which is a concern given that locust flight metabolic rates have been shown to increase with lift (Armstrong and Mordue 1985; Weis-Fogh 1964a). Indeed, in other insects, such as the fruit fly *Drosophila melanogaster*, tethering can underestimate peak flight performance by around 20% (Lehmann and Dickinson 1997), and the rate of oxygen uptake by tethered sphinx moths *Manduca sexta* is one-half that of free-flying moths (Heinrich 1971).

If tethering does encourage sub-maximal flight efforts, then it might explain why locust flight metabolic rates appear to be lower than those of other insects. For example, pioneering work by Krogh and Weis-Fogh showed that energy expenditure during tethered-flight in the desert locust *Schistocerca gregaria* is in the range of 450-1300 μmol O_2 g^{-1} h^{-1} (Weis-Fogh 1967; Weis-Fogh 1952; Krogh and Weis-Fogh 1951). This has more recently been verified in the American locust *S. americana* where metabolic rates during tethered-flight are around 1150 μmol O_2 g^{-1} h^{-1} (Rascon and Harrison 2005; calculated from CO_2 production assuming RQ = 0.83, Hadley and Quinlan 1993). However, these rates are much lower than similar size bees, beetles and moths where flight oxygen consumption rates are generally within the range of 2000-4000 μmol O_2 g^{-1} h^{-1} (Suarez et al., 2005; Auerswald et al., 1998; Casey et al., 1985; Bartholomew and Casey 1978).

Because tethering can elicit sub-maximal flight efforts, and given that some insects reveal a hidden metabolic reserve when extra demands are placed on the flight system, we hypothesise that the apparently low oxygen consumption rate of flying locusts may not reflect their true metabolic potential. Therefore, the aim of this study is to clarify whether previous estimates of energy consumption during locust flight are representative of maximum aerobic metabolic values, and whether the energy requirements for locust flight can be further increased by the attachment of small weights onto the wings.

3. Methods

3.1. Animals

Gregarious-phase locusts *Locusta migratoria* were reared at 33 ± 1°C, under a 12:12 h light-dark cycle, with *ad libitum* access to seedling wheatgrass and wheat germ, as previously described (Chapter Two). Newly emerged adults were identified from the breeding colony and placed into separate plastic terraria with other adults of similar age. Respirometry during rest and flight, and measurements of lift and wing-stroke frequency, were conducted on adult male locusts two to three weeks post-final moult, by which time the flight muscles are fully developed (Mizisin and Ready 1986). All insects were fasted 6-10 h prior to experiments to minimise elevation in oxygen consumption due to the heat increment of feeding (Nespolo et al., 2005; Gouveia et al., 2000).

3.2. Respirometry system

Flow-through respirometry was carried out using a dual-channel oxygen analyser (FC-2 Sable Systems, Las Vegas, NV, USA). First, outside air was pushed through an air pressure buffer cylinder (Sparmax, AT-250A, Taipei, Taiwan) before being scrubbed of H_2O vapour and CO_2 using a series of Drierite (W. A. Hammond Drierite Co. Ltd, Xenia, OH, USA), soda lime, and Drierite columns. This dry, CO_2-free air was then split into an experimental and reference line, both of which were directed through mass flow controllers (Sierra Instruments Inc. Mass-Trak, Monterey, CA, USA, Model 810C 0-100 ml min^{-1} used for resting measurements and 0-1000 ml min^{-1} used for flight measurements; calibrated with a bubble flow meter, Gilibrator, Sensidyne, Clearwater, FL, USA) where their flow rates were matched. Both lines then entered a temperature cabinet set to 35 ± 2°C, where the experimental line was connected to a metabolic chamber that contained the locust. Upon exiting the temperature cabinet, the reference line was directed straight into the oxygen analyser, whereas the experimental line was first scrubbed of H_2O vapour and CO_2 using a

small Drierite, Ascarite (A. H. Thomas Co., Philadelphia, PA, USA), Drierite column. The experimental line also had a bypass line around the metabolic chamber which was controlled with two 3-way valves at the connection points and allowed for baseline measurements of oxygen concentration before and after measurements with locusts.

The differential mode of the oxygen analyser was used to measure the difference in oxygen level between the reference and experimental line at 1 s intervals. The analog outputs from the oxygen analyser and both mass flow controllers were recorded to a computer with a PowerLab data acquisition system and LabChart software (ADInstruments, Bella Vista, NSW, Australia). Baseline measurements of ambient oxygen concentration taken before and after locust measurements were used to correct experimental data for drift. Oxygen consumption rates were then calculated as:

$$(1) \qquad \mathrm{MR_{non-inst.}} = \mathrm{M_I} \cdot \left(\mathrm{F_{I_{O_2}}} - \mathrm{F_{E_{O_2}}}\right) / \left(1 - \mathrm{F_{E_{O_2}}}\right)$$

where $MR_{non\text{-}inst.}$ is the oxygen consumption rate (μmol O_2 h^{-1}) of the locust prior to instantaneous correction, M_I is the flow rate (μmol h^{-1}) of the dry CO_2-free air prior to entering the metabolic chamber, F_{IO_2} is the fractional O_2 concentration of the dry CO_2-free air (i.e. 0.2095) prior to entering the metabolic chamber, and F_{EO_2} is the fractional O_2 concentration in air that has exited the metabolic chamber following the removal of CO_2 and H_2O vapour. This calculation for the rate of oxygen consumption is appropriate for respirometry set-ups where both H_2O vapour and CO_2 are removed prior to measurement of M_I and F_{EO_2} (Withers 2001).

Oxygen consumption rates were then instantaneously corrected as:

$$(2) \qquad \mathrm{MR} = \left(\mathrm{MR_{non-inst.\ 1}} - \mathrm{MR_{non-inst.\ 2}} \cdot \mathrm{e}^{\mathrm{k}(\mathrm{t_2} - \mathrm{t_1})}\right) / \left(1 - \mathrm{e}^{\mathrm{k}(\mathrm{t_2} - \mathrm{t_1})}\right)$$

where MR is the instantaneous oxygen consumption rate of the locust, $MR_{non\text{-}inst.\ 1}$ and $MR_{non\text{-}inst.\ 2}$ are the oxygen consumption rates of the locust at time t_1 and t_2, respectively, and k is the washout constant determined for each chamber at the appropriate flow rate (Seymour et al., 1998).

Instantaneous oxygen consumption rates (MR) were then used for all analyses. Resting oxygen consumption rates (RMR) were calculated for each individual by averaging the lowest oxygen consumption rate over 2 min during an initial period of rest. In a number of experiments, individuals exhibited cyclic gas exchange and in such cases RMR was calculated by averaging over two or more successive ventilation cycles. Maximum oxygen consumption rates during flight (MMR) were calculated for each individual by averaging the highest oxygen consumption rate over a 30 s period (consistent with hopping MMR, Chapter

Two). The maximum metabolic rate of the flight muscle ($MMR_{flight\ muscle}$) was calculated by subtracting RMR from MMR in locusts from which data for both metabolic states were available (N=13). This ignores the metabolic contribution made by the flight muscle to overall RMR; however, the high aerobic scope associated with insect flight means the error in this approach is likely to be small.

3.3. Respirometry during rest

Prior to each flight experiment, resting rates of oxygen consumption (N=28 individuals) were recorded from locusts sitting in a cylindrical 50 ml polymethyl methacrylate metabolic chamber that was orientated with the flat side down. The chamber was sealed at the top and bottom with rubber stoppers, where incurrent and excurrent air-flow ports were located, through which air was pushed at a rate of 200 ml min^{-1} STPD. Each locust was given 30 min to acclimate to the conditions of the chamber, during which time a starting baseline oxygen level was recorded. Using the 3-way valves, incurrent air was then directed from the bypass line into the chamber so that the locust's resting oxygen consumption rate could be recorded for 10 min (up to 30 min if cyclic gas exchange occurred). During this time, locusts were monitored for movement although most individuals settled within minutes of the initial acclimation period. Following resting measurements, the chamber was bypassed and baseline values were measured for the final 10 min of the trial.

3.4. Respirometry during flight

Locusts were then transferred to a cylindrical 500 ml polymethyl methacrylate metabolic flight chamber for measurements of flight oxygen consumption rate (N=23 individuals). The flight chamber was orientated with the cylinder tube positioned horizontally and was sealed at both ends with rubber stoppers, where incurrent and excurrent air-flow ports were located, through which air was pushed at a rate of 1000 ml min^{-1} STPD. Locusts were tethered to a metal rod descending from the roof of the chamber which was attached to the pronotum of the insect with warm depilatory wax (Klorane, Boulogne, France) (Fig. 1A). Careful attention was paid to ensure the wax was not excessively hot upon application. Each locust was given 10 min to acclimate to the conditions of the flight chamber, during which time a starting baseline oxygen level was recorded. Using the 3-way valves, incurrent air was then directed from the bypass line into the chamber so that the insect's oxygen consumption during flight could be measured over a 5 min exercise period. Following flight measurements, the chamber was bypassed and baseline values were measured for the final 10 min of the trial.

Tethered-flight was induced by invoking the 'tarsal reflex' (Weis-Fogh 1956). This involved the rapid removal of a metal perch from beneath the locust using a rare-earth magnet located outside the chamber. In addition, flight was encouraged by positioning the incurrent air stream directly in front of the locust's head which provided stimulation of the aerodynamic sense organ also known to elicit a flight response (Weis-Fogh 1949). Locust flight was generally associated with an initial high wing-stroke frequency, which over the course of a few minutes could decline (also noted in locusts flying on round-a-bouts; Weis-Fogh 1952). In such instances it was necessary to re-perch the insect and reinitiate the tarsal reflex. This took <1 s as the perch was positioned within close proximity of the locust. Immediately following the experiment each locust was weighed to 0.1 mg on an analytical balance (AE163, Mettler, Greifensee, Switzerland). No insects were reused.

3.5. Respirometry during flight with weight attachments

In an attempt to increase maximum oxygen consumption rate from the exercising flight muscles, a second cohort of adult male locusts (N=15 individuals) were exercised exactly as previously described but with a steel plate attached with putty (Bostik, Regency Park, SA, Australia) to the mid-proximal part of each of the four wings (Fig. 1B). It was important that the weight was not positioned too distally as this inhibited normal wing-stroke. The combined mass of the four steel plates (including putty mass) ranged between 30-45% of body mass for all locusts. Maximum oxygen consumption rates from individuals with weights attached to their wings (MMR_{weight}) were calculated exactly as described for individuals without weights.

3.6. Lift and wing-stroke frequency

Lift and wing-stroke frequency during flight were measured in a third cohort of adult male locusts (N=15 individuals). Individuals performed flight exercise while tethered to a vertical force-displacement transducer (FT03, Grass Instrument Co., Quincy, MA, USA) coupled to a polygraph (79D, Grass Instrument Co., USA) with analog output recorded every 0.001 s to a computer with a PowerLab data acquisition system and LabChart software.

Experiments were conducted in a temperature cabinet set to 35 ± 2°C, consistent with flight respirometry. Warm depilatory wax was used to attach a metal rod that descended from the vertical force-displacement transducer to the pronotum of the insect. Once again, attention was paid to ensure the wax was not excessively hot upon application. Locusts were tethered so the body was ~10° to the horizontal, head-up, consistent with locusts in free-flying

swarms (Baker et al., 1981). A 4 × 4 cm variable speed fan (XC5054, Sirocco, Taipei, Taiwan) was positioned 3 cm in front of the locust to replicate the flow of air that would occur during free-forward flight (Cloupeau et al., 1979). With the use of a calibrated hot wire anemometer (AM-4204HA, Lutron Electronic Enterprise Co., Taipei, Taiwan), the velocity of air flowing over the locust was maintained at 4-5 m s^{-1}, similar to the forward velocity of locusts in free-flight (Baker et al., 1981).

Immediately after each locust was tethered to the vertical force-displacement transducer, it was provided with a metal perch and given a few minutes to settle. The perch was then removed very slowly from beneath the locust so as to prevent flight by tarsal reflex. With the locust suspended in still air, but not making any wing movements, the baseline vertical force voltage of the locust's body mass was zeroed using the polygraph, and then this was recorded for 60 s. A precision calibration weight (2.5 g) was then carefully attached to the tether above the locust and another 60 s baseline vertical force voltage was recorded. The vertical force voltage produced by the 2.5 g calibration weight was used to calculate a gram-voltage equivalent, and so it was imperative that no wing movements occurred during these initial baseline measurements. The calibration weight was then carefully removed from the tether (vertical force voltage went back to zero) and then flight was initiated by engaging the variable speed fan and when necessary, inducing the tarsal reflex. The vertical force voltage produced during tethered-flight was recorded over a 5 min exercise bout, consistent with the duration of flight respirometry. Immediately following flight exercise, locusts were weighed to 0.1 mg on the analytical balance. No insects were reused.

The vertical force voltage produced during flight was plotted for the entire 5 min of exercise, and then a 30 s period in which the force voltages were greatest was extracted for analysis, consistent with flight MMR calculation. From the 30 s of extracted data, lift was calculated for each locust as:

$$L = V_1 \cdot M_w / V_2 \quad (3)$$

where L is lift (g), V_1 is the vertical force voltage produced during flight averaged over the highest 30 s period (Volts), V_2 is the vertical force voltage produced by the calibration weight (Volts), and M_W is the mass of the precision calibration weight (2.5 g).

The percent of body mass supported by flight was calculated for each locust as:

$$P = (L/M_b) \cdot 100 \quad (4)$$

where P is the percent of locust body mass supported by flight (%), L is lift (g) calculated for each locust in Equation (3), and M_b is the body mass of the insect (g). Values of P>100%

represent ascending flight, P<100% represent descending flight, and P=100% represent level or horizontal flight.

The vertical force voltage recorded during flight exercise was cyclic due to wing flapping with downstrokes representing a peak in lift production (Robertson and Johnson 1993; Cloupeau et al., 1979). Wing-stroke frequency was calculated for each locust by averaging the number of complete wing-stroke cycles during three random 1 s periods within the 30 s period of maximum lift.

All mean values and allometric exponents include 95% confidence intervals (CI). Statistical significance between means was tested using paired and unpaired T-tests for equal or unequal variance, as appropriate. Allometric data were transformed into $\log_{10}$ base before statistical analysis using ordinary least squares regressions. ANCOVA comparisons of regressions (Zar 1998) and T-tests were carried out with GraphPad Prism 5 statistical software (GraphPad Software, La Jolla, CA, USA).



Fig. 1A. Tethered locust undertaking flight exercise.



Fig. 1B. Tethered locust with weights attached to each wing.

4. Results

4.1. Body mass

Adult males 2-3 weeks post-moult used for respirometry had a mean body mass of 1.010 ± 0.046 g, and adult males used for lift and wing-stroke frequency measurements had a statistically indistinguishable mean body mass of 0.983 ± 0.055 g (T-test, P=0.51).

4.2. Respirometry

During rest, locusts regularly exhibited cyclic gas exchange, which is indicative of inactivity (Chown et al., 2006). Mean mass-specific RMR was 28 ± 2 μmol O_2 g^{-1} h^{-1} (Fig. 2). During flight, oxygen consumption rates increased 35-fold, with mean mass-specific MMR reaching 1032 ± 69 μmol O_2 g^{-1} h^{-1}, which is significantly higher than resting levels (T-test, P<0.0001) (Fig. 2).

The maximum oxygen consumption rate of the flight muscles was calculated by subtracting RMR from MMR measurements. Mean mass-specific $MMR_{flight\ muscle}$ was 967 ± 76 μmol O_2 g^{-1} h^{-1}, which is statistically indistinguishable from MMR (T-test, P=0.25) (Fig. 2).

In an effort to elicit higher metabolic rates during flight a second cohort of locusts were flown with weights attached to their wings. Mean mass-specific MMR_{weight} in these locusts was 896 ± 101 μmol O_2 g^{-1} h^{-1}, which is approximately 15% lower than the mean MMR of unweighted individuals (T-test, P<0.05) (Fig. 2).

4.3. Allometry

When the flight MMR of locusts in the current study are combined with flight metabolic data from larger desert locusts *Schistocerca gregaria* (Krogh and Weis-Fogh 1951), it is possible to generate the allometric equation, $MR_{locust\ flight} = 1018 M_b^{0.77 \pm 0.18\ (95\%\ CI)}$ μmol O_2 h^{-1} (r^2=0.68, N=37) (Fig. 3). Flight metabolic rate from 56 other insect species published in the literature scales with body mass according to the equation, $MR_{other\ insect\ flight} = 2631 M_b^{0.85 \pm 0.07}$ μmol O_2 h^{-1} (r^2=0.87, N=96 measurements) (Fig. 3) (data from White et al., 2008). The slopes of the two allometric regressions are not significantly different (ANCOVA, $F_{1, 129}$=0.33; P=0.57), however their elevations are significantly different (ANCOVA, $F_{1, 130}$=201; P<0.0001), such that the metabolic cost of flight in other insects is approximately 2.6-fold higher compared to that of locusts.

4.4. Lift and wing-stroke frequency

Mean maximum lift was on average sufficient to support 90 ± 14% of locust body mass (Fig. 4). In free-flight, this would equate to a gradual descent. However, there was variability between individuals, with 8 of the 15 locusts recording lift that exceeded body mass, and in three locusts lift was sufficient to support only around one-half of body mass. If these three locusts are excluded, mean maximum lift was sufficient to support 100 ± 10% of body mass, which equates to level flight.

Corresponding mean wing-stroke frequency during flight averaged 23.9 ± 0.8 Hz, although one locust recorded a frequency of just 20 Hz (Fig. 4). Over the narrow range of wing-stroke frequencies recorded, there was no clear-cut relationship with lift, Lift = $-2.7 \cdot f +$ 154 % (r^2=0.02, N=15) (Fig. 5).

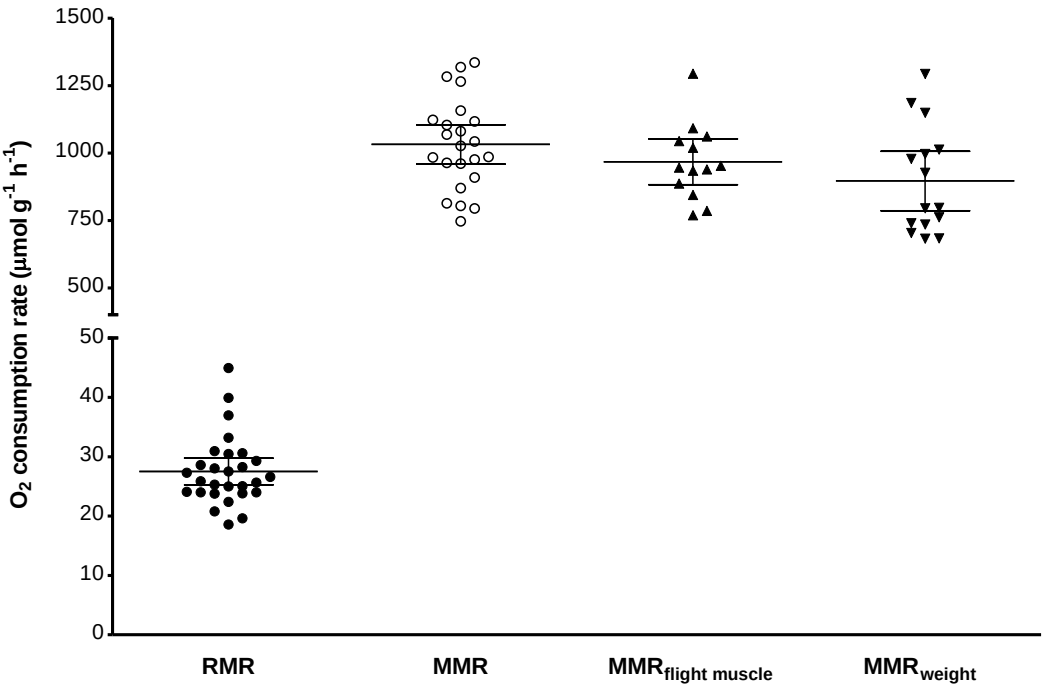


Fig. 2. Body mass-specific resting metabolic rate (RMR; N=28), maximum metabolic rate during flight (MMR; N=23), maximum metabolic rate of the flight muscles ($MMR_{flight\ muscle}$; N=13), and maximum metabolic rate during flight with weights attached to each wing (MMR_{weight}; N=15). Each data point represents the mean of an individual adult locust. The grand mean ± 95% CI is also presented.

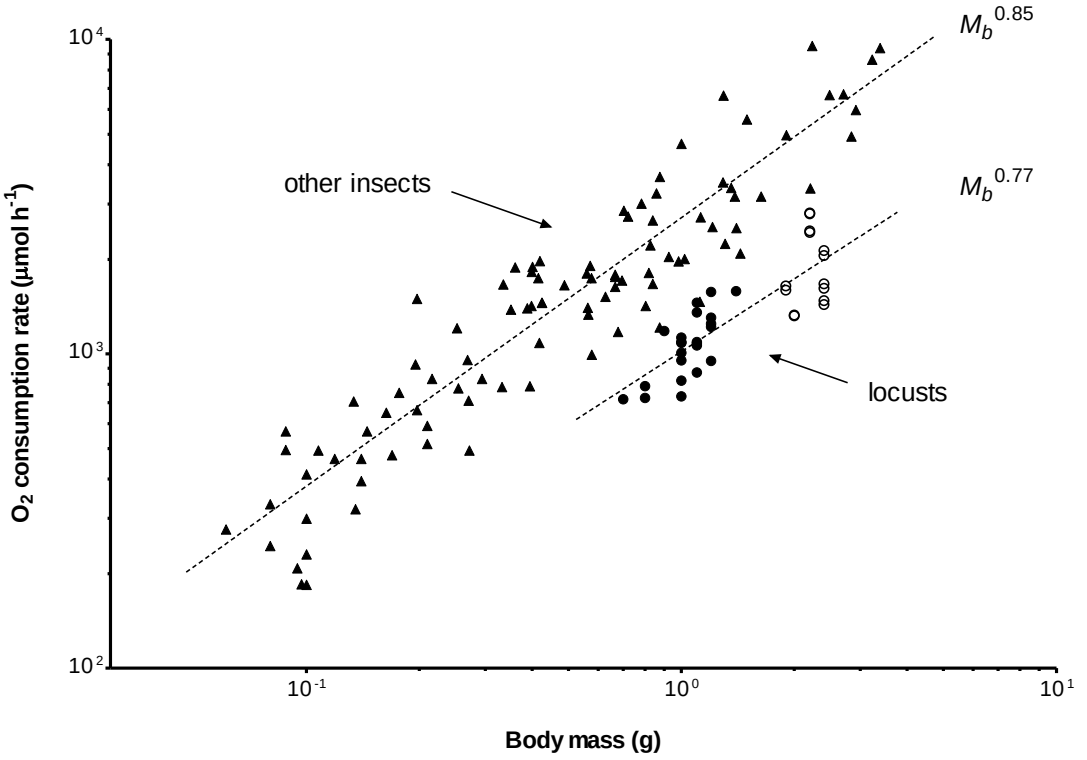


Fig. 3. Relationship between body mass (M_b) and oxygen consumption rate during tethered-flight in locusts from the current study (filled circles; N=23) and *Schistocerca gregaria* measured by Krogh and Weis-Fogh (1951) (unfilled circles; N=14). Also shown are flight oxygen consumption rates from 56 other insect species (filled triangles; N=96 measurements, comprised of 64 moths, 26 bees, three beetles, one cicada, one dragonfly, and one tachinid fly) (data from White et al., 2008).

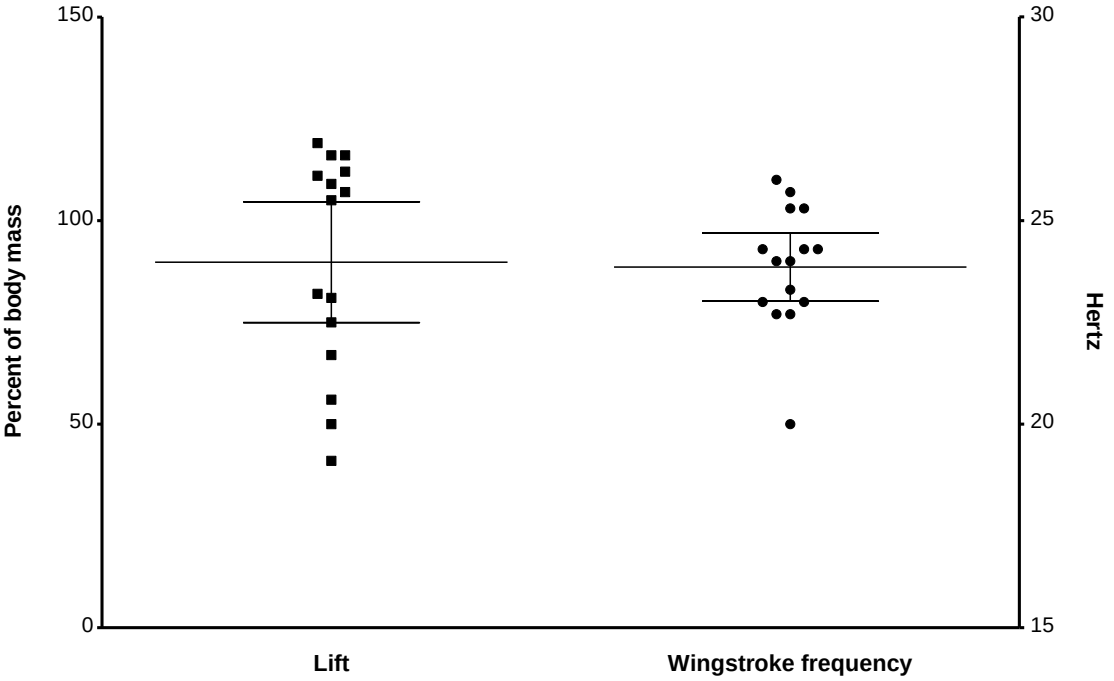


Fig. 4. Mean maximum lift expressed as a percent of body mass supported during tethered-flight (N=15). Also shown is the corresponding mean wing-stroke frequency (N=15). Each data point represents the mean of an individual adult locust. The grand mean ± 95% CI is also presented.

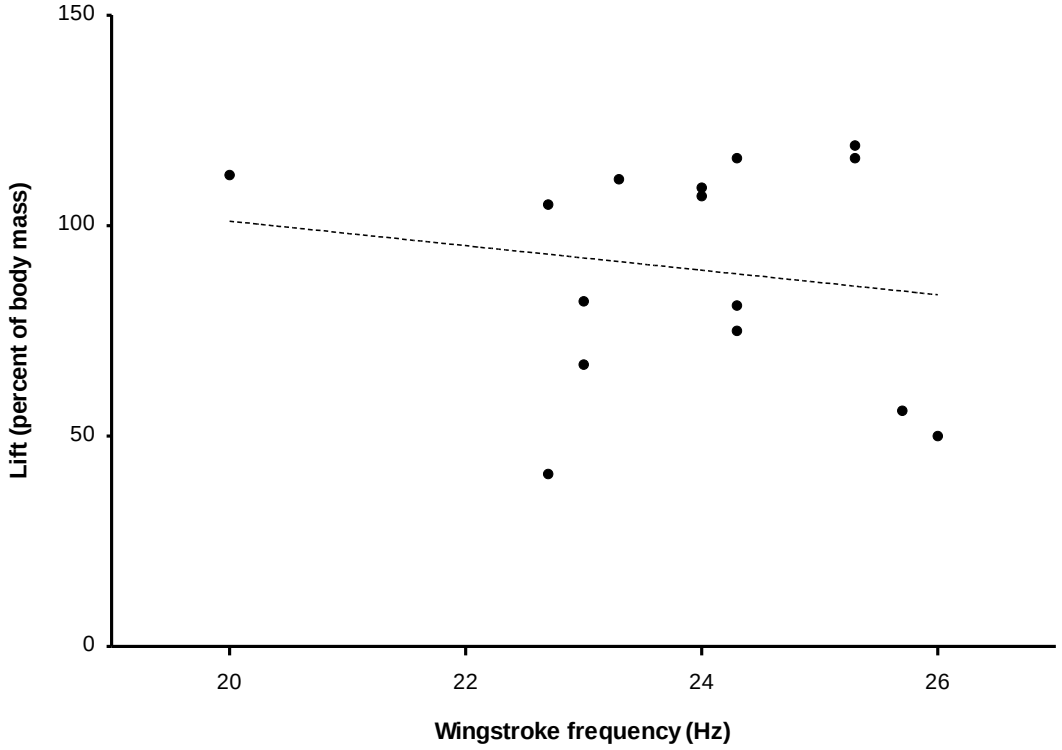


Fig. 5. Relationship between mean maximum lift and mean wing-stroke frequency during tethered-flight in adult locusts (N=15).

5. Discussion

5.1. Resting metabolic rate

The mean resting oxygen consumption rate of adult migratory locusts is approximately 28 μmol O_2 g^{-1} h^{-1} at 35°C (Fig. 2), which is consistent with data from adult desert locusts *Schistocerca gregaria* (1.69 g) where values around 25 μmol O_2 g^{-1} h^{-1} have been reported (Armstrong and Mordue 1985; corrected to 35°C assuming Q_{10} = 1.83, Harrison et al., 1991). Elsewhere in the literature there is variability; at the upper end American locusts *Schistocerca americana* (1.22 g) consume 39 μmol O_2 g^{-1} h^{-1} (Rascon and Harrison 2005; calculated from CO_2 production assuming RQ = 0.83, Hadley and Quinlan 1993) and resting two-striped grasshoppers *Melanoplus bivittatus* (1.65 g) consume 46 μmol O_2 g^{-1} h^{-1} (Harrison et al., 1991). At the lower end, the large and flightless eastern lubber grasshopper *Romalea guttata* (2.92 g) has a resting rate of around 16 μmol O_2 g^{-1} h^{-1} (Hadley and Quinlan 1993; corrected to 35°C assuming Q_{10} = 1.83). The large body mass and absence of flight muscles in *R. guttata* more than likely contribute to a low resting metabolic rate in this species.

5.2. Maximum metabolic rate

The mean maximum oxygen consumption rate of adult migratory locusts during tethered-flight is 1032 μmol O_2 g^{-1} h^{-1}, while the mean maximum oxygen uptake of the flight muscles is 967 μmol O_2 g^{-1} h^{-1} (Fig. 2). This means that when the flight muscles are working they contribute close to 95% of the locust's whole-body energy expenditure. These oxygen consumption rates align well with those of American locusts, which consume around 1150 μmol O_2 g^{-1} h^{-1} during tethered-flight (Rascon and Harrison 2005; calculated from CO_2 production assuming RQ = 0.83), and are also towards the upper estimated range of 450-1300 μmol O_2 g^{-1} h^{-1} determined for desert locusts (Armstrong and Mordue 1985; Weis-Fogh 1967; Weis-Fogh 1952; Krogh and Weis-Fogh 1951). However, compared to other insect groups, flight metabolic rates in locusts are relatively modest. On average, other insects expend 2.6-fold more energy during flight than locusts, after allometrically correcting for the effect of body mass (Fig. 3). The apparently low energetic cost of flight in locusts could either reflect a naturally low flight metabolic rate in these insects, or alternatively, it could arise if metabolic rates have been underestimated because of the need to tether locusts for flight respirometry. It is well established that tethering can lead to sub-maximal flight efforts because it interrupts sensory feedback loops, and also because there is no requirement for

insects to support their own body mass (Kutsch et al., 1999; Preiss and Gewecke 1991; Dudley and Ellington 1990; Zarnack and Wortmann 1989).

5.3. Attachment of weights

To address the potential problem that tethered locusts might be underperforming, a second cohort of insects were made to perform flight exercise with a small weight attached to each wing. This proved quite successful in that locusts appeared unperturbed by the weights and exhibited a flight effort that seemed consistent with that of unweighted individuals. It was therefore reasoned that the increased work required per wing-stroke might reveal untapped metabolic potential. Instead, weighted locusts have a slightly lower MMR than unweighted locusts (Fig. 2). The lack of a significant increase in MMR might occur if the wing muscles are already operating close to their aerobic limits, and so little potential exists to increase oxygen uptake beyond levels attained during unweighted flight. However, the fact that MMR is slightly lower in weighted locusts might also suggest that the extra effort required to move the 'heavy' wings was annulled by a decrease in wing-stroke frequency or amplitude, although data for this are unavailable. Either way, it seems likely that if the flight muscles were significantly underperforming during tethered-flight, then the weights should have induced at least some increase in maximum oxygen consumption rate.

5.4. Lift and wing-stroke frequency

Measurements of lift and wing-stroke frequency can also provide insight into whether insects are underperforming during tethered-flight. Mean maximum lift generated by locusts in the current study is on average sufficient to support 90% of body mass, which equates to a slow descending flight (Fig. 4). Other locust studies also report lift values below that required to maintain level flight (Gee and Robertson 1998; Robertson and Johnson 1993; Kutsch and Gewecke 1979; Gewecke 1975), and in some instances net lift is as low as 0-25% of body mass (Wolf 1993). However, a closer examination of mean lift data in the current study reveals significant variation between individuals (Fig. 4). In fact, if the three locusts with the lowest recorded lift values are excluded, the mean maximum lift of the 12 remaining individuals is 100%, which then supports the view that tethered locusts can generate enough lift to maintain level flight (Zarnack and Wortmann 1989; Armstrong and Mordue 1985; Cloupeau et al., 1979; Weis-Fogh 1964a).

The variability in mean maximum lift might suggest variability in the motivation of tethered locusts to undertake strenuous flight efforts, however, wing-stroke frequency data

suggests otherwise. The mean wing-stroke frequency of tethered locusts in the current study is 24 Hz (Fig. 4), which compares well with estimates around 22-26 Hz in tethered- and free-flying locusts (Kutsch et al., 1999; Robertson and Johnson 1993; Baker et al., 1981; Gewecke and Kutsch 1979; Goldsworthy and Coupland 1974). However, of particular interest is that over the narrow range of wing-stroke frequencies recorded, there is no clear-cut relationship with lift (Fig. 5). Other factors must be influencing lift production, such as wing-stroke amplitude, stroke plane angle, or the angle of attack (Kutsch et al., 1999; Baker 1979; Weis-Fogh 1964a; Jensen 1956; Weis-Fogh and Jensen 1956). Because these variables were not measured, it is difficult to speculate on their relative contribution to the variation in lift recorded from locusts in the current study.

The fact that seven out of the 15 locusts tested failed to generate enough lift to support entire body mass also raises the possibility that overall mean MMR during tethered-flight could have been underestimated by the inclusion of underperforming individuals. Because measurements of oxygen uptake were made on a separate cohort of locusts from those used for lift and wingstroke frequency measurements it is not possible to directly exclude individuals that failed to produce adequate lift from the respirometry data. However, if the finding that half of tethered locusts do not generate substantial lift is used as a representative guide, and the bottom-half of the respirometry data are thus excluded, the re-calculated mean mass-specific MMR increases from 1032 ± 69 μmol O_2 g^{-1} h^{-1} to 1160 ± 63 – a modest 12% increase. Potentially, many of the locusts that failed to generate substantial lift may have been working very hard during tethered-flight, and thus recorded a relatively high MMR, but a large fraction of the aerodynamic forces produced by the beating wings was translated as thrust, which was not measured. In addition, variation in the wings' angle of attack and stroke plane angle may have also influenced lift production without necessarily affecting the rate of oxygen uptake.

5.5. Low energy expenditure of locust flight

Several lines of evidence suggest that locusts in the present study were exerting themselves to the extent that near-maximum metabolic rates were attained during tethered-flight. Firstly, oxygen consumption rates are within the upper range of those recorded by other researchers. Secondly, the addition of weights failed to increase the energy cost of flight. Thirdly, the wing-stroke frequency of tethered locusts is comparable with free-flight. And lastly, although mean maximum lift was sufficient to support nine-tenths of body mass, the confidence interval overlaps with level flight, which is suggestive of a high work rate.

If the aerobic metabolic rates measured from flying locusts are representative of near-maximum values, as the evidence suggests, then locusts must consume less energy during flight compared to other insects. This might be linked to the low wing-loading and modest wing-stroke frequency of locusts (Harrison et al., 1996; Casey et al., 1985; Casey et al., 1981; Curtsinger and Laurie-Ahlberg 1981; May 1981; Bartholomew and Casey 1978; Casey 1976; Bartholomew and Heinrich 1973; Heinrich 1971). However, it is also reasonable to suspect that the energetics of insect flight, together with wing-loading and wing-stroke frequency, might also correlate with the size and efficiency of the insect flight motor. Interestingly, a recent morphometric analysis of the locust flight system indentifies two factors that probably contribute to the low flight metabolic rate of locusts. The first is that the flight muscle of locusts represents just 17% of body mass (Chapter Five), which compared to other insects is at the low end of a range that spans 17-56% (Marden 1987). The second is that the mitochondrial density of locust flight muscle is approximately 20% (Chapter Five), which is also relatively low compared to flight muscle in other insects where densities are around 40% have been reported (Suarez 1996; Smith 1963).

What is the biological significance behind the modest flight metabolic rate and relatively small flight motor of locusts? An obvious advantage of a relatively small flight motor is that it costs less to synthesise and maintain, which presumably allows more energy to be directed towards other requirements, such as reproduction and migration. The fact that many insect flight muscles are labile and adjust in size depending on short-term requirements for flight is indirect evidence of the significant energetic burden the flight motor represents (Robertson 1998; Dingle and Winchell 1997; Zera and Denno 1997). Of course, the disadvantage of a small flight motor is reduced flight performance. It is noteworthy that in order for insects to fly, the ratio between flight muscle mass and body mass cannot fall much below the 17% determined for locusts, and indeed, the ability to lift loads and to accelerate increases linearly from this minimum set-point (Marden 2000; Marden 1987). It is perhaps unsurprising then, that locusts do not always generate relative lift values significantly above that required to support entire body mass. However, a small flight motor seems to meet the needs of a locust. Although they are periodically required to remain airborne for extended periods, there is little requirement, or ability, for locusts to hover in still air, lift heavy loads (e.g. large prey items), compete in aerial mating challenges, initiate flight solely under the power of the flight muscles (locusts must jump forward into the air to initiate flight, Kirkton and Harrison 2006; Katz and Gosline 1993), or overcome low muscle temperatures (locust flight is restricted to air temperatures >24-25^{0}C, Neville and Weis-Fogh 1963) – all of which

require, to a variable extent, a relatively large flight muscle mass (Marden 2000). Thus, it would seem that the locust flight system functions with absolute minimum operational and maintenance costs, however, this comes with an evolutionary trade-off in the form of reduced aerial performance.

6. Acknowledgements

This research was supported by the Australian Research Council, project no. DP0879605.

Chapter Four: Symmorphosis and the insect respiratory system: allometric variation

Preamble

The following chapter forms the basis of a published co-authored manuscript* and is reproduced with permission from the *Journal of Experimental Biology*. Snelling fixed the tissue, collected and analysed the images, and wrote the manuscript. Seymour provided valuable input into the complete design of the study, Runciman provided assistance with tissue fixation methods, electron microscopy, and image analysis techniques, and Matthews and White contributed to the synthesis of ideas discussed in the paper. They each give permission** for the inclusion of the manuscript in the thesis.

*Snelling EP, Seymour RS, Runciman S, Matthews PGD, White CR (2011) Symmorphosis and the insect respiratory system: allometric variation. *Journal of Experimental Biology* **214**, 3225-3237.

**Signatures of co-authors:

Roger Seymour

Sue Runciman

Philip Matthews

Craig White

1. Abstract

Taylor and Weibel's theory of symmorphosis predicts that structures of the respiratory system are matched to maximum functional requirements with minimal excess capacity. We test this hypothesis in the respiratory system of the migratory locust *Locusta migratoria* by comparing the aerobic capacity of the jumping muscles with the morphology of the oxygen cascade in the hopping legs using an intra-specific allometric analysis of different body mass (M_b) at selected juvenile life stages. The maximum oxygen consumption rate of the hopping muscle during jumping exercise scales as $M_b^{1.02 \pm 0.02 \text{ (95\% CI)}}$, which parallels the scaling of mitochondrial volume in the hopping muscle, $M_b^{1.02 \pm 0.08}$, and the total surface area of mitochondrial inner membrane, $M_b^{0.99 \pm 0.10}$. Likewise, at the oxygen supply end of the insect respiratory system, there is congruence between aerobic capacity and the total volume of tracheoles in the hopping muscle, $M_b^{0.99 \pm 0.16}$, the total inner surface area of the tracheoles, $M_b^{0.99 \pm 0.16}$, the anatomical lateral diffusing capacity of the tracheoles, $M_b^{0.99 \pm 0.17}$, and the anatomical radial diffusing capacity of the tracheoles, $M_b^{0.99 \pm 0.18}$. Therefore, the principles of symmorphosis are upheld at each step of the oxygen cascade in the respiratory system of the migratory locust.

2. Introduction

In 1981, Taylor and Weibel together with their co-workers introduced the theory of symmorphosis. The principle was defined as the 'state of structural design commensurate to functional needs resulting from regulated morphogenesis, whereby the formation of structural elements is regulated to satisfy but not exceed the requirements of the functional system' (Taylor and Weibel 1981b). The assertion that each step in a biological system is quantitatively matched to the overall maximum functional task of the system is essentially an optimality theory, which was motivated by the belief that animals are built economically, because maintaining superfluous structure is energetically expensive (Weibel et al., 1981b).

In a seminal series of papers, Taylor and Weibel tested their theory on the respiratory system of mammals (Taylor and Weibel 1981a). First, the functional capacity of the respiratory system was determined by measuring maximum oxygen consumption rate (MMR) of mammals during exercise of progressive increasing intensity (Seeherman et al., 1981). Next, a number of structural variables crucial in the delivery and consumption of oxygen during exercise were morphometrically quantified (Gehr et al., 1981; Hoppeler et al., 1981a; Hoppeler et al., 1981b; Mathieu et al., 1981; Weibel et al., 1981a). The effect of body mass on the MMR of mammals and the amount of respiratory structure they possess was expressed as an allometric equation, $y = a \cdot M_b^{b}$, where y is the variable of interest, a is the coefficient, M_b is body mass, and b is the scaling exponent. Taylor and Weibel predicted that if their theory of symmorphosis holds for the mammalian respiratory system, then MMR should scale with an exponent (b) that is statistically indistinguishable from the exponents derived for each of the structural variables (Taylor and Weibel 1981b). They found that MMR scales with body mass with an exponent of b=0.80 (Taylor et al., 1981), and that this is congruent with the allometric scaling of mitochondrial volume in the diaphragm and locomotory muscles, b=0.80 to 0.82 (Mathieu et al., 1981). It was also established that total capillary length in selected muscles scales roughly parallel with MMR, b=0.86 to 0.91, but due to scatter in the data it was not possible to determine whether the slopes were statistically similar (Hoppeler et al., 1981b; Weibel et al., 1981b). Interestingly, the study also found that the diffusing capacity of the lung scales with an exponent, b=0.99, that is significantly steeper than MMR, which means that larger mammals appear to possess excess lung structure (Gehr et al., 1981). It was suggested that large mammals may have a lower alveolar pressure head for diffusion and therefore require a greater pulmonary diffusing capacity to transfer oxygen from the lungs to the blood at the same rate as smaller mammals (Gehr et al., 1981). In contrast, the pulmonary anatomical diffusing capacity of birds appears to be symmorphotic, both phylogenetically and

ontogenetically (Canals et al., 2011; Seymour et al., 2008; Runciman et al., 2005; Seymour et al., 2004).

Since its conception, symmorphosis has received the support of a number of workers who view the optimal design idea as a useful null hypothesis of biological design on which to base analytical studies (Suarez 1996; Diamond 1992). Where these simple economy-based expectations breakdown, an opportunity arises to analyse the reasons for such a breakdown (Diamond 1992). However, symmorphosis has also evoked criticism, especially from evolutionary biologists, who argue that natural selection leads to adequate or sufficient design but not optimal or symmorphotic design (Garland 1998; Dudley and Gans 1991; Garland and Huey 1987; Smith 1978). They argue that symmorphosis is not an inevitable outcome because environmental unpredictability means that evolutionary selective forces vary too much in space and time to produce a structure that is functionally optimal (Dudley and Gans 1991). It is suggested that symmorphotic-like matching between structure and function may only ever be realised when the selective forces influencing design have either been static for a long time (Dudley and Gans 1991) or when selective pressures have been directed towards extreme performance (Jones and Lindstedt 1993). Criticism of symmorphosis is supported by a number of instances in which animals appear to be in possession of unnecessary structure. Not only does the mammalian lung appear to have an excess capacity (Canals et al., 2010; Hsia et al., 1992; Karas et al., 1987a; Gehr et al., 1981), but excess structure may also exist at oxygen delivery steps further downstream. For example, MMR in athletic humans, racehorses, and mice, increases under hyperoxic conditions (Gebczynski and Konarzewski 2011; Jones and Lindstedt 1993; Powers et al., 1989), which suggest that in some animals the mitochondria have an aerobic reserve that is never fully exploited.

Whether there are physiological or adaptive explanations for instances where symmorphosis must be rejected is open to debate, but first it is worth considering two other factors important in animal design. Firstly, it is likely that many physiological systems have a built-in safety margin, analogous to the safety margin engineers build in to bridges, buildings, and elevators. If a structure has no safety margin, then it is at risk of breakage when its performance approaches maximum. For example, the cardiovascular system of racehorses has been artificially selected for high oxygen flux to the extent that the safety margin for pulmonary blood pressure has been significantly compromised, and when physically exerted, some horses experience pulmonary bleeding (Pascoe et al., 1981). The second point worth considering is that some structures in the body are multifunctional and this can complicate the interpretation of results. For example, the design of the cardiovascular system could be

geared towards oxygen delivery, or it could reflect some other physiological requirement, such as substrate delivery, lactate removal, carbon dioxide removal, pH regulation or heat dispersal (Dudley and Gans 1991; Garland and Huey 1987). It is also reasoned that optimal matching between structural elements in a system becomes increasingly unlikely as the number of elements increases, along with the number of functions performed by each element (Dudley and Gans 1991). Clearly, some systems offer a more suitable model on which to test for symmorphotic design. The insect respiratory system appears to be a case in point.

In insects, oxygen delivery occurs along a series of steps (Hartung et al., 2004; Schmitz and Perry 1999). First, atmospheric oxygen enters the air-filled tubes of the insect's tracheal system through small pores located along its lateral margins, called spiracles. It then moves in the gas-phase through a branching system of successively smaller tracheae, before arriving at the terminal tracheoles. Here, it exits the tracheal system and diffuses across the tracheal cuticle and epidermal layers (Fig. 1), before diffusing into tissue where it is used by mitochondria to oxidise substrate to produce ATP for work. Carbon dioxide produced by the respiring cells does not take the exact same path as oxygen in reverse. Due to its greater solubility in tissue and haemolymph, some carbon dioxide may be temporarily retained in the tissue before diffusing into tracheae or passing directly through the integument (Bridges and Scheid 1982). In some stick insects for example, up to 25% of carbon dioxide is expelled directly across the exoskeleton (Wigglesworth 1965). As such, a system capable of bringing an adequate supply of oxygen to the tissues should also suffice to remove carbon dioxide (Schmitz and Perry 1999; Chapman 1998).

The primary function of the insect tracheal system, therefore, is to deliver oxygen to the mitochondria, which makes it an ideal model on which to test for symmorphosis. However, there are other characteristics that make it appealing. Oxygen flux through the insect respiratory system is higher than in any other animal group (Suarez 2000; Sacktor 1976), and so the selective pressure for optimal design has likely been strong (Jones and Lindstedt 1993). The high metabolic scope of insects also means that the oxygen requirement of the exercising muscle greatly exceeds metabolism in the remaining tissues, and this makes the work due to exercise easier to quantify (Weis-Fogh 1952). Furthermore, insect locomotory muscles are often easy to identify and therefore analyse without including non-locomotory tissues. For example, hopping in locusts is performed by just two muscles contained within each metathoracic femur. It is also noteworthy that although there is significant lactate produced in the initial stages of hopping, after 2 min of exercise ATP is thought to be synthesised almost entirely aerobically (Kirkton et al., 2005; Harrison et al.,

1991). Lastly, for the purpose of an allometric study of symmorphosis, the fact that locust body mass increases more than 30-fold from first to fifth instar is also a key advantage.

The aim of this study is to test whether the respiratory system of the migratory locust *Locusta migratoria* is designed according to the economical principles of symmorphosis. To achieve this, allometric variation in the structural properties of the locust respiratory system in the hopping femurs is quantified and compared to the maximum functional rate that oxygen flows through the system during intense hopping exercise in first, third and fifth instar juveniles. Earlier respirometry showed the aerobic capacity of hopping muscle scales throughout juvenile locust development according to the allometric equation, $MMR_{\text{juvenile hop muscle}} = 103 M_b^{1.02 \pm 0.02 \text{ (95\% CI)}}$ μmol O_2 h^{-1} at 35°C (r^2=0.98, N=145) (Chapter Two). If the theory of symmorphosis holds for the insect respiratory system, then similar scaling exponents should also exist for mitochondrial volume, mitochondrial inner membrane surface area, tracheal volume, tracheal surface area, and tracheal diffusing capacity in the juvenile locust hopping muscle.

3. Methods

3.1. Animals

Gregarious-phase locusts *Locusta migratoria* were reared at 33 ± 1°C, under a 12:12 h light-dark cycle, with *ad libitum* access to seedling wheatgrass and wheat germ, as previously described (Chapter Two). The developmental stage of each locust was determined based on instar-specific differences in wing morphology. Newly moulted individuals were transferred into separate plastic terraria with other locusts of the same age. Morphometric quantification of the metathoracic femur (hopping leg femur) was conducted on locusts in their first, third, and fifth instar life stages. Three insects were used from each life stage (N=9 individuals). Insects were measured three to four days post-moult to provide sufficient time for the exoskeleton to stiffen while minimising compression of the tracheal system due to growth (Greenlee and Harrison 2004b; Queathem 1991). Locusts were fasted 6-10 h prior to tissue fixation consistent with earlier respirometry experiments (Chapter Two).

3.2. Specimen preparation

The procedure used to dissect and fix locust tissue was modified based on the methods of previous electron microscopy studies of insects and spiders (Biserova and Pfluger 2004; Hartung et al., 2004; Kohnert et al., 2004; Schmitz and Perry 2002a; Schmitz and Perry 2002b). The large extensor tibialis muscle and the smaller flexor tibialis muscle, which are

used during hopping locomotion, constitute the entire muscle mass of the metathoracic femur (Gabriel 1985b; Gabriel 1985a; Bennet-Clark 1975), and were identified from published illustrations (Albrecht 1953; Snodgrass 1929).

To begin, locusts were cold anaesthetised for 20 min in a refrigerator at 4°C. They were then weighed to 0.1 mg on an analytical balance (AE163, Mettler, Greifensee, Switzerland). Both metathoracic femurs on each locust were then carefully removed with angled spring scissors. Each femur was weighed to 0.1 mg before being sliced along the transverse plane into equal length pieces using a razor. Femurs from first instar locusts were sliced into three pieces, third instar femurs were sliced into six pieces, and fifth instar femurs were sliced into 12 pieces. Each piece of femur tissue was sequentially numbered proximally to distally and labelled left or right. The pieces were immediately immersed into a chemical fixative solution of 2.5% glutaraldehyde and 2% formaldehyde in 0.2 M phosphate buffer with pH 7.4, and left overnight in a refrigerator at 4°C. On the second day, each piece was given a series of buffer rinses; the first rinse was 20 min followed by four, 60-min rinses. Then there were three, 20-min distilled water rinses and then the tissue was placed into a 1% aqueous solution of osmium tetroxide for secondary fixation and left overnight at room temperature. On the third day, each piece was given five, 20-min rinses in distilled water and then placed into a 2% aqueous solution of uranyl acetate and left overnight at room temperature. On the fourth day, the pieces were given four, 20-min rinses in distilled water and then dehydrated in ethyl alcohol in 10% incremental steps starting from 50% to 80%, each for 20 min. The tissue was then further dehydrated in consecutive, 20-min immersion in 90% ethanol (×2), 100% ethanol (×2), and finally pure propylene oxide (×2). Following dehydration, the samples were incrementally infiltrated with embedding resin (Durcupan, Fluka, Buchs, Switzerland) at ratios of 3:1, 2:2, 1:3 (propylene oxide : resin) each for a duration of 60 min, and then left overnight at room temperature in pure resin. On the fifth day, each piece was aligned longitudinally and in a proximal to distal orientation in individually labelled embedding moulds where they were covered with pure embedding resin and left to polymerise in a 70°C oven for 48 h.

3.3. Light microscopy

One metathoracic femur from each locust was randomly selected for light microscopy analysis. From each femur, 12 parallel, transverse and equidistant 1-µm thick sections were cut proximally to distally along the leg using 8 mm glass knives and an ultramicrotome (EM UC6, Leica Microsystems, Wetzlar, Germany). The sections were placed onto glass slides,

stained with toluidine blue, rinsed with distilled water, and air-dried. Each section was viewed between ×4 and ×20 magnification under an optical microscope (BX51, Olympus, Hamburg, Germany), photographed with a mounted digital colour camera (ColorView III, Soft Imaging System, Olympus, Germany), which generated 24-bit 2576 × 1932 pixel resolution images. Each section image was imported into a computer graphics program (CorelDRAW 11, Corel Corp., Ottawa, ON, Canada) where a point grid test system was superimposed randomly over the image which allowed transverse area and volume estimates using the following stereological equations (Howard and Reed 1998; Mayhew 1991; Cruz-Orive and Weibel 1990).

3.3.1. Femur transverse area

The number of points that fell over the femur was counted and the transverse area (T; μm^2) was estimated for each section along the leg using:

$$T = P \cdot (a/p) \quad (1)$$

where P is the number of points falling over the femur per transverse section, and a/p is the area (μm^2) associated with each point in the grid. A mean transverse area was calculated for each section along the leg for each of the three life stages. A mean transverse area distribution curve was then generated proximally to distally along the femur for each life stage.

3.3.2. Femur volume

The number of points falling on muscle tissue, connective tissue, exoskeleton, class IV tracheae and air sacs (tracheae with a diameter >20 µm), tendon, nerve, and haemolymph were also counted. The total volume (V; μm^3) of each structure was then estimated for both metathoracic femurs in each locust according to the Cavalieri principle:

$$V = D \cdot P \cdot (a/p) \cdot 2 \quad (2)$$

where D is the distance (µm) between sections, P is the total number of points falling on the structure summed from all 12 section images in each locust, a/p is the area (μm^2) associated with each point in the grid, and 2 provides a volume estimate for both metathoracic femurs per locust.

3.4 Electron microscopy

While one metathoracic femur was randomly selected for light microscopy and Cavalieri volume calculation, the remaining femur was used for transmission electron microscopy analysis. The sampling scheme used for electron microscopy randomised section position and

angle to produce vertical uniform random sections (Howard and Reed 1998; Mayhew 1991). Six equidistant 70-nm sections were cut proximally to distally along the leg using a diamond knife (Diatome, Biel, Switzerland) and ultramicrotome. For the first locust of each life stage, the first section was cut at a random angle between 0° and 18° relative to the vertical plane. For the second locust, the first section was cut at a random angle between 36° and 54°, and for the third locust, the first section was cut at a random angle between 72° and 90°. For the remaining five sections in each locust, 18° was added to the cutting angle with every successive section. This meant that for each locust femur, the full range of angles around the vertical plane was randomly sampled.

Sections were placed onto 3 mm copper mesh grids, stained with lead citrate, and viewed with a transmission electron microscope (CM 100, Philips, Eindhoven, The Netherlands) where random 8-bit 1280 × 1024 pixel resolution images were captured with a mounted digital camera (MegaView II, Soft Imaging System, Olympus, Germany) at appropriate magnifications (Table 1). To obtain unbiased sampling of the femur, it was necessary to weight the number of random images taken from different sections along the leg because the femur tapers significantly as it approaches the tibial joint. The mean transverse area distribution curve generated in Equation (1) for each life stage was used to determine the extent that sampling should be weighted towards the larger proximal regions of the leg. Accordingly, the number of random images taken from each section along the femur was adjusted as a fraction of the total number of images taken per femur, while the total number of images taken per femur was kept approximately the same for all locusts (Table 1). All images were exported to CorelDRAW for analyses, where a test system was randomly superimposed over the image which allowed estimates to be made of volume density, surface area density, and thickness using the following stereological equations (Howard and Reed 1998; Mayhew 1991; Cruz-Orive and Weibel 1990) appropriate for vertical sections (Baddeley et al., 1986). The average time to process each locust from initial fixation to the final quantification of femur ultrastructure was ~6 weeks. This significant investment in time restricted the study to 9 individuals from 3 developmental stages.

Table 1. Number (and magnification) of random electron micrographs taken along the length of the femur per locust.

	Low magnification femur tissue images	High magnification muscle cell images	Mitochondria images	Trachea images
First instars (*N=3*)	40 (×1950)	40 (×7900)	23 (×64000)	40 (×620-64000)
Third instars (*N=3*)	41 (×1950)	41 (×7900)	22 (×64000)	41 (×620-64000)
Fifth instars (*N=3*)	44 (×1100)	44 (×4600)	22 (×64000)	44 (×620-64000)

3.4.1. Volume calculations

Low magnification images of random femur tissue (Table 1) were analysed with a point grid test system that was randomly superimposed over the image. The total number of points falling on muscle, muscle nuclei, extracellular haemolymph, secretory cells, nerve, tendon, lipid droplets, unidentified cells, and tracheae were counted. Whether points fell on tracheal lumen, cuticle, epidermis or nuclei was noted, and whether tracheae were intracellular or extracellular was also recorded. Tracheae were categorised into four size classes based on their inner diameter: class I tracheae had an inner diameter of 0-2 μm (hereafter referred to as tracheoles; Thesis Appendix), class II were 2-5 μm, class III were 5-20 μm, and class IV tracheae and air sacs were those with an inner diameter >20 μm (consistent with Hartung et al., 2004). The total volume of each structure ($V_{structure}$; μm^3) (except class IV tracheae which was calculated in Equation (2)) within both metathoracic femurs of each locust was calculated as:

$$V_{structure} = Vv_{structure} \cdot V_{muscle\ tissue} \quad (3)$$

where $Vv_{structure}$ is the fraction of muscle tissue occupied by the structure determined from point grid counts, and $V_{muscle\ tissue}$ is the muscle tissue volume (μm^3) of both metathoracic femurs in each locust calculated in Equation (2).

High magnification images of random muscle cells (Table 1) were then analysed. A point grid test system was randomly superimposed over the muscle cell image and the number of points falling on mitochondria organelles, myofibril+sarcoplasmic reticulum organelles, and cytosol was counted. Their respective volumes ($V_{organelle}$; μm^3) within both metathoracic femurs of each locust were calculated as:

$$V_{organelle} = Vv_{organelle} \cdot V_{muscle} \quad (4)$$

where $Vv_{organelle}$ is the fraction of muscle cell occupied by the organelle or cytosol in each locust determined from point grid counts, and V_{muscle} is the muscle volume (μm^3) of both metathoracic femurs in each locust calculated in Equation (3).

3.4.2. Mitochondrial inner membrane surface area

Mitochondria images (Table 1) were analysed with a cycloid arc test system that was randomly translated onto the image with the minor axis of the cycloid arc parallel with the vertical direction of the image (Baddeley et al., 1986). The surface area-to-volume ratio of the inner mitochondrial membrane (Sv_{inner}; μm^{-1}) for each mitochondrion in each locust was calculated as:

$$(5) \qquad Sv_{inner} = 2 \cdot I/L$$

where I is the number of intersections of the test lines with the inner mitochondrial membrane surface, L is the total length (μm) of test lines falling over the mitochondrion, and 2 is the coefficient used to transform intersection points to a surface area estimate.

The total surface area of inner mitochondrial membrane (S_{inner}; μm^2) within both femurs of each locust was calculated as:

$$(6) \qquad S_{inner} = Sv_{inner} \cdot V_{mito}$$

where Sv_{inner} is the mean surface area-to-volume ratio (μm^{-1}) of inner membrane in the mitochondria of each locust calculated in Equation (5), and V_{mito} is the volume (μm^3) of mitochondria in both femurs of each locust calculated in Equation (4).

3.4.3. Tracheal surface areas

Trachea images (Table 1) were analysed with a cycloid arc test system that was randomly translated onto the image with the minor axis of the cycloid arc parallel with the vertical direction of the image (Baddeley et al., 1986). The ratio of tracheal inner cuticle surface area-to-lumen volume (Sv_{cut}; μm^{-1}), and tracheal outer epidermal surface area-to-lumen+cuticle+epidermis volume (Sv_{epi}; μm^{-1}) (Fig. 1) for each trachea in each locust was calculated as:

$$(7) \qquad Sv_{cut} = 2 \cdot I_{cut}/L_{lum}$$

$$(8) \qquad Sv_{epi} = 2 \cdot I_{epi}/L_{lum+cut+epi}$$

where I_{cut} and I_{epi} is the number of intersections of the test lines with the inner cuticle surface and outer epidermal surface, respectively, L_{lum} and $L_{lum+cut+epi}$ is the total length (μm) of test lines falling over the tracheal lumen and tracheal lumen+cuticle+epidermis, respectively, and 2 is the coefficient used to transform intersection points to a surface area estimate.

The total surface area of the inner cuticle layer (S_{cut}; μm^2) and outer epidermal layer (S_{epi}; μm^2) for each trachea size class (I, II, III, IV) within both femurs of each locust was calculated as:

(9) $S_{cut} = Sv_{cut} \cdot V_{trach\ lum}$

(10) $S_{epi} = Sv_{epi} \cdot V_{trach\ lum+cut+epi}$

where Sv_{cut} and Sv_{epi} is the mean tracheal inner cuticle surface area-to-lumen volume ratio (μm^{-1}), and mean tracheal outer epidermal surface area-to-lumen+cuticle+epidermis volume ratio (μm^{-1}), respectively, which was calculated for each trachea size class for each locust in Equations (7) and (8), respectively. $V_{trach\ lum}$ and $V_{trach\ lum+cut+epi}$ is the lumen volume (μm^3) and the lumen+cuticle+epidermis volume (μm^3) in both femurs of each locust, respectively, both of which were calculated in Equation (3) for class I, II, III tracheae, and in Equation (2) for class IV tracheae.

3.4.4. Tracheal thickness measurements

Trachea images (Table 1) were reanalysed, this time to determine the thickness of both the cuticular and epidermal layers (Fig. 1). Four random intersections made by the superimposed cycloid arc test system with the inner cuticular layer were used as the starting point of the measurement, from which the thickness of the inner cuticle and the outer epidermal layers were measured in a random direction (consistent with Hartung et al., 2004; Schmitz and Perry 2001). The harmonic mean barrier thickness of the cuticular (τ_{cut}; μm) and epidermal (τ_{epi}; μm) layers for each trachea size class (I, II, III, IV) in each locust was calculated as:

(11) $\tau = (N / \sum_{i=1}^{N} \frac{1}{L_i}) \cdot 2/3$

where N is the number of measurements, L_i are the individual measured lengths (μm), and 2/3 compensates for an overestimation due to the random orientation of measured intercepts (Weibel and Knight 1964).

3.4.5. Lateral diffusing capacity

The lateral diffusing capacity for oxygen (i.e. lateral conductance) was determined separately for the cuticle layer ($GL_{cut,\ class\ X}$; μmol O_2 kPa^{-1} h^{-1}) and epidermal layer ($GL_{epi,\ class\ X}$; μmol O_2 kPa^{-1} h^{-1}) (Fig. 1) of each trachea size class (I, II, III, IV) for both femurs of each locust. It was calculated as:

(12) $GL_{cut,\ class\ X} = S_{cut,\ class\ X} / \tau_{cut,\ class\ X} \cdot K_{cut}$

(13) $GL_{epi,\ class\ X} = S_{cut,\ class\ X} / \tau_{epi,\ class\ X} \cdot K_{epi}$

where $S_{cut,\ class\ X}$ is the tracheal inner cuticle surface area (μm^2) for each trachea size class for both femurs of each locust calculated in Equation (9), $\tau_{cut,\ class\ X}$ and $\tau_{epi,\ class\ X}$ is the harmonic mean barrier thickness (μm) of the cuticle and epidermal layers, respectively, for each trachea

size class in each locust calculated in Equation (11), and K_{cut} and K_{epi} are the Krogh diffusion coefficients for chitin (3.95×10^{-9} μmol O_2 kPa^{-1} h^{-1} μm^{-1}) and rat lung tissue (6.31×10^{-8} μmol O_2 kPa^{-1} h^{-1} μm^{-1}), respectively, corrected to 35°C using Q_{10} = 1.1 (Bartels 1971), consistent with the temperature of respirometry experiments (Chapter Two). Inner cuticle surface area was used in Equation (13) rather than outer epidermal surface area because the maximum lateral flow of oxygen across the tracheal wall will be limited by the smaller of the two surfaces, which in this case is the inner cuticle layer of the trachea (except for large class IV tracheae).

The lateral diffusing capacity ($GL_{class\ X\ trach}$; μmol O_2 kPa^{-1} h^{-1}) of each trachea size class (I, II, III, IV) within both femurs of each locust was calculated as:

(14) $$GL_{class\ X\ trach} = 1/\left(1/GL_{cut,\ class\ X} + 1/GL_{epi,\ class\ X}\right)$$

where $GL_{cut,\ class\ X}$ and $GL_{epi,\ class\ X}$ are the lateral diffusing capacities (μmol O_2 kPa^{-1} h^{-1}) of the cuticular and epidermal layers, respectively, calculated for each trachea size class in each locust in Equations (12) and (13), respectively. This is appropriate for determining overall conductance in series (Weibel 1970).

The lateral diffusing capacity of the entire tracheal system ($GL_{trach\ sys}$; μmol O_2 kPa^{-1} h^{-1}) within both femurs of each locust was calculated as:

(15) $$GL_{trach\ sys} = GL_{class\ I\ trach} + GL_{class\ II\ trach} + GL_{class\ III\ trach} + GL_{class\ IV\ trach}$$

where $GL_{class\ I,\ II,\ III,\ IV\ trach}$ are the lateral diffusing capacities (μmol O_2 kPa^{-1} h^{-1}) of each trachea size class within both femurs of each locust calculated in Equation (14).

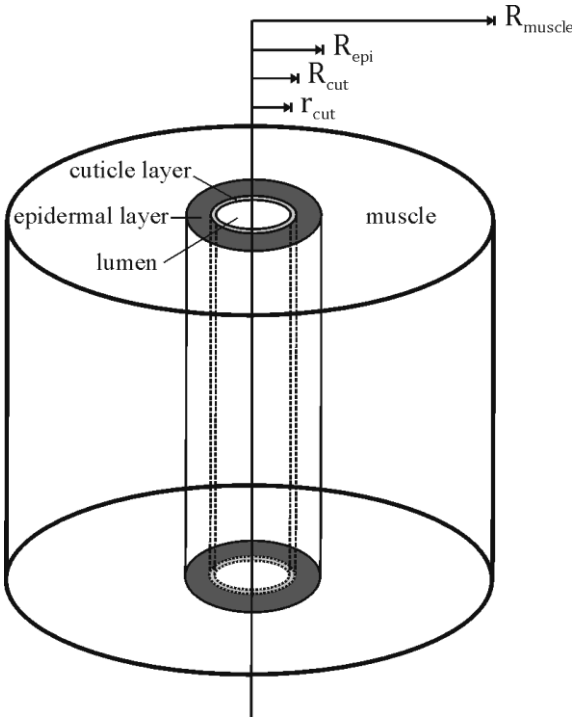


Fig. 1. Krogh's cylinder model for radial diffusion was originally devised for the diffusion of oxygen out of a vertebrate capillary and into the surrounding muscle. Here we have adapted this and applied it to an insect tracheole. r_{cut} is the mean radius (μm) of the tracheole to the inner surface of the cuticle layer, R_{cut} is the mean radius (μm) of the tracheole to the outer surface of the cuticle layer, R_{epi} is the mean radius (μm) of the tracheole to the outer surface of the epidermal layer, and R_{muscle} is the radius (μm) of the mean transverse area of muscle serviced by each tracheole (after Kreuzer 1982). Not to scale.

3.4.6. Radial diffusing capacity

The radial diffusing capacity for oxygen (i.e. radial conductance) out of the class I tracheae (tracheoles) and into the surrounding muscle was calculated for each locust according to Krogh's cylinder model for radial diffusion (Kreuzer 1982; Krogh 1919). Krogh's cylinder (Fig. 1) was adapted only for tracheoles because they are the most relevant in the supply of oxygen to the tissues (see Results).

Images of tracheoles were reanalysed and the inner cuticular radius (r_{cut}; μm) was measured and averaged for each locust. According to Krogh's model, the tracheoles and the surrounding muscle they service are cylindrical in shape. Therefore, the mean radius (μm) to the outer surface of the cuticle layer (R_{cut}), epidermal layer (R_{epi}), and serviced muscle (R_{muscle}), can be calculated for each locust according to:

(16) $$R_{cut} = r_{cut} + \tau_{cut}$$

(17) $$R_{epi} = R_{cut} + \tau_{epi}$$

(18) $$R_{muscle} = \sqrt{r_{cut}^{2} \cdot (T_{muscle} / T_{lum})}$$

where τ_{cut} and τ_{epi} is the harmonic mean barrier thickness (μm) of the cuticular and epidermal layers of the tracheoles, respectively, calculated for each locust in Equation (11), and T_{muscle}/T_{lum} is the ratio between the mean transverse area of muscle that surrounds each tracheole and the mean transverse area of the tracheole lumen. This is equal to the ratio between the volume of muscle and the volume of tracheole lumen which were quantified for each locust in Equation (3).

The radial diffusing capacity (μmol O_2 kPa^{-1} h^{-1}) of the inner cuticle layer of the tracheoles ($GR_{cut,\ class\ I}$), the outer epidermal layer of the tracheoles ($GR_{epi,\ class\ I}$), and the muscle that surrounds the tracheoles ($GR_{muscle,\ class\ I}$), within both femurs for each locust was calculated according to Krogh's cylinder model for radial diffusion (adapted from Kreuzer 1982):

$$(19)\quad GR_{cut,\ class\ I} = K_{cut} \Big/ \left[\frac{R_{cut}^{\ 2}}{2} \ln \frac{R_{cut}}{r_{cut}} - \frac{R_{cut}^{\ 2} - r_{cut}^{\ 2}}{4}\right] \cdot V_{cut}$$

$$(20)\quad GR_{epi,\ class\ I} = K_{epi} \Big/ \left[\frac{R_{epi}^{\ 2}}{2} \ln \frac{R_{epi}}{r_{cut}} - \frac{R_{epi}^{\ 2} - r_{cut}^{\ 2}}{4}\right] \cdot V_{epi}$$

$$(21)\quad GR_{muscle,\ class\ I} = K_{muscle} \Big/ \left[\frac{R_{muscle}^{\ 2}}{2} \ln \frac{R_{muscle}}{r_{cut}} - \frac{R_{muscle}^{\ 2} - r_{cut}^{\ 2}}{4}\right] \cdot V_{muscle}$$

where r_{cut} is the mean inner cuticular radius (μm) measured from images of tracheoles for each locust, and R_{cut}, R_{epi}, and R_{muscle} are the mean radii (μm) to the tracheole outer cuticle surface, the tracheole outer epidermal surface, and the muscle that surrounds and is serviced by each tracheole, respectively, calculated for each locust in Equations (16), (17), and (18), respectively. V_{cut}, V_{epi}, and V_{muscle} are the tracheole cuticle, tracheole epidermal, and muscle volumes (μm^3) in both femurs, respectively, calculated for each locust in Equation (3). K_{cut}, K_{epi}, and K_{muscle} are the Krogh diffusion coefficients for chitin, rat lung tissue, and frog muscle (4.16×10^{-8} μmol O_2 kPa^{-1} h^{-1} μm^{-1}), respectively, corrected to 35°C using Q_{10} = 1.1 (Bartels 1971).

Finally, the total radial diffusing capacity for oxygen across the cuticular and epidermal layers of the tracheoles and through the surrounding muscle serviced by the tracheoles ($GR_{class\ I\ trach}$; μmol O_2 kPa^{-1} h^{-1}) in both femurs for each locust was calculated as:

$$(22)\quad GR_{class\ I\ trach} = 1/(1/GR_{cut,\ class\ I} + 1/GR_{epi,\ class\ I} + 1/GR_{muscle,\ class\ I})$$

where $GR_{cut,\ class\ I}$, $GR_{epi,\ class\ I}$, and $GR_{muscle,\ class\ I}$ are the tracheole radial diffusing capacities (μmol O_2 kPa^{-1} h^{-1}) of the cuticle, epidermis, and surrounding muscle, respectively, calculated for both hopping femurs in each locust in Equations (19), (20), and (21), respectively.

All mean values and allometric exponents include 95% confidence intervals (CI). Allometric data were transformed into $\log_{10}$ base before statistical analysis using ordinary least squares regressions. ANCOVA comparisons of regressions (Zar 1998) were carried out with GraphPad Prism 5 statistical software (GraphPad Software, La Jolla, CA, USA).

4. Results

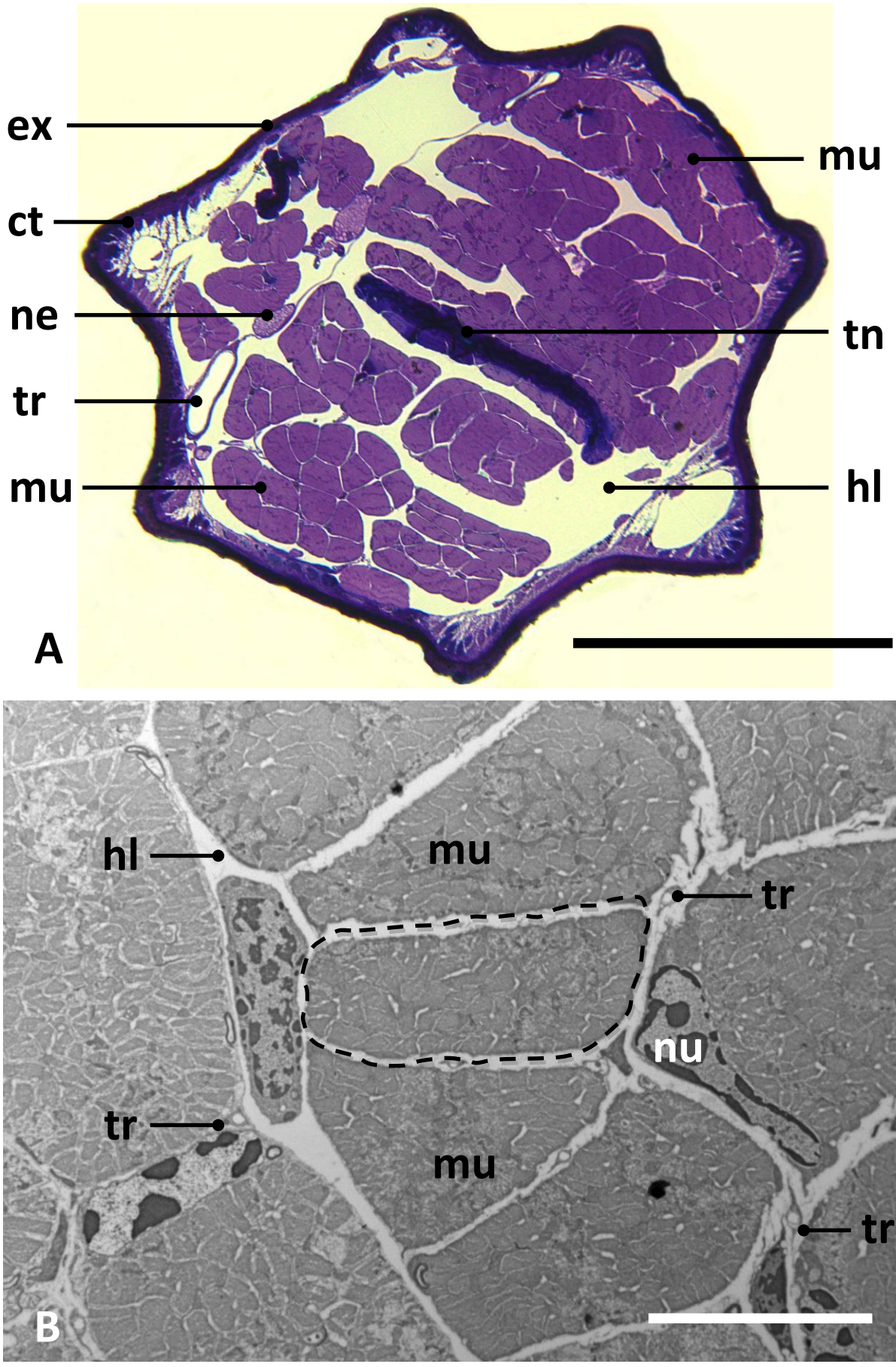
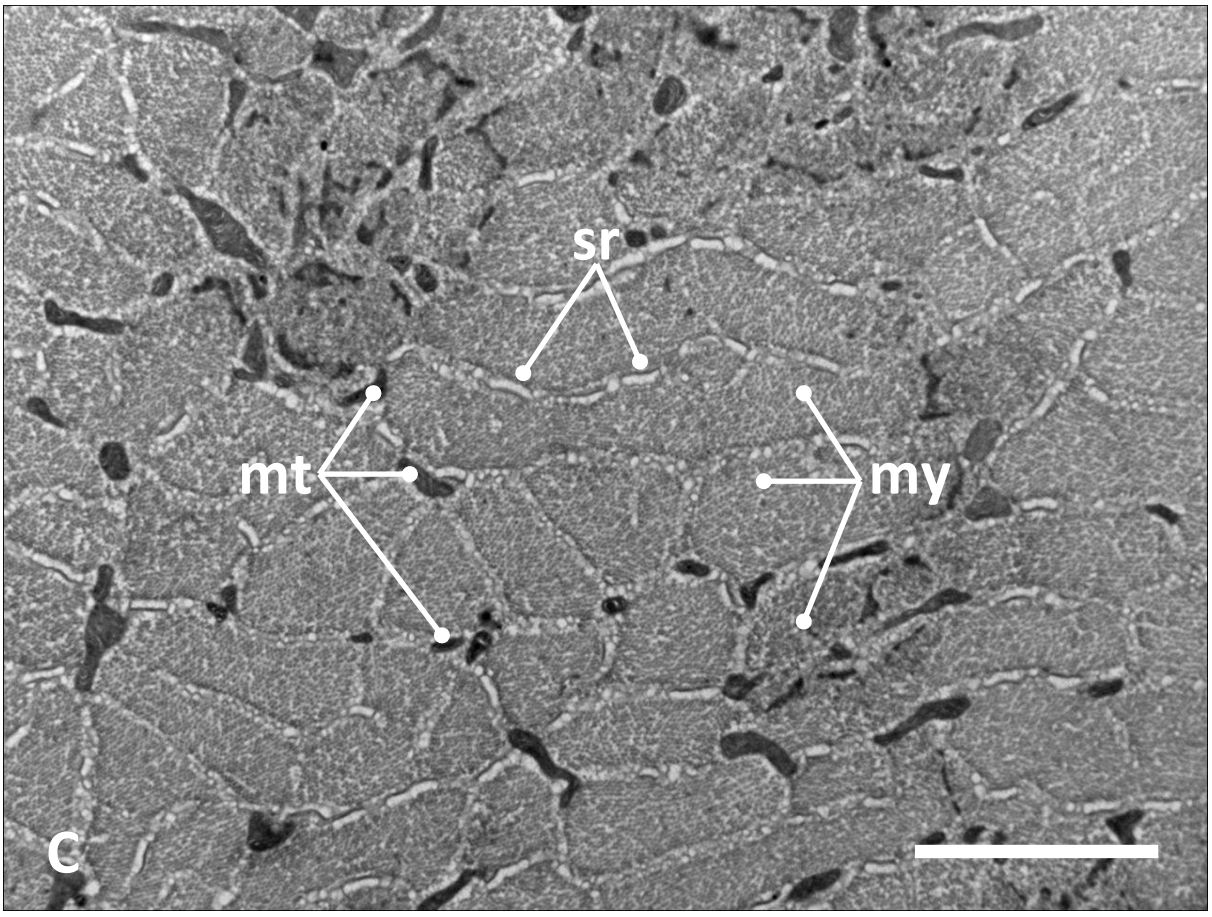


Fig. 2. Micrographs from the metathoracic femur of a single first instar locust, presented from low to high magnification, showing the hierarchy of magnifications used to quantify every structure referred to in the Methods (see Table 1 for electron micrograph magnifications). A (scale bar = 200 μm) is an example of a low magnification light micrograph from which the volume of muscle tissue (and other tissue types) was calculated according to the Cavalieri principle. B (scale bar = 10 μm) is a low magnification electron micrograph from which the volume fraction of muscle tissue occupied by muscle cells (a single muscle cell is indicated by the dashed outline in the image), tracheae, and other structures was calculated. Abbreviations; cl, cuticle layer; cr, mitochondrial crista; ct, connective tissue; ep, epidermal layer; ex, exoskeleton; hl, haemolymph; lu, lumen; mt, mitochondrion; mu, muscle; my, myofibril; ne, nerve; nu, nucleus; sr, sarcoplasmic reticulum; tn, tendon; tr, trachea.


sr
mt
my
C

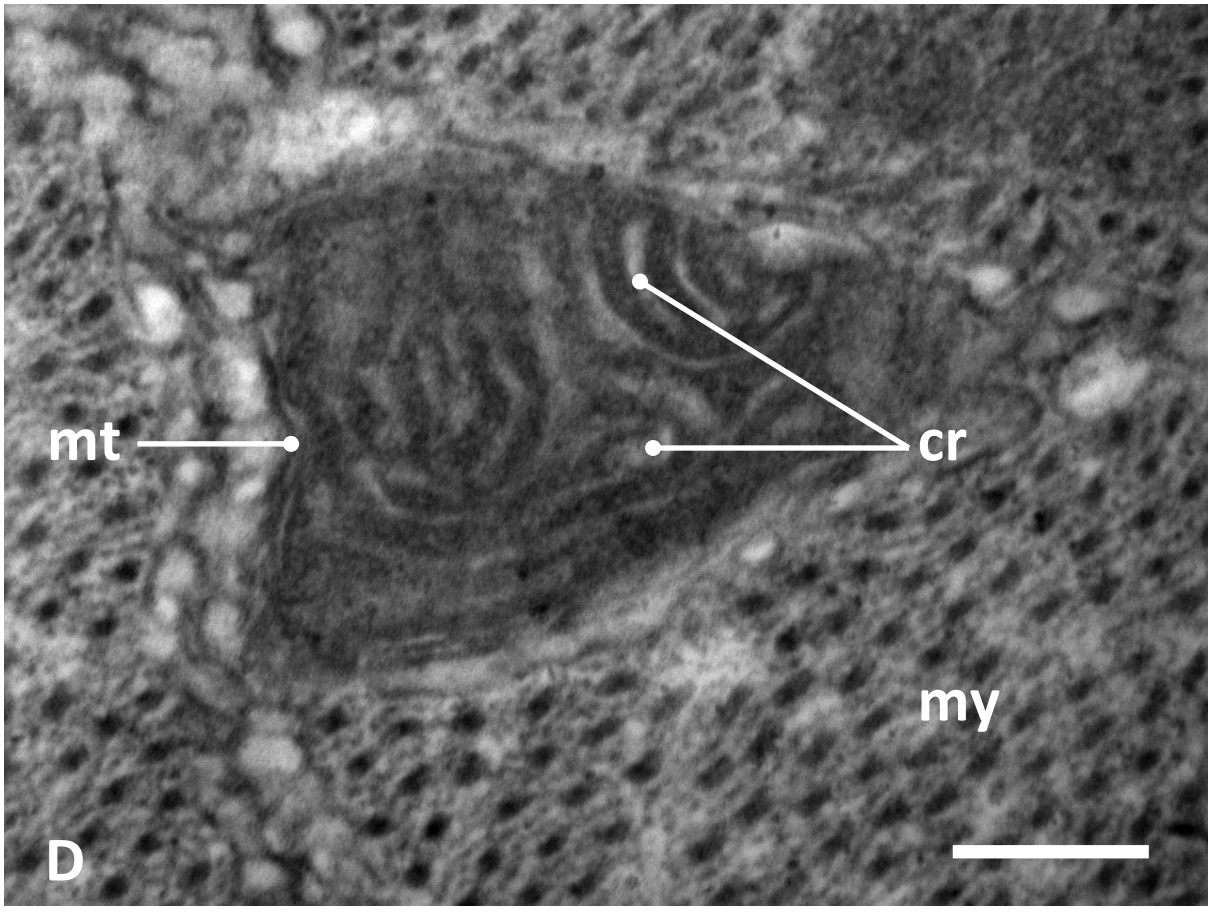

mt
cr
my
D

Fig. 2 (*continued*). C (scale bar = 5 μm) is a high magnification electron micrograph of the ultra-structure of a random muscle cell from which the volume fraction occupied by mitochondria and myofibril+sarcoplasmic reticulum organelles was calculated. D (scale bar = 0.2 μm) is a very high magnification electron micrograph of a random mitochondrion from which the surface area-to-volume ratio of the inner mitochondrial membrane was calculated.

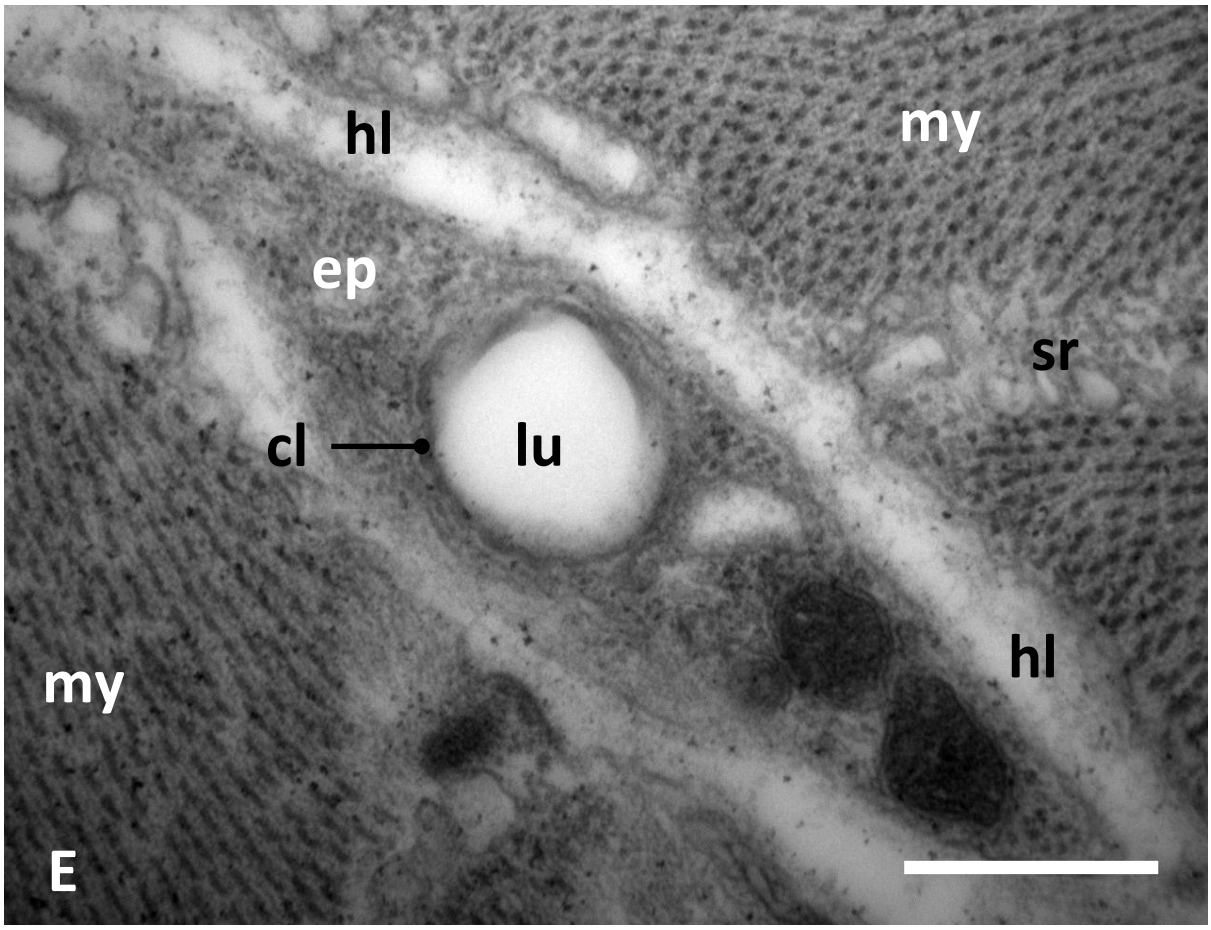


Fig. 2 (*continued*). E (scale bar = 0.5 μm) is a very high magnification electron micrograph of a random class I trachea (tracheole) from which the surface area-to-volume ratio and harmonic mean barrier thickness of the cuticular intima and epidermal layer was calculated.

4.1. Body mass

Body mass increased 32-fold throughout juvenile development. First instars had a mean body mass of 0.019 ± 0.001 g (N=3), which increased to 0.122 ± 0.007 g by the third instar stage (N=3), and 0.611 ± 0.010 g by the fifth instar stage (N=3). There was no significant difference between the body mass of locusts used in the current study and those used in earlier respirometry experiments for each life stage (Mann-Whitney U-test, P>0.05) (Chapter Two).

4.2. Allometric variation

4.2.1. Muscle volume

Muscle occupies around half the volume of the metathoracic femur (Fig. 2A,B). Muscle volume scales according to the allometric power equation, $V_{muscle} = 4.3\times10^{10}M_b^{1.05 \pm 0.08 \text{ (95\% CI)}}$ μm^3 (r^2=0.99, N=9) (Fig. 3). Earlier respirometry experiments found that the maximum functional rate at which oxygen is consumed by jumping muscle during intense hopping exercise scales according to the equation, $MMR_{juvenile\ hop\ muscle} = 103M_b^{1.02 \pm 0.02}$ $\mu mol\ O_2\ h^{-1}$ at 35°C (r^2=0.98, N=145) (Chapter Two). The exponent for $MMR_{juvenile\ hop\ muscle}$ is not significantly different to V_{muscle} (ANCOVA, $F_{1, 150}$=0.43; P=0.51).

4.2.2. Mitochondrial volume

Mitochondria occupy approximately 3.5% of muscle cell volume regardless of life stage (Fig. 2C, Table 2). This is indicated in the allometric power equation for mitochondrial volume density, $Vv_{mito} = 0.032M_b^{-0.03 \pm 0.09}$ (r^2=0.10, N=9). The absolute volume of mitochondria in the hopping muscle is highly dependent on body mass and scales according to the equation, $V_{mito} = 1.3\times10^{9}M_b^{1.02 \pm 0.08}$ μm^3 (r^2=0.99, N=9) (Fig. 4). The exponent for V_{mito} is not significantly different to $MMR_{juvenile\ hop\ muscle}$ (ANCOVA, $F_{1, 150}$=0.01; P=0.94).

4.2.3. Mitochondrial inner membrane surface area

The surface density of inner membrane within the mitochondria is similar for all life stages and averages around 33 $\mu m^2\ \mu m^{-3}$ (Fig. 2D, Table 2). Inner mitochondrial membrane surface density scales according to the allometric power equation, $Sv_{inner} = 31M_b^{-0.03 \pm 0.05}$ μm^{-1} (r^2=0.23, N=9). The total surface area of inner mitochondrial membrane in the hopping muscle is highly dependent on body mass and scales according to the equation, $S_{inner} = 4.2\times10^{10}M_b^{0.99 \pm 0.10}$ μm^2 (r^2=0.99, N=9) (Fig. 5). The exponent for S_{inner} is not significantly different to $MMR_{juvenile\ hop\ muscle}$ (ANCOVA, $F_{1, 150}$=0.52; P=0.47).

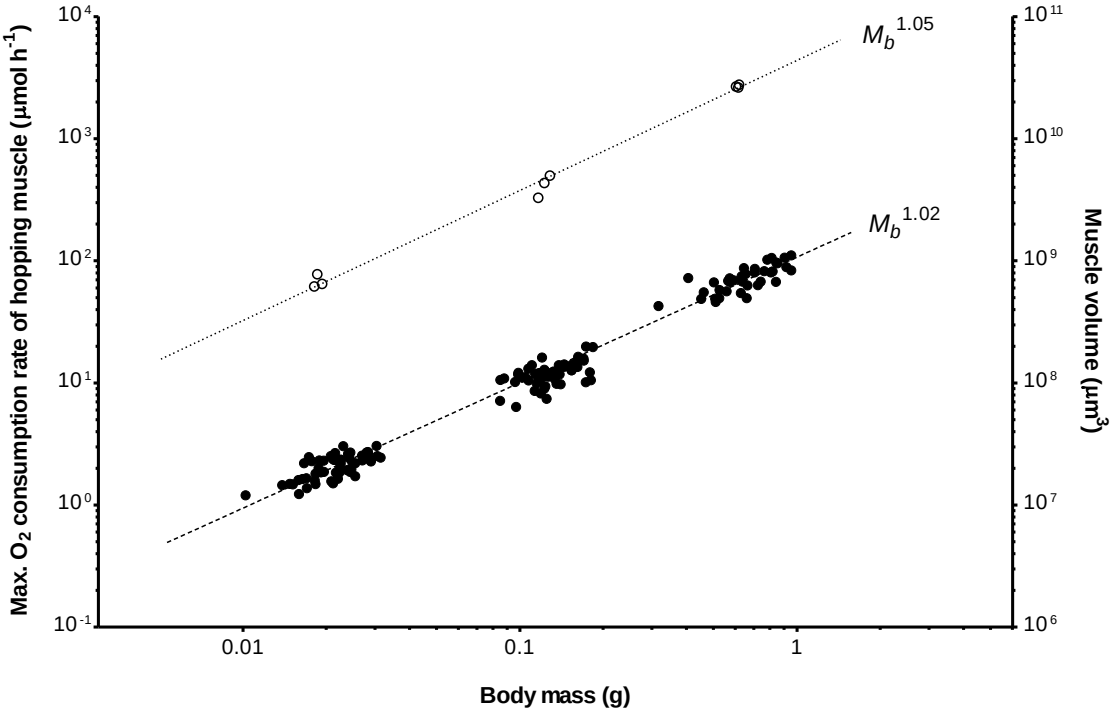


Fig. 3. Relationship between body mass and the volume of muscle contained within both metathoracic femurs (unfilled circles; dotted line) of first (N=3), third (N=3), and fifth instar locusts (N=3). Also shown is the relationship between body mass and the maximum functional rate of oxygen consumption by the juvenile hopping muscle $MMR_{\text{juvenile hop muscle}}$ during intense jumping exercise (filled circles; dashed line) in first (N=55), third (N=53), and fifth instar locusts (N=37).

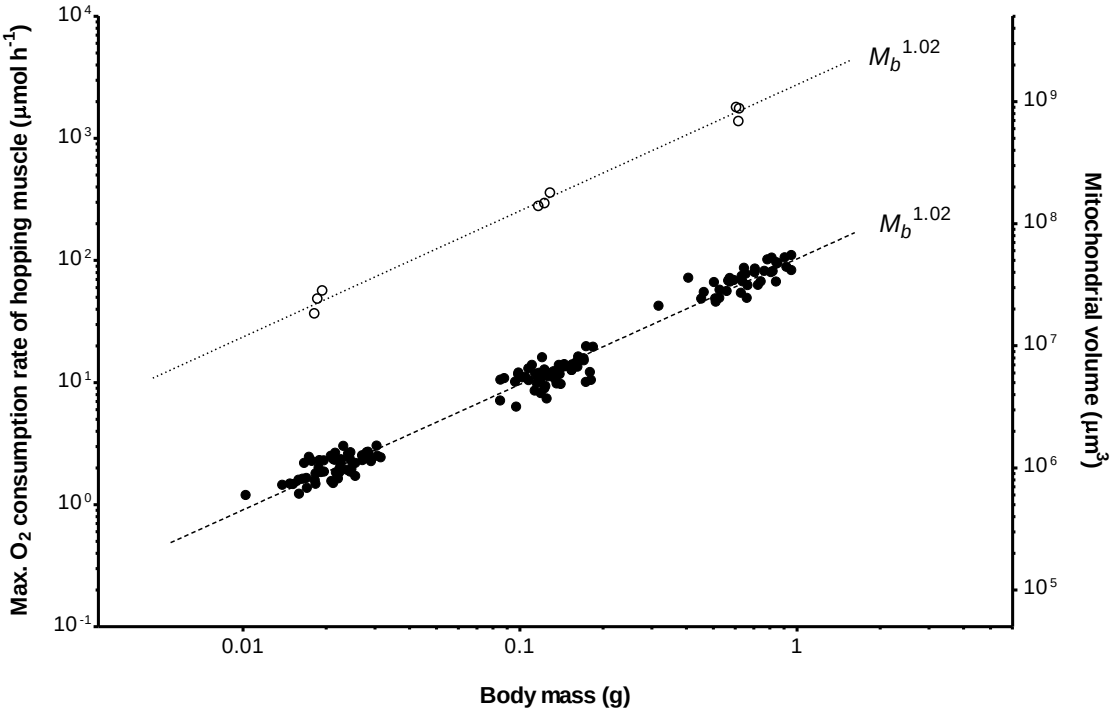


Fig. 4. Relationship between body mass and mitochondrial volume within both metathoracic femurs (unfilled circles; dotted line) of first (N=3), third (N=3), and fifth instar locusts (N=3). Also shown is the maximum oxygen consumption rate of juvenile hopping muscle (filled circles; dashed line) (see Fig. 3).

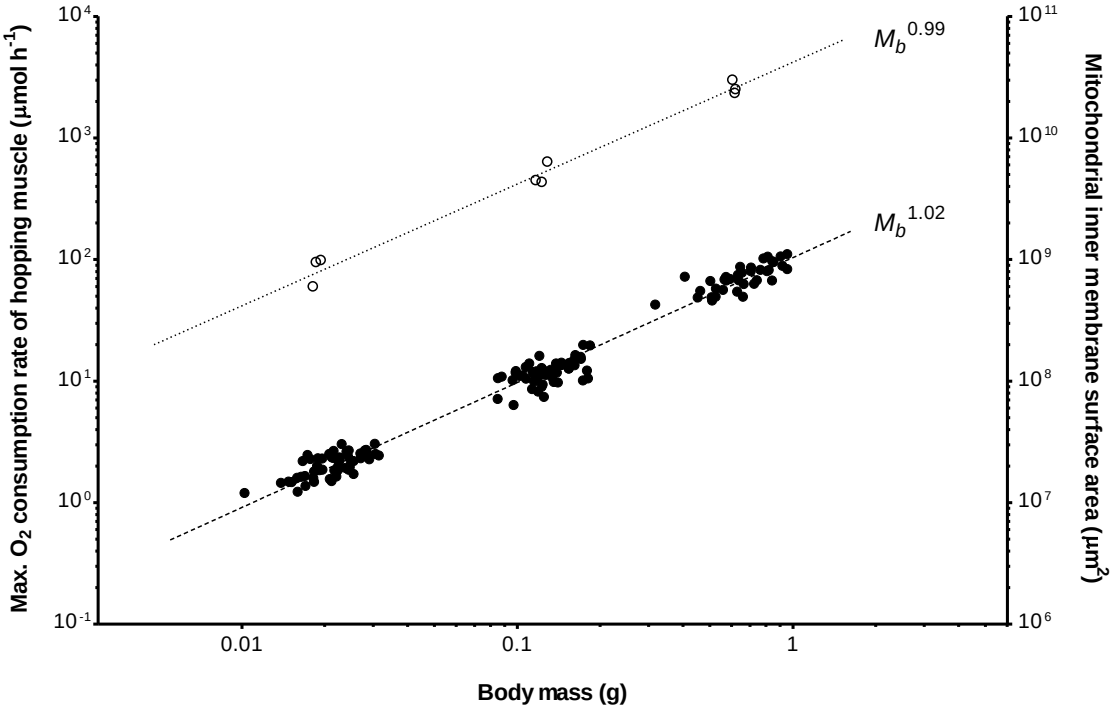


Fig. 5. Relationship between body mass and mitochondrial inner membrane surface area within both metathoracic femurs (unfilled circles; dotted line) of first (N=3), third (N=3), and fifth instar locusts (N=3). Also shown is the maximum oxygen consumption rate of juvenile hopping muscle (filled circles; dashed line) (see Fig. 3).

Table 2. Volume (µm^3, ± 95% CI) of hopping muscle, myofibril + sarcoplasmic reticulum, and mitochondria within both metathoracic femurs in first (N=3), third (N=3) and fifth instar locusts (N=3). Also shown is the volume density (%, ± 95% CI) of myofibril + sarcoplasmic reticulum and mitochondria in the hopping muscle, and the mitochondrial inner membrane surface area (µm^2, ± 95% CI) and surface density (µm^{-1}, ± 95% CI).

	First instars	Third instars	Fifth instars
Muscle volume of femur	$6.8\times10^8 \pm 9.6\times10^7$	$4.2\times10^9 \pm 9.7\times10^8$	$2.7\times10^{10} \pm 7.7\times10^8$
Myofibril + s/reticulum volume in muscle	$6.3\times10^8 \pm 9.3\times10^7$	$3.9\times10^9 \pm 9.1\times10^8$	$2.5\times10^{10} \pm 6.2\times10^8$
Mitochondrial volume in muscle	$2.4\times10^7 \pm 5.7\times10^6$	$1.6\times10^8 \pm 2.4\times10^7$	$8.3\times10^8 \pm 1.3\times10^8$
Myofibril + s/reticulum density in muscle	92.8 ± 1.7	92.5 ± 0.9	94.4 ± 0.6
Mitochondrial density in muscle	3.5 ± 0.9	3.8 ± 0.5	3.1 ± 0.4
Mitochondrial inner membrane surface area	$8.5\times10^8 \pm 2.4\times10^8$	$5.1\times10^9 \pm 1.3\times10^9$	$2.6\times10^{10} \pm 3.9\times10^9$
Mitochondrial inner membrane surface density	35.5 ± 3.7	32.4 ± 3.4	32.0 ± 3.3

4.2.4. Tracheal volume

The tracheal system occupies approximately 3% of metathoracic femur volume. The volume of the tracheal system within both metathoracic femurs scales hypermetrically with body mass following the allometric power equation, $V_{trach\ sys} = 2.4\times10^{9}M_b^{1.12\pm0.09}$ μm^3 (r^2=0.99, N=9) (Fig. 6), which has an exponent that is significantly steeper than the exponent derived for $MMR_{juvenile\ hop\ muscle}$ (ANCOVA, $F_{1,\ 150}$=4.44; P<0.05). However, class IV tracheae and air sacs account for much of the tracheal system's volume; 68% in first instars, 71% in third instars, and 78% in fifth instars (Table 3). The volume of class IV tracheae and air sacs increase disproportionately with body mass according to the power equation, $V_{trach\ class\ IV\ \&\ air\ sacs} = 1.9\times10^{9}M_b^{1.16\pm0.16}$ μm^3 (r^2=0.98, N=9). If class IV tracheae and air sacs are excluded, then the volume of the remaining tracheal system scales with a much lower exponent following the equation, $V_{trach\ sys\ (no\ class\ IV\ trach)} = 5.4\times10^{8}M_b^{1.02\pm0.14}$ μm^3 (r^2=0.98, N=9), which has an exponent that is statistically indistinguishable from that derived for $MMR_{juvenile\ hop\ muscle}$ (ANCOVA, $F_{1,\ 150}$=0.00; P=0.97). Class II and III tracheae are relatively uncommon representing just 5-10% of the tracheal system's volume despite their reasonably large size (Table 3).

Class I tracheae (tracheoles) contribute 10-15% of the tracheal system's volume (Table 3) and because of their small size are far more numerous than the other trachea size classes (Fig. 2B,E). The volume density of tracheoles in the muscle is largely invariant with body mass and scales according to the allometric equation, $Vv_{trach\ class\ I} = 0.0073M_b^{0.06\pm0.24}$ (r^2=0.04, N=9). The volume density of tracheole lumen in the muscle is less, and scales according to the equation, $Vv_{trach\ class\ I\ (lumen\ only)} = 0.00051M_b^{-0.06\pm0.15}$ (r^2=0.12, N=9). On the other hand, the absolute volume of tracheoles in the femurs is highly dependent on body mass and scales according to the equation, $V_{trach\ class\ I} = 3.1\times10^{8}M_b^{1.11\pm0.23}$ μm^3 (r^2=0.95, N=9). The absolute volume of tracheole lumen in the femurs is less, and scales according to the equation, $V_{trach\ class\ I\ (lumen\ only)} = 2.2\times10^{7}M_b^{0.99\pm0.16}$ μm^3 (r^2=0.97, N=9) (Fig. 7). Neither the exponent for $V_{trach\ class\ I}$ (ANCOVA, $F_{1,\ 150}$=2.87; P=0.09) nor that for $V_{trach\ class\ I\ (lumen\ only)}$ (ANCOVA, $F_{1,\ 150}$=0.35; P=0.56) are significantly different to $MMR_{juvenile\ hop\ muscle}$.

4.2.5. Tracheal surface area

The area of the tracheal system's outer epidermal surface in both femurs scales according to the allometric power equation, $S_{epi,\ trach\ sys} = 1.8\times10^{9}M_b^{1.10\pm0.17}$ μm^2 (r^2=0.97, N=9). The class I trachea (tracheole) outer epidermal surface area scales with juvenile body mass following the equation, $S_{epi,\ class\ I} = 1.5\times10^{9}M_b^{1.11\pm0.23}$ μm^2 (r^2=0.95, N=9), which is not significantly

different to the exponent derived for $MMR_{juvenile\ hop\ muscle}$ (ANCOVA, $F_{1, 150}$=2.87; P=0.09). The area of the tracheal system's inner cuticular surface in both femurs scales according to the allometric equation, $S_{cut, trach\ sys} = 8.5\times10^{8}M_b^{1.16 \pm 0.43}$ μm^2 (r^2=0.85, N=9). The tracheole inner cuticle surface area scales with body mass following the equation, $S_{cut, class\ I} = 2.0\times10^{8}M_b^{0.99 \pm 0.16}$ μm^2 (r^2=0.97, N=9) (Fig. 8), which is similar to the exponent derived for $MMR_{juvenile\ hop\ muscle}$ (ANCOVA, $F_{1, 150}$=0.35; P=0.56).

4.2.6. Tracheal harmonic mean barrier thickness

The harmonic mean barrier thickness of the cuticular and epidermal layers increases with trachea size class. Class I tracheae (tracheoles) thus have the thinnest walls. The harmonic mean barrier thickness of the tracheole cuticle and epidermal layers does not vary with body mass. Tracheole harmonic mean barrier cuticle thickness scales according to the allometric equation, $\tau_{cut, class\ I} = 0.027M_b^{-0.01 \pm 0.05}$ μm (r^2=0.05, N=9), and the harmonic mean barrier epidermal thickness scales according to the equation, $\tau_{epi, class\ I} = 0.19M_b^{0.04 \pm 0.17}$ μm (r^2=0.04, N=9).

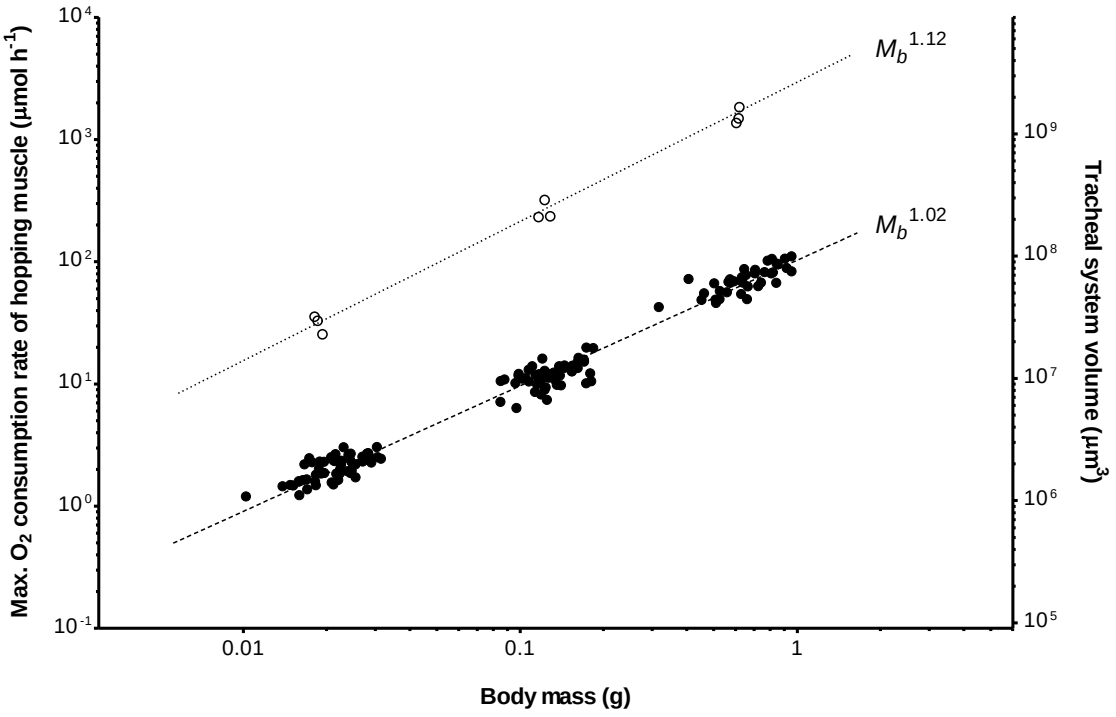


Fig. 6. Relationship between body mass and total tracheal volume within both metathoracic femurs (unfilled circles; dotted line) of first (N=3), third (N=3), and fifth instar locusts (N=3). Also shown is the maximum oxygen consumption rate of juvenile hopping muscle (filled circles; dashed line) (see Fig. 3).

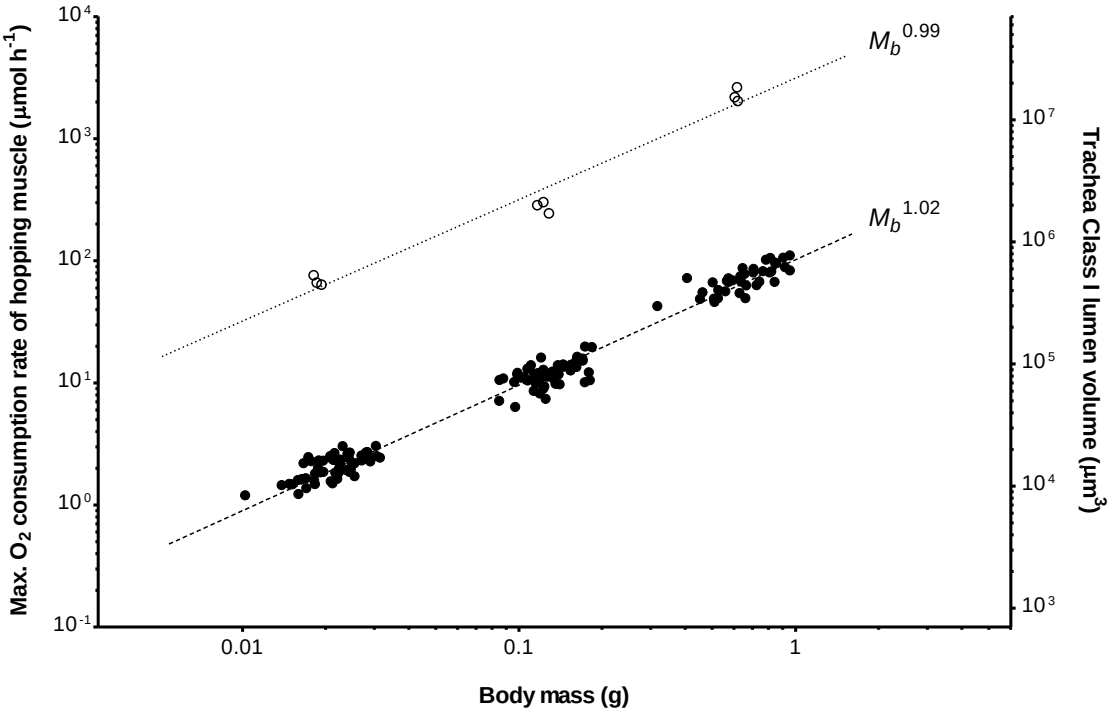


Fig. 7. Relationship between body mass and class I tracheal (tracheole) lumen volume within both metathoracic femurs (unfilled circles; dotted line) of first (*N*=3), third (*N*=3), and fifth instar locusts (*N*=3). Also shown is the maximum oxygen consumption rate of juvenile hopping muscle (filled circles; dashed line) (see Fig. 3).

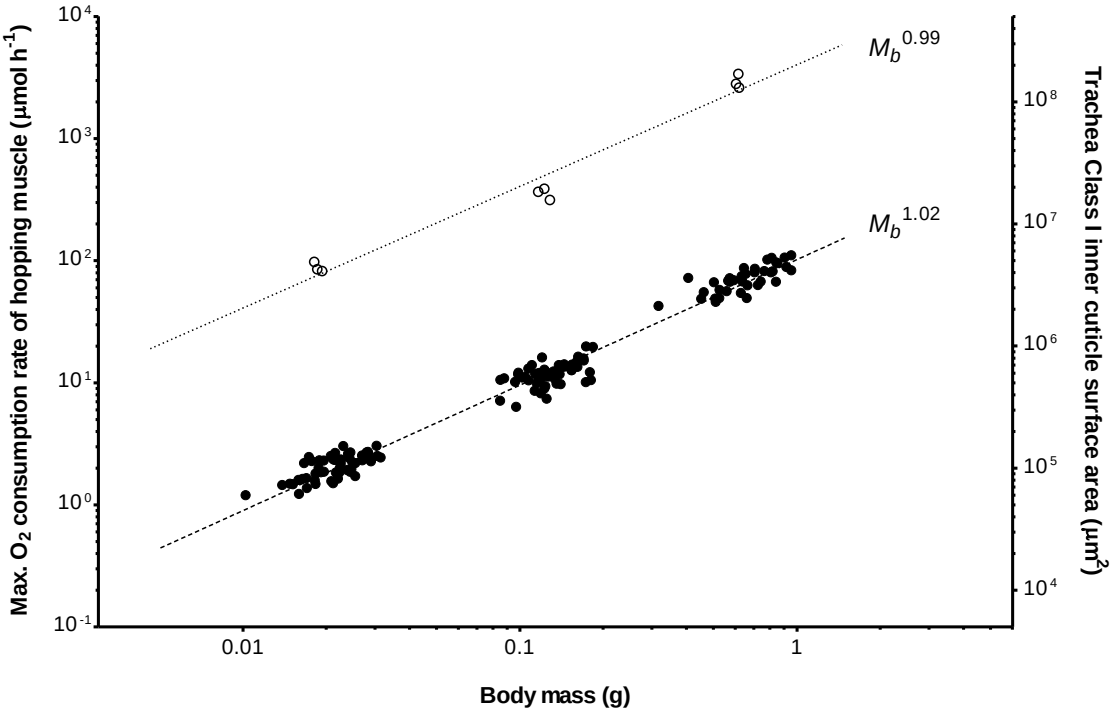


Fig. 8. Relationship between body mass and the inner cuticle surface area of class I tracheae (tracheoles) within both metathoracic femurs (unfilled circles; dotted line) of first (*N*=3), third (*N*=3), and fifth instar locusts (*N*=3). Also shown is the maximum oxygen consumption rate of juvenile hopping muscle (filled circles; dashed line) (see Fig. 3).

Table 3. Class I tracheal (tracheole) inner cuticle and outer epidermal surface area (μm^2, ± 95% CI), class I tracheal volume density (%, ± 95% CI), class I, II, III, IV tracheal volume (μm^3, ± 95% CI), and the total tracheal system volume within both metathoracic femurs in first (*N*=3), third (*N*=3) and fifth instar locusts (*N*=3).

	First instars	Third instars	Fifth instars
Class I tracheal inner cuticle surface area	$4.4\times10^6 \pm 4.7\times10^5$	$1.8\times10^7 \pm 2.1\times10^6$	$1.5\times10^8 \pm 2.3\times10^7$
Class I tracheal outer epidermal surface area	$2.0\times10^7 \pm 3.3\times10^6$	$1.2\times10^8 \pm 6.4\times10^7$	$1.0\times10^9 \pm 2.9\times10^8$
Class I tracheal density in muscle - lumen only	0.072 ± 0.015	0.048 ± 0.015	0.060 ± 0.011
Class I tracheal density in muscle	0.645 ± 0.173	0.638 ± 0.496	0.802 ± 0.209
Class I tracheal volume - lumen only	$4.8\times10^5 \pm 5.1\times10^4$	$1.9\times10^6 \pm 2.3\times10^5$	$1.6\times10^7 \pm 2.5\times10^6$
Class I tracheal volume	$4.3\times10^6 \pm 7.1\times10^5$	$2.5\times10^7 \pm 1.4\times10^7$	$2.2\times10^8 \pm 6.1\times10^7$
Class II tracheal volume	$1.2\times10^6 \pm 7.5\times10^5$	$7.4\times10^6 \pm 5.4\times10^6$	$4.0\times10^7 \pm 1.6\times10^7$
Class III tracheal volume	$3.5\times10^6 \pm 1.2\times10^6$	$3.8\times10^7 \pm 4.1\times10^7$	$7.0\times10^7 \pm 5.7\times10^7$
Class IV tracheal volume	$1.9\times10^7 \pm 4.3\times10^6$	$1.7\times10^8 \pm 7.7\times10^7$	$1.1\times10^9 \pm 1.6\times10^8$
Total tracheal volume	$2.8\times10^7 \pm 5.4\times10^6$	$2.4\times10^8 \pm 5.1\times10^7$	$1.4\times10^9 \pm 2.5\times10^8$

4.2.7. Tracheal lateral diffusing capacity

The lateral diffusing capacity (lateral conductance) of the entire tracheal system in the femurs scales isometrically with body mass following the equation, $GL_{trach\ sys} = 23M_b^{1.00 \pm 0.21}$ μmol O_2 kPa^{-1} h^{-1} at 35°C (r^2=0.95, *N*=9), which is not significantly different to the exponent derived for $MMR_{juvenile\ hop\ muscle}$ (ANCOVA, $F_{1, 150}$=0.21; *P*=0.64). Class I tracheae (tracheoles) provide ~90% of the lateral diffusing capacity of the entire tracheal system in the femurs (Table 4). The lateral diffusing capacity of tracheoles scales according to the allometric equation, $GL_{class\ I\ trach} = 20M_b^{0.99 \pm 0.17}$ μmol O_2 kPa^{-1} h^{-1} at 35°C (r^2=0.96, *N*=9) (Fig. 9), which also has an exponent that is statistically indistinguishable from that derived for $MMR_{juvenile\ hop\ muscle}$ (ANCOVA, $F_{1, 150}$=0.40; *P*=0.53).

4.2.8. Tracheole radial diffusing capacity

The average transverse area of muscle serviced by each tracheole is 440 μm^2 (radius = 12 μm) and scales independently with body mass according to the allometric relationship, $T_{muscle\ per\ single\ class\ I\ trach} = 482M_b^{0.06 \pm 0.15}$ μm^2 (r^2=0.12, *N*=9). The radial diffusing capacity (radial conductance) for oxygen through the tracheole cuticle, epidermis, and surrounding muscle, scales with juvenile body mass according to the allometric equation, $GR_{class\ I\ trach} = 5.8M_b^{0.99 \pm}$

$^{0.18}$ µmol O_2 kPa^{-1} h^{-1} at 35°C (r^2=0.96, N=9) (Fig. 10), which has an exponent that is statistically indistinguishable from that derived for $MMR_{juvenile\ hop\ muscle}$ (ANCOVA, $F_{1, 150}$=0.55; P=0.46).

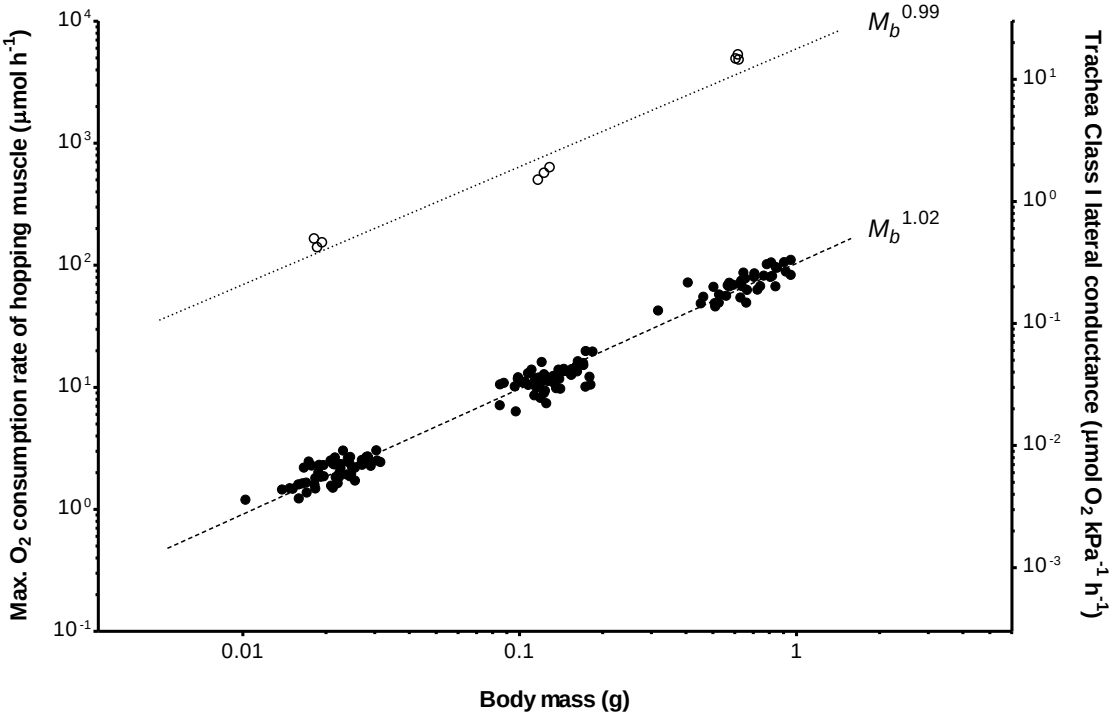


Fig. 9. Relationship between body mass and the lateral diffusing capacity of class I tracheae (tracheoles) within both metathoracic femurs (unfilled circles; dotted line) of first (N=3), third (N=3), and fifth instar locusts (N=3). Also shown is the maximum oxygen consumption rate of juvenile hopping muscle (filled circles; dashed line) (see Fig. 3).

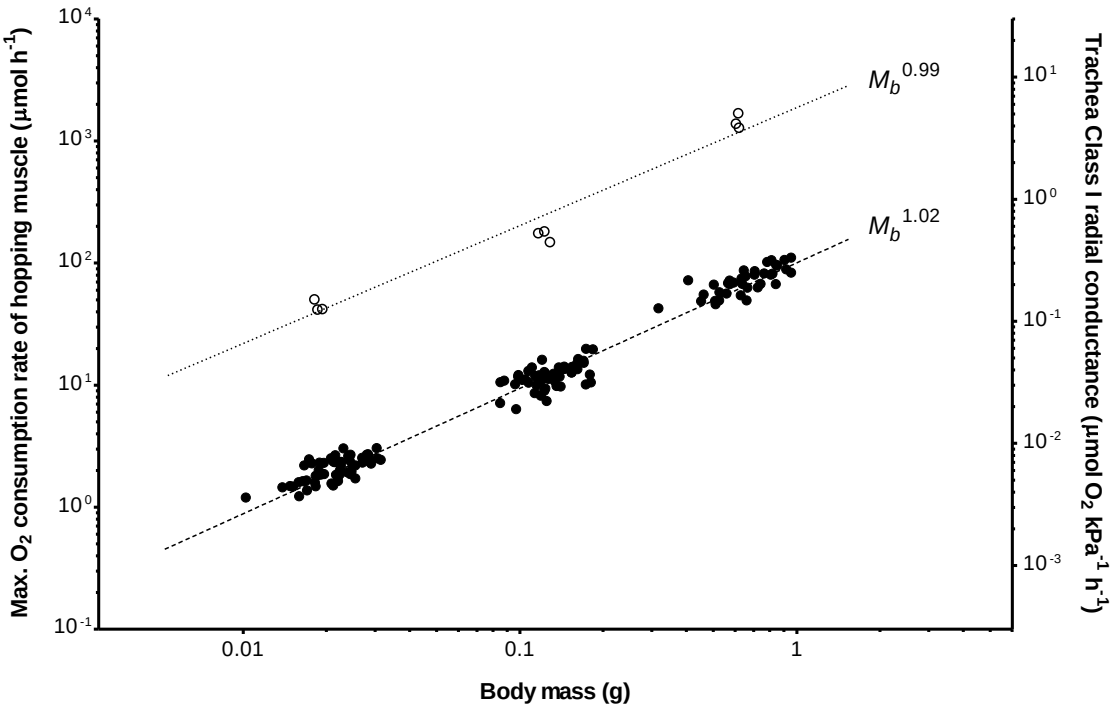


Fig. 10. Relationship between body mass and the radial diffusing capacity of class I tracheae (tracheoles) within both metathoracic femurs (unfilled circles; dotted line) of first (N=3), third (N=3), and fifth instar locusts (N=3). Also shown is the maximum oxygen consumption rate of juvenile hopping muscle (filled circles; dashed line) (see Fig. 3).

Table 4. Anatomical radial diffusing capacity (µmol O_2 kPa^{-1} h^{-1}, ± 95% CI) of class I tracheae (tracheoles), and the anatomical lateral diffusing capacity (µmol O_2 kPa^{-1} h^{-1}, ± 95% CI) of class I, II, III, IV tracheae, and the entire tracheal system within both metathoracic femurs in first (N=3), third (N=3) and fifth instar locusts (N=3).

	First instars	Third instars	Fifth instars
Class I radial conductance	0.134 ± 0.017	0.506 ± 0.060	4.353 ± 0.714
Class I lateral conductance	0.461 ± 0.044	1.712 ± 0.229	15.144 ± 0.896
Class II lateral conductance	0.017 ± 0.006	0.030 ± 0.024	0.248 ± 0.006
Class III lateral conductance	0.010 ± 0.006	0.037 ± 0.019	0.125 ± 0.040
Class IV lateral conductance	0.053 ± 0.067	0.050 ± 0.026	2.595 ± 4.388
Total tracheal lateral conductance	0.541 ± 0.025	1.829 ± 0.213	18.112 ± 5.322

5. Discussion

Respirometry conducted prior to the current study revealed that the maximum functional rate at which oxygen is delivered and consumed by the juvenile hopping muscle during strenuous jumping exercise, $MMR_{juvenile\ hop\ muscle}$, scales with body mass with an exponent of 1.02 ± 0.02 (Chapter Two). According to the principles of symmorphosis, structures involved in the delivery (tracheal system) and consumption (mitochondria) of oxygen should scale congruently with $MMR_{juvenile\ hop\ muscle}$ (Weibel et al., 1991).

5.1. Mitochondria as oxygen sinks

The volume of hopping muscle contained within the metathoracic femurs (Fig. 2A,B) scales with an exponent of 1.05 (Fig. 3). Contained within the muscle fibres are mitochondria (Fig. 2C) that occupy approximately 3.5% of muscle volume in all locusts (Table 2), which agrees well with the results of another study that estimated a mitochondrial density of around 2-4% in the hopping muscle of American locusts *Schistocerca americana* (Hartung et al., 2004). However, it is considerably less than the 20-50% mitochondrial density estimated for insect flight muscle (Chapter Five; Mizisin and Ready 1986; Smith 1963), which is no doubt related to the much higher energetic requirements for flight compared with terrestrial locomotion.

The volume of mitochondria in the hopping muscle scales with an exponent of 1.02 and is parallel with the scaling of the hopping muscle's aerobic capacity (Fig. 4). The congruent scaling between structure and function suggests that no more mitochondria exist than are necessary to meet the maximum energy requirements of the exercising muscle, which is indicative of symmorphotic design. Matching at this step of the oxygen cascade has also been shown in the locomotory and diaphragm muscles of mammals (Weibel et al., 2004; Schwerzmann et al., 1989; Mathieu et al., 1981).

Within the mitochondria, the respiratory enzymes for oxidative phosphorylation are located in the inner membrane (Fig. 2D), and so it is reasonable to argue that quantifying the inner membrane surface area is a more relevant test for symmorphosis. Mitochondria in locust hopping muscle have a mean inner membrane surface density of approximately 33 μm^2 μm^{-3} (Table 2). This is similar to cat muscle mitochondria, which have an inner membrane surface density around 35 μm^2 μm^{-3} (Schwerzmann et al., 1989), but is much less than the flight muscle of flies (Smith 1963) and hummingbirds (Suarez et al., 1991), which are in the vicinity of 50-60 μm^2 μm^{-3}. It is speculated that in these animals, the inner membrane surface density is at the upper limit, beyond which there would be insufficient room in the mitochondrial matrix for Krebs cycle enzymes to function properly (Suarez 1996).

The mitochondrial inner membrane surface density in hopping muscle decreases very slightly with age (Table 2), which probably reflects the gradual increase in mitochondrion size that occurs during development, rather than a decrease in the density at which cristae are packed. The absolute surface area of mitochondrial inner membrane therefore scales with an exponent of 0.99, which is statistically similar to the exponent derived for the hopping muscle's aerobic capacity (Fig. 5). Therefore, at this final step of the oxygen cascade the principles of symmorphosis are evident.

5.2. Oxygen delivery and the tracheal system

The volume of the entire tracheal system within the metathoracic femur scales with an exponent of 1.12, which is significantly steeper than the scaling of the hopping muscle's maximum oxygen consumption rate (Fig. 6). This suggests that larger locusts may have more tracheae than they require, which runs counter to the principles of economic design and the symmorphosis hypothesis. However, it is worth examining each trachea size class separately because different sized tracheae appear to perform different functions.

More than half the tracheal volume can be attributed to large class IV tracheae and air sacs (Table 3), which scale with a rather steep exponent of 1.16. This means that large locusts have relatively more large-sized tracheae. However, the harmonic mean barrier thickness of class IV tracheae is very thick, and so although they represent more than half the total tracheal volume, they provide less than 5% of the overall lateral diffusing capacity (Table 4). The large size and poor lateral conductance of class IV tracheae suggest that their main function is to ventilate the tracheal system (Westneat et al., 2003; Maina 1989; Weis-Fogh 1967). If this is correct, then the disproportionately greater volume of class IV tracheae in older locusts could be necessary to overcome the physiological diffusion limitations often associated with long tracheal tubes in larger insects (Greenlee et al., 2009; Kaiser et al., 2007; Harrison et al., 2005). The idea that large insects are diffusion limited is central to the hypothesis that insect gigantism during the late Palaeozoic was facilitated by high atmospheric oxygen levels (ca. 30%) that occurred during this period (Dudley 1998; Graham et al., 1995).

Class II and III tracheae each represent just ~3% of the tracheal system's volume and total surface area in the femurs (Table 3). Compared with larger class IV tracheae, their walls are thinner and so they probably allow a small amount of oxygen to diffuse across, but because they are so uncommon, they account for less than 3% of the tracheal system's overall lateral diffusing capacity (Table 4). Therefore, it seems that the primary function of class II and III tracheae is to serve as an intermediary between class IV tracheae and class I tracheae.

Small class I tracheae (tracheoles), represent the terminal endings of the tracheal system, and contribute 13% to overall tracheal volume and less than 1% to muscle volume in the femurs (Table 3). Tracheole volume scales with an exponent of 1.11, which is higher than the 1.02 derived for the hopping muscle's aerobic capacity, but the difference is not significant. However, oxygen is delivered along the tracheoles in the gas-phase, and so it is more useful to analyse the lumen volume only, which excludes the volume contribution made by the cuticular and epidermal layers, which are important only in the across-wall diffusion of oxygen. The lumen volume of tracheoles scales with an exponent of 0.99 and this is well matched to the aerobic capacity of the juvenile hopping muscle (Fig. 7). Thus, although the volume of the entire tracheal system is not symmorphotic, the functional part is.

To reach the exercising muscle, oxygen must first diffuse across the tracheole inner cuticle layer followed by the outer epidermal layer. The tracheole outer epidermal layer has a surface density around 4 $\mu m^2\ \mu m^{-3}$, and its total surface area scales with body mass with an exponent of 1.11, which is somewhat higher than the exponent derived for the hopping muscle's maximum oxygen consumption rate. However, given that the outer epidermal surface covers a larger area than the inner cuticle surface, it would seem that the inner cuticle layer is far more important in terms of limiting oxygen flow out of the tracheoles (Fig. 2E, Table 3). The tracheole inner cuticle layer has a surface density around 8 $\mu m^2\ \mu m^{-3}$, and its total surface area scales with body mass with an exponent of 0.99, which is congruent with the hopping muscle's aerobic capacity as predicted by symmorphosis (Fig. 8).

The lateral diffusing capacity of the entire tracheal system within the femurs scales isometrically with body mass and around 90% of the system's lateral conductance for oxygen can be attributed to the tracheoles (Table 4), which are intimately associated with the muscle (Fig. 2B,E). Therefore, tracheoles represent the primary site for oxygen transfer from the tracheal system to the muscle, which is in agreement with the results of other morphometric studies on insects (Hartung et al., 2004; Schmitz and Perry 1999). The harmonic mean barrier thickness of the tracheole cuticle and epidermal layers does not vary much throughout development, and so the tracheole lateral diffusing capacity scales with an exponent of 0.99 (Fig. 9), following a similar slope to that of the inner cuticle surface area. The exponent for tracheole lateral diffusing capacity matches the scaling of the hopping muscle's maximum oxygen consumption rate, as predicted by symmorphosis.

However, the congruent scaling between lateral diffusing capacity and the hopping muscle's aerobic limits is a little surprising because the ontogenetic growth of the hopping muscle is associated with an observed increase in the size of muscle cells (also observed by

Hartung et al., 2004), which would lead to longer average diffusion distances for oxygen through the muscle. In response to the longer diffusion distance, it is reasonable to suspect that larger locusts may have a disproportionate investment in the abundance of tracheoles as a means to compensate for this. Instead, larger locusts appear to overcome this potential diffusion problem in part by investing more in large class IV tracheae (Table 3), which function to ventilate the tracheal system and maintain a high pressure head for oxygen diffusion (Westneat et al., 2003; Maina 1989; Weis-Fogh 1967), and in part by increasing the number of tracheoles that penetrate the muscle cell, such that they become functionally intracellular and therefore in closer proximity to mitochondria deep within the muscle fibre. Small first instars lack these intracellular tracheoles; however, in large fifth instars 5% of tracheoles are intracellular. The occurrence of tracheoles that penetrate the surface of other cells has been reported in a number of studies, although they appear to be particularly prevalent in large and highly aerobic insect flight muscle fibres (Wigglesworth 1983; Whitten 1972).

The observation that some tracheoles are functionally intracellular leads to the realisation that the lateral diffusion of oxygen may not be the most appropriate model to apply to tracheoles because it does not account for the extra distance oxygen must travel as it diffuses through the surrounding muscle, or the inevitable dissipation of oxygen molecules as they diffuse further from the tracheole source. In this respect, the flow of oxygen out of tracheoles and into the surrounding muscle in insects is analogous to the flow of oxygen out of capillaries and into the surrounding tissue in vertebrate animals. Therefore, Krogh's cylinder for radial diffusion should offer a more appropriate model on which to estimate the true anatomical conductance for oxygen out of the tracheoles and into the hopping muscle. The results of the current study show that the average transverse area of muscle serviced by each tracheole is around 440 μm^2 and this does not vary significantly with increasing body mass. Consequently, the maximum average distance oxygen must diffuse from a tracheole into the muscle fibre is ~12 μm in locusts at all stages of development. This compares to a maximum oxygen diffusion distance of 8 μm in the muscle capillary network of the 2 g Etruscan shrew (Hoppeler et al., 1981b). From the estimate of maximum diffusion distance, it was calculated that the tracheole radial diffusing capacity scales with an exponent of 0.99, which is congruent with both the tracheole lateral diffusing capacity and the aerobic capacity of the hopping muscle (Fig. 10). The matching between the anatomical tracheole diffusing capacity and the aerobic capacity of the hopping muscle is evidence of symmorphosis in the

insect tracheal system, and it complements the results of an earlier ontogenetic study on American locusts, which showed that the convective capacity of large tracheae located between the spiracles and the digestive tract matches the metabolic rate of locusts shortly after feeding (Harrison et al., 2005).

5.3. Oxygen partial pressure in the terminal tracheoles

By combining the aerobic capacity of the juvenile hopping muscles ($MMR_{\text{juvenile hop muscle}}$; μmol O_2 h^{-1}) with the radial diffusing capacity of the tracheoles ($GR_{\text{class I trach}}$; μmol O_2 kPa^{-1} h^{-1}), and assuming that during strenuous jumping exercise the partial pressure of oxygen in the hopping muscle at the furthest average distance from a tracheole is 0.1 kPa ($PO_{2\ \text{muscle}}$; kPa), the average partial pressure of oxygen in the tracheoles ($PO_{2\ \text{class I trach}}$; kPa) can be calculated according to Fick's Law of Diffusion:

$$(23) \quad PO_{2_{\text{class I trach}}} = (MMR_{\text{juvenile hop muscle}}/GR_{\text{class I trach}}) + PO_{2_{\text{muscle}}}$$

$$PO_{2_{\text{class I trach}}} \approx 17 \text{ kPa}$$

The average oxygen partial pressure in the terminal tracheoles required to overcome the diffusion barrier and meet the oxygen needs of the hopping muscle during heavy exercise is approximately 17 kPa at 35°C, or expressed as an allometric equation, $PO_{2\ \text{class I trach}} = 19M_b^{0.05 \pm 0.15\ (95\%\ CI)}$ kPa at 35°C (r^2=0.08, N=9). It is not possible to measure directly the partial pressure of oxygen in the terminal tracheoles given their small size (<2 μm diameter; Thesis Appendix), however, in resting American locusts direct measurements in the upper regions of the tracheal system reveal that the partial pressure of oxygen is 19kPa (Gulinson and Harrison 1996). Given that oxygen is delivered along the tracheal system in the gas-phase, it is reasonable to suspect that there may not be a large pressure drop in oxygen between the upper regions of the tracheal system measured by Gulinson and Harrison, and the terminal tracheoles estimated in the present study. Therefore, our estimate of approximately 17kPa in the terminal tracheoles seems reasonable.

5.4. Critique

Along each step of the oxygen cascade there is matching between the maximum functional rate at which oxygen flows through the respiratory system and the quantitative investment made into the structures of the respiratory system. This provides strong evidence that the insect respiratory system is designed according to the economic principles of symmorphosis. However, it should be recognised that the variation in the scaling exponents for the tracheal system might reduce the power of an ANCOVA to distinguish differences with the scaling of

the hopping muscle's aerobic capacity. This variation exists despite the analysis of 108 light micrographs and 1326 electron micrographs from nine individuals spanning a 32-fold range in body mass.

Some of the variation in the tracheal exponents could arise because the allometric equation may not accurately reflect changes in tracheal dimensions that occur during ontogeny. While muscle volume increases continually throughout development, the tracheal system on the other hand, undergoes significant expansion only at moulting (Wigglesworth 1981; Ryerse and Locke 1978). Therefore, in reality, the dimensions of the tracheal system during ontogeny would likely resemble a series of five instar steps, rather than a straight line, and this has probably lead to some of the variation. Taking this into account, it is plausible that the reason that third instar locusts consistently lie below the tracheole regression lines (Figs 7-10) could be because they were fixed late in their life stage, when the ratio between muscle and tracheole volume is at its widest. Either way, it is unlikely that the third instars bear a strong influence on the final scaling exponent, given that the allometric slope tends to be more affected by data at the upper and lower regions of the analysed body mass range.

It is also important to recognise that a proportional relationship between structural investment and functional capacity, while consistent with symmorphosis, does not necessarily prove that the investment is the absolute minimum required to carry out the structure's maximum functional task. For instance, the congruent allometric scaling of aerobic capacity ($M_b^{1.02}$) and mitochondrial volume ($M_b^{1.02}$) determined for the hopping muscle of juvenile locusts in the present study might also arise if the muscle were over-supplied with mitochondria to the same relative extent at all life stages. Ideally, morphometric analyses of the kind undertaken here are complemented with additional measurements that search for hidden excess capacities by manipulating ambient oxygen partial pressures on exercising locusts. If maximum oxygen uptake increases significantly under hyperoxia then it suggests an over-supply of mitochondria, and if maximum oxygen uptake is maintained under moderate hypoxia then it suggests an over-investment in the tracheal system.

The other point worth considering is that in adult locusts, the flight muscles become functional and the insect is capable of oxygen consumption rates far in excess of those attained during terrestrial locomotion. It is reasonable to argue that symmorphosis might be most evident in respiratory systems geared toward extreme performance, such as insect flight. To this end, we have tested whether the vastly different aerobic metabolic rates attained during hopping and flight in the adult locust is matched by a proportional difference in the

amount of respiratory structure associated with the hopping and flight muscles. This will be dealt with in the following chapter (Chapter Five).

6. Acknowledgements

This research was supported by the Australian Research Council, project no. DP0879605. Mr Kerry Gascoigne and Dr Mike Teo of Flinders Microscopy and Ms Ruth Williams and Ms Lyn Waterhouse of Adelaide Microscopy shared their expertise in the field of electron microscopy, which was greatly appreciated. The author also acknowledges two anonymous reviewers who improved an earlier version of this manuscript.

Chapter Five: Symmorphosis and the insect respiratory system: a comparison between flight and hopping muscle

1. Abstract

Taylor and Weibel's theory of symmorphosis predicts that structural components of the respiratory system are quantitatively adjusted to satisfy, but not exceed, maximum functional requirement. We test this in the respiratory system of the adult migratory locust *Locusta migratoria* by comparing the aerobic capacity of hopping and flight muscle with the morphology of the oxygen cascade. Maximum oxygen uptake by flight muscle during tethered-flight is 967 ± 76 (95% CI) $\mu mol\ h^{-1}\ g^{-1}$ body mass, whereas hopping muscle consumes a maximum of 158 ± 8 during jumping exercise. The 6.1-fold difference in aerobic capacity between the two muscles is matched by a 6.4-fold difference in tracheole lumen volume, which is $3.5\times10^{8} \pm 1.2\times10^{8}\ \mu m^{3}\ g^{-1}$ in flight muscle and $5.5\times10^{7} \pm 1.8\times10^{7}$ in hopping muscle. It is also matched by a 6.4-fold difference in tracheole inner cuticle surface area, which is $3.2\times10^{9} \pm 1.1\times10^{9}\ \mu m^{2}\ g^{-1}$ in flight muscle and $5.0\times10^{8} \pm 1.7\times10^{8}$ in hopping muscle, and by a 6.8-fold difference in tracheole anatomical radial diffusing capacity, which is 113 ± 47 $\mu mol\ kPa^{-1}\ h^{-1}\ g^{-1}$ in flight muscle and 16.7 ± 6.5 in hopping muscle. However, there is little congruence between the 6.1-fold difference in aerobic capacity and the 19.8-fold difference in mitochondrial volume, which is $3.2\times10^{10} \pm 3.9\times10^{9}\ \mu m^{3}\ g^{-1}$ in flight muscle and only $1.6\times10^{9} \pm 1.4\times10^{8}$ in hopping muscle. Therefore, symmorphosis is upheld in the design of the tracheal system, but not in relation to the amount of mitochondria. Potentially, factors operating on the molecular level are responsible for this apparent economical breakdown.

2. Introduction

Taylor and Weibel's theory of symmorphosis posits that the oxygen delivery steps of the respiratory system are quantitatively adjusted so that no single component limits maximum oxygen flow during strenuous exercise (Weibel et al., 1998; Weibel et al., 1992; Weibel et al., 1991). They reason that natural selection should act to minimise excess capacity along each step of the oxygen cascade because building and maintaining unused respiratory structure is a waste of resources and places unnecessary loads on the body. To test the theory, Taylor and Weibel performed an allometric comparative analysis on mammals over a wide range of body mass to assess whether size-related differences in maximum metabolic rate are associated with parallel changes in the morphology of the respiratory system (Taylor and Weibel 1981a). On the one hand, they found that the volume of mitochondria in exercising muscle scales proportionately with maximum oxygen consumption rate (Mathieu et al., 1981). But on the other hand, they found that the anatomical pulmonary diffusing capacity increases disproportionately, such that larger mammals appear to have more lung structure than they require (Gehr et al., 1981). The study concluded that symmorphosis is upheld with respect to the amount of mitochondria, but not in relation to the design of the pulmonary gas exchanger.

Interestingly, Taylor and Weibel also noticed that wild, more athletic mammals, tend to have a higher maximum oxygen consumption rate and pulmonary diffusing capacity than similar sized domestic mammals (Gehr et al., 1981). Unfortunately, the difference in aerobic capacity between the wild and domestic mammals was not quite large enough to assess whether it was congruent with differences in the amount of respiratory structure, as predicted by symmorphosis (Weibel et al., 1981b), and so six years later they published a second study in which they formally tested this hypothesis (Weibel et al., 1987b). In this study, they showed that the 2.5-fold higher maximum oxygen consumption rate of the 'athletic' dog and pony compared to the 'nonathletic' goat and calf (Taylor et al., 1987a) is matched by a similar difference in the volume of mitochondria between the two groups (Hoppeler et al., 1987). They also found that the athletic mammals combine an increase in muscle capillary supply with an increase in blood oxygen carrying capacity to meet their 2.5-fold higher maximum oxygen consumption rate (Conley et al., 1987). Similarly, a larger heart size and higher red blood cell concentration in the athletic mammals combine to increase the oxygen transport capacity of the circulatory system by a factor of 2.5-fold (Karas et al., 1987b). However, the study also found that the higher aerobic capacity of athletic mammals is only partly met by an increase in lung diffusing capacity (Weibel et al., 1987a), and that all mammals appear to have more lung and pulmonary capillary structure than they require to saturate blood with

oxygen (Karas et al., 1987a). Thus, the comparison between athletic and nonathletic mammals, as well as the earlier allometric analysis, both conclude that symmorphosis is upheld for each step of the mammalian respiratory system, except for the lung, where an excess capacity is evident (Taylor et al., 1987b).

However, the mammalian respiratory system may not be the best model on which to test for symmorphosis. Some authors argue that because the cardiovascular system of mammals serves a number of important functions, it is difficult to establish whether its design is geared towards oxygen delivery, and not some other function, such as substrate supply, carbon dioxide removal, lactate removal, or heat dispersal (Garland 1998; Dudley and Gans 1991; Garland and Huey 1987). It is also reasoned that optimal matching between structural elements in a system becomes increasingly unlikely as the number of elements increases, along with the number of functions performed by each element (Dudley and Gans 1991). On this basis, insects might provide a more suitable model because in these animals the task of oxygen delivery is met entirely by the tubular branching networks of the tracheal system, which ultimately terminate as fine tracheoles that function primarily to service the oxygen needs of the insect tissue (Chapter Four; Schmitz and Perry 1999; Chapman 1998; Wigglesworth 1965). Furthermore, oxygen flux through the insect respiratory system is higher than in any other animal (Chapter Three; Suarez 2000; Casey et al., 1985; Bartholomew and Casey 1978; Weis-Fogh 1964b), and if animals are designed optimally, as symmorphosis suggests, then it should be most evident in species that have experienced strong selective pressure for high aerobic performance (Jones and Lindstedt 1993).

An allometric assessment of the design characteristics of the insect respiratory system has recently been undertaken in an ontogenetic study on the migratory locust *Locusta migratoria* (Chapter Four). It was shown that throughout juvenile development, the aerobic capacity of the hopping muscle scales in proportion with the total volume of tracheoles in the hopping muscle, the total inner surface area of the tracheoles, the anatomical diffusing capacity of the tracheoles, and the total volume and inner membrane surface area of mitochondria in the hopping muscle. The study therefore provides strong evidence that the insect respiratory system conforms to the economic design principles of symmorphosis. However, the assessment is only half-complete because a non-allometric study, analogous to Taylor and Weibel's comparison of athletic versus nonathletic mammals, has not yet been undertaken. The challenge is to find either a pair of similar sized insects with vastly different aerobic metabolic ceilings, or alternatively, one insect that utilises different locomotory

modes requiring very different energy inputs. For example, a comparison could be made between highly aerobic flight muscles and less aerobic running or hopping muscles.

The aim of this study is to assess whether the difference in aerobic capacity between the flight and hopping muscle in the adult migratory locust *L. migratoria* is matched by a proportional difference in the amount respiratory structure associated with the two muscles, as predicted by symmorphosis. Earlier respirometry revealed that the maximum functional rate that adult hopping muscle consumes oxygen during jumping exercise is 158 ± 8 μmol O_2 h^{-1} g^{-1} body mass at 35°C (*N*=23) (Chapter Two), whereas the maximum functional rate that adult flight muscle consumes oxygen during tethered-flight is 967 ± 76 μmol O_2 h^{-1} g^{-1} body mass at 35°C (*N*=13) (T-test, *P*<0.05) (Chapter Three). Therefore, the aerobic metabolic ratio between the two muscles is 6.1-fold, and according to the principles of symmorphosis, a similar ratio should exist for the total volume of tracheoles in the two muscles, the total inner surface area of the tracheoles, the anatomical diffusing capacity of the tracheoles, and the total volume and inner membrane surface area of mitochondria in the two muscles.

3. Methods

3.1. Animals

Gregarious-phase locusts *Locusta migratoria* were reared at 33 ± 1°C, under a 12:12 h light-dark cycle, with *ad libitum* access to seedling wheatgrass and wheat germ, as previously described (Chapter Two). Newly emerged adults were identified from the breeding colony and were placed into separate plastic terraria with other adults of similar age. Morphometric analysis of the flight muscles housed within the pterothorax (mesothorax and metathorax) was conducted on adult locusts (*N*=3 individuals) two to three weeks post-final moult, by which time the flight muscles have fully developed (Mizisin and Ready 1986). Morphometric analysis of the metathoracic femur (hopping leg femur) was conducted on adult locusts (*N*=3 individuals) three to four days post-final moult, which is sufficient time for the exoskeleton to stiffen while minimising compression of the tracheal system due to growth (Greenlee and Harrison 2004b; Queathem 1991). All locusts were fasted 6-10 h prior to tissue fixation consistent with earlier respirometry (Chapters Two & Three).

3.2. Specimen preparation

3.2.1. Dissection

The procedure used to dissect and fix locust tissue was modified based on the methods of previous electron microscopy studies of insects and spiders (Chapter Four; Biserova and

Pfluger 2004; Hartung et al., 2004; Kohnert et al., 2004; Schmitz and Perry 2002a; Schmitz and Perry 2002b). The dorsal longitudinal muscle and dorsoventral muscles (tergosternal, tergocoxal, basalar, subalar, and tergotrochanteral muscles) constitute almost the entire muscle mass of the pterothorax and are all recruited for flight (Table 1, pp 671, Wilson 1962). These muscles were identified in dissected locusts from published illustrations (Wilson 1962; Albrecht 1953; Snodgrass 1929). Adults used to obtain morphological data on the flight muscles were initially cold anaesthetised for 20 min in a refrigerator at 4°C, and then weighed to 0.1 mg on an analytical balance (AE163, Mettler, Greifensee, Switzerland). The wings and legs were removed with angled spring scissors, while the head, prothorax, and abdomen were removed with a razor. The gut and other organs were withdrawn from the remaining pterothoracic cavity, which was then weighed to 0.1 mg. The left and right sides of the pterothorax were then separated with a razor, and from each half, the dorsal longitudinal muscle was removed, and the dorsoventral muscles of the mesothorax separated from those of the metathorax. Each muscle piece was labelled left or right and by its anatomical name.

The large extensor tibialis muscle and the smaller flexor tibialis muscle, which are used during hopping locomotion, constitute the entire muscle mass of the metathoracic femur (Gabriel 1985a; Gabriel 1985b; Bennet-Clark 1975), and were identified from published illustrations (Albrecht 1953; Snodgrass 1929). Adults used to obtain morphological data on the metathoracic femur were cold anaesthetised for 20 min, weighed to 0.1 mg, and then both femurs from each locust were carefully removed with angled spring scissors and weighed to 0.1 mg. A razor was then used to slice each femur along the transverse plane into 12 equal length pieces that were sequentially numbered proximally to distally and labelled left or right.

3.2.2. Fixation & embedding

The fixation and embedding process was performed over five consecutive days as detailed in an earlier study (Chapter Four). Briefly, immediately following dissection, the tissue pieces were immersed into a chemical fixative solution of 2.5% glutaraldehyde and 2% formaldehyde in 0.2 M phosphate buffer with pH 7.4. The tissue was then rinsed and placed into a 1% aqueous solution of osmium tetroxide for secondary fixation, and then rinsed again and placed into a 2% aqueous solution of uranyl acetate. The tissue was then rinsed and dehydrated in a 50% to 100% ethyl alcohol series followed by immersion in pure propylene oxide. Lastly, the tissue was incrementally infiltrated with embedding resin (Durcupan, Fluka, Buchs, Switzerland), then placed into individually labelled embedding moulds, and covered with pure resin which was left to polymerise in a 70°C oven for 48 h.

3.3. Light microscopy

One pterothorax-half and one femur from each locust were randomly selected for light microscopy analysis. Twelve sections were cut along the length of the flight muscles, starting with the anterior end of the dorsal longitudinal muscle, followed by the dorsal end of the mesothoracic dorsoventral muscle, and then the dorsal end of the metathoracic dorsoventral muscle. Twelve sections were also cut proximally to distally along the length of the femur. All sections were 1-µm thick, parallel, transverse, equidistant and cut with 8 mm glass knives and an ultramicrotome (EM UC6, Leica Microsystems, Wetzlar, Germany). The sections were placed onto glass slides, stained with toluidine blue, rinsed with distilled water, and air-dried. Each section was viewed at ×4 magnification under an optical microscope (BX51, Olympus, Hamburg, Germany) and photographed with a mounted digital colour camera (ColorView III, Soft Imaging System, Olympus, Germany), which generated 24-bit 2576 × 1932 pixel resolution images. Each section image was imported into a computer graphics program (CorelDRAW 11, Corel Corp., Ottawa, ON, Canada) where a point grid test system was superimposed randomly over the image. The Cavalieri principle, which estimates the volume of a structure as the product of the structure's total cross-sectional area and the distance between parallel sections (Howard and Reed 1998; Mayhew 1991; Cruz-Orive and Weibel 1990), provided volume estimates for muscle tissue, connective tissue, exoskeleton, class IV tracheae and air sacs (tracheae with a diameter >20 µm), tendon, nerve, and haemolymph for each locust. Full details of these measurements and calculations are provided in an earlier study (Chapter Four).

3.4 Electron microscopy

The remaining pterothorax-half and femur from each locust were used for transmission electron microscopy analysis. The sampling scheme randomised section position and angle to produce vertical uniform random sections (Howard and Reed 1998; Mayhew 1991). Six sections were cut along the length of the flight muscles and along the length of the femur, in the same order as that used for light microscopy. Each section was 70-nm thick, equidistant, and cut with a diamond knife (Diatome, Biel, Switzerland) and ultramicrotome. For the first locust of each group, the first section was cut at a random angle between 0° and 18° relative to the vertical plane. For the second locust, the first section was cut at a random angle between 36° and 54°, and for the third locust, the first section was cut at a random angle between 72° and 90°. For the remaining five sections in each locust, 18° was added to the

cutting angle with every successive section. This meant that for each locust, the full range of angles around the vertical plane was randomly sampled.

Sections were placed onto 3 mm copper mesh grids, stained with lead citrate, and viewed with a transmission electron microscope (CM 100, Philips, Eindhoven, The Netherlands) where random 8-bit 1280 × 1024 pixel resolution images were captured with a mounted digital camera (MegaView II, Soft Imaging System, Olympus, Germany) at appropriate magnifications (Table 1). To obtain unbiased sampling of the flight muscle and femur, the number of random images taken from each section was adjusted relative to the amount of muscle present (Chapter Four). All images were exported to CorelDRAW where they were analysed using stereological principles (Howard and Reed 1998; Mayhew 1991; Cruz-Orive and Weibel 1990) appropriate for vertical sections (Baddeley et al., 1986).

Low magnification tissue images (Table 1) were analysed with a point grid test system, which allowed density and volume estimates of muscle, muscle nuclei, extracellular haemolymph, secretory cells, nerve, tendon, lipid droplets, unidentified cells, and tracheal lumen, cuticle, epidermis and nuclei, in each locust. Tracheae were categorised into four size classes: class I tracheae had an inner diameter of 0-2 μm (hereafter referred to as tracheoles; Thesis Appendix), class II were 2-5 μm, class III were 5-20 μm, and class IV tracheae and air sacs were those with an inner diameter >20 μm. Whether tracheoles were intracellular or extracellular was also recorded. High magnification images of random muscle cells (Table 1) were also analysed with a point grid test system and this allowed density and volume estimates of mitochondria, myofibril+sarcoplasmic reticulum, and cytosol in each locust. Mitochondria images (Table 1) were analysed with a cycloid arc test system, which provided the surface area-to-volume ratio of the inner and outer mitochondrial membrane from which the total inner and outer membrane surface area was calculated for each locust. Trachea images (Table 1) were also analysed with a cycloid arc test system and the ratio of tracheal inner cuticle surface area-to-lumen volume, and tracheal outer epidermal surface area-to-lumen+cuticle+epidermis volume was calculated for each trachea size class (I, II, III, IV) in each locust. The total inner cuticle and outer epidermal surface areas were then calculated for each trachea size class in each locust. Finally, the cuticle and epidermal thicknesses were measured from the trachea images (Table 1) and this was used to calculate the harmonic mean barrier thickness of the respective layers for each trachea size class in each locust. A more detailed account of the methods used to analyse vertical sections using point grid and cycloid

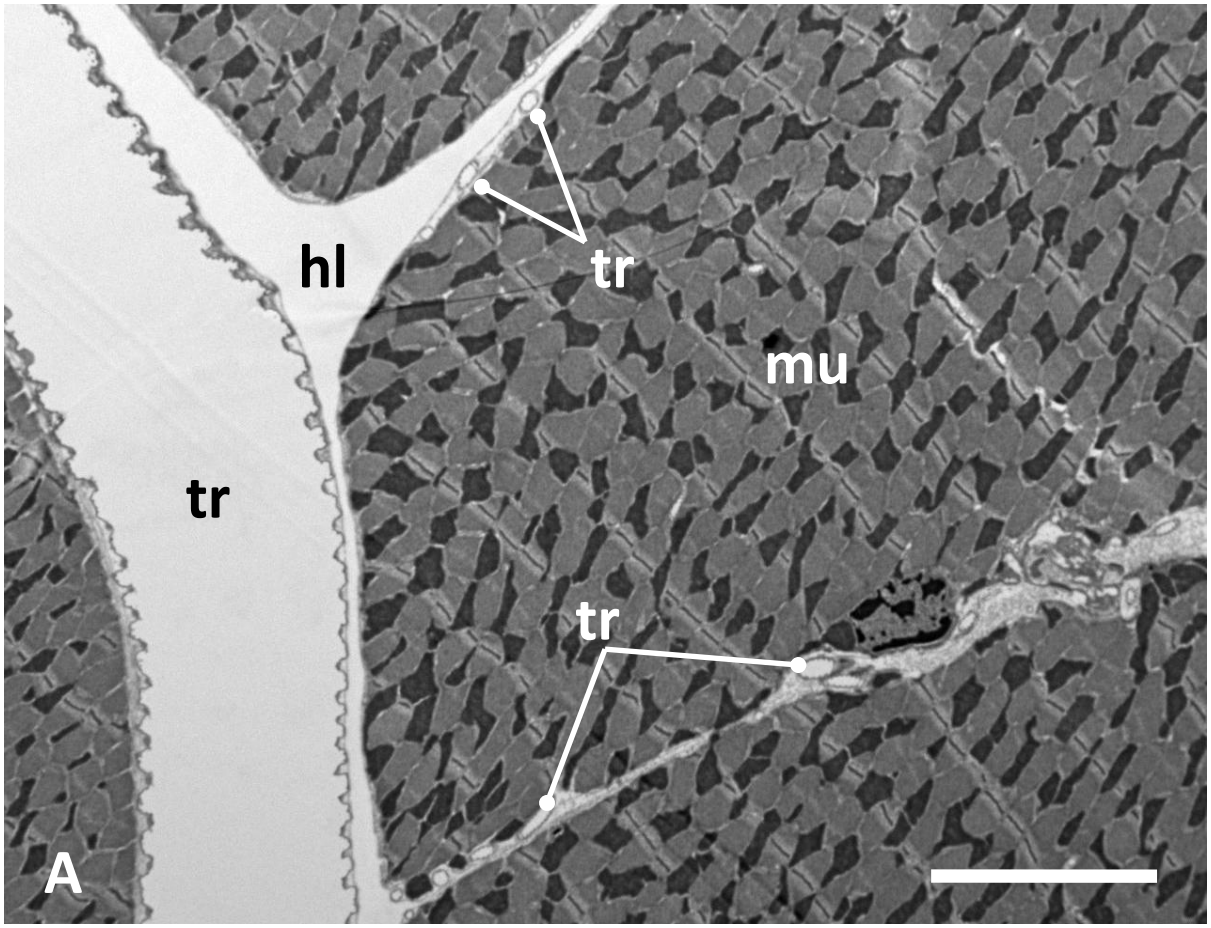
arc test systems, as well as the appropriate calculations, are provided in an earlier study (Chapter Four).

The anatomical lateral diffusing capacity for oxygen across the tracheal wall (i.e. lateral conductance) was calculated for each trachea size class (I, II, III, IV) in each locust as a function of inner cuticle surface area, cuticle and epidermal harmonic mean barrier thickness, and Krogh's diffusion coefficients for chitin (cuticle layer) and rat lung tissue (epidermal layer) corrected to 35°C using Q_{10} = 1.1 (Bartels 1971), consistent with the temperature of earlier respirometry (Chapters Two & Three). The sum of the lateral diffusing capacities for each trachea size class provided an overall estimate of lateral diffusing capacity for the entire tracheal system associated with the flight muscle/femurs in each locust. Finally, the anatomical radial diffusing capacity for oxygen out of the tracheoles and into the surrounding muscle (i.e. radial conductance) was determined for each locust according to Krogh's cylinder model for radial diffusion (Chapter Four; Kreuzer 1982; Krogh 1919). This calculation takes into account the tracheoles' inner cuticular radius, outer cuticular radius, outer epidermal radius, the mean radius of the surrounding muscle serviced by each tracheole, and Krogh's diffusion coefficients for chitin (cuticle layer), rat lung tissue (epidermal layer), and frog muscle (locust muscle), which were once again corrected to 35°C using Q_{10} = 1.1 (Bartels 1971). Full details of every calculation briefly summarised above are provided in an earlier study (Chapter Four). The average time to process each locust from initial fixation to the final quantification of flight muscle/femur ultrastructure was ~6 weeks. This significant investment in time restricted the study to six individuals.

All mean values are body mass-specific (except volume density, surface density, and thickness estimates) and include 95% confidence intervals (CI). Statistical significance between means was tested using paired and unpaired T-tests for equal or unequal variance, as appropriate. When three or more means were compared, an ANOVA was performed followed by a Tukey's post-hoc test (Zar 1998). ANOVAs and T-tests were carried out with GraphPad Prism 5 statistical software (GraphPad Software, La Jolla, CA, USA).

Table 1. Number (and magnification) of random electron micrographs taken per adult locust.

	Low magnification tissue images	High magnification muscle cell images	Mitochondria images	Trachea images
Pterothorax and flight muscle (*N*=3)	36 (×1450)	36 (×4600)	20 (×64000)	36 (×620-64000)
Femur and hopping muscle (*N*=3)	44 (×1100)	44(×4600)	22 (×64000)	44 (×620-64000)


hl
tr
mu
tr
tr
A

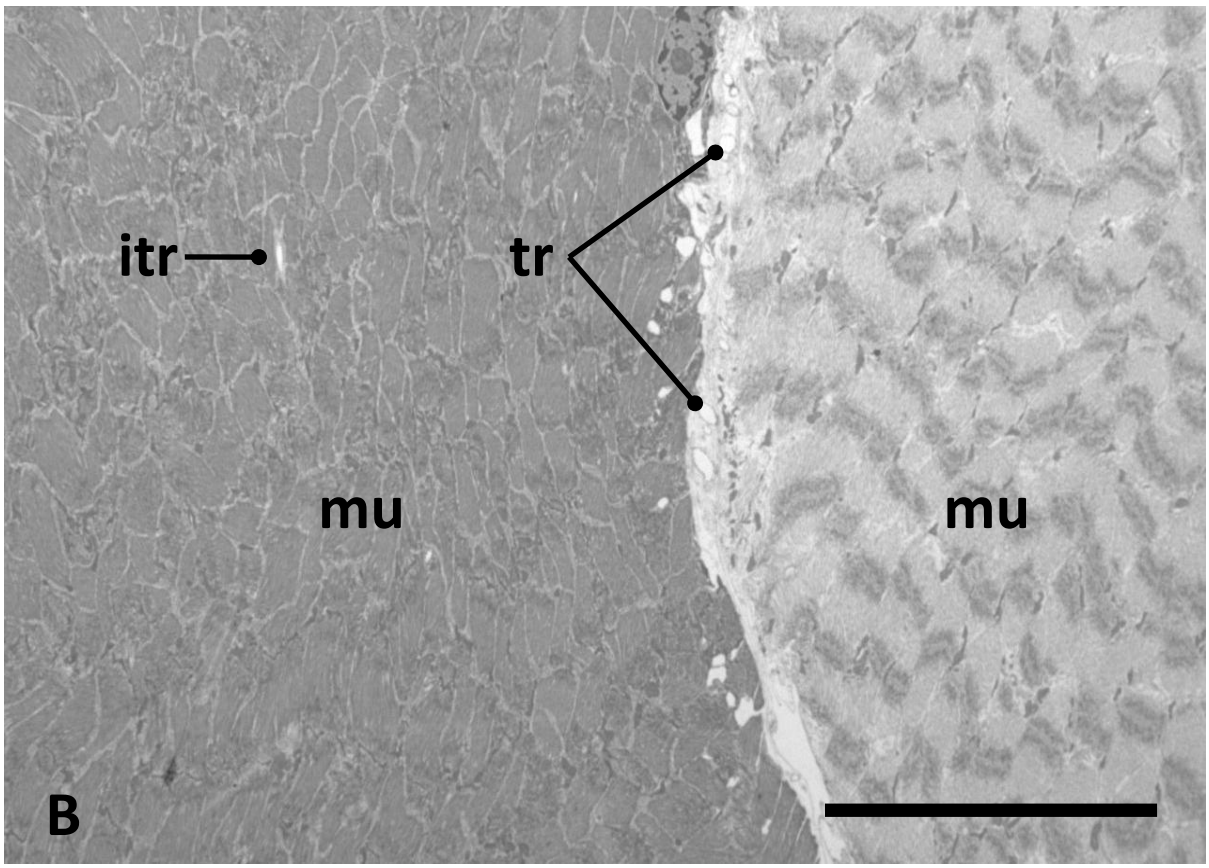
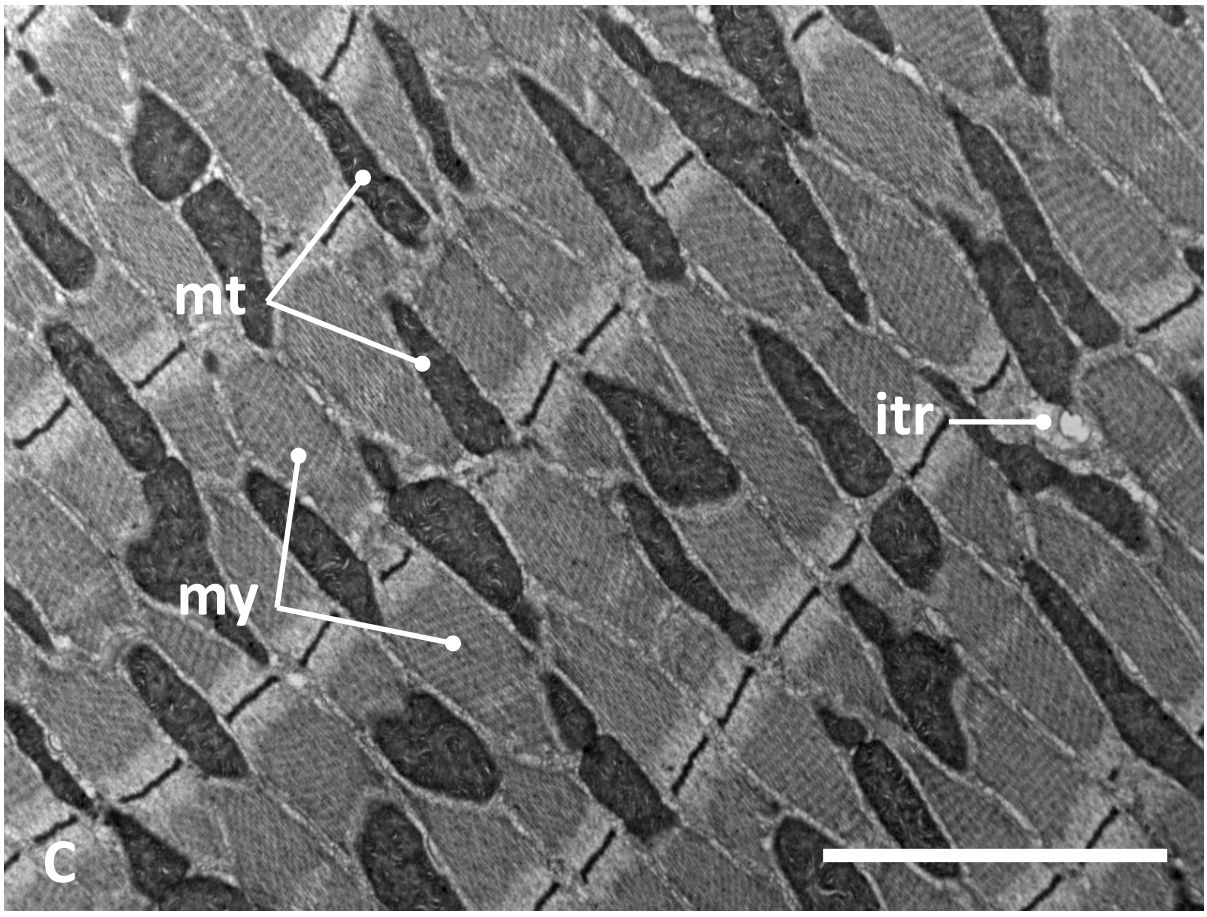

itr
tr
mu
mu
B

Fig. 1. Electron micrographs of flight and hopping muscle in the adult locust (see Table 1 for magnifications). A (scale bar = 10 μm) and B (scale bar = 20 μm) are low magnification micrographs of flight and hopping muscle, respectively, from which the volume fraction of muscle tissue occupied by muscle cells, tracheae, and other structures was calculated. Abbreviations; cl, cuticle layer; cr, mitochondrial crista; ep, epidermal layer; hl, haemolymph; itr, intracellular trachea; lu, lumen; mt, mitochondrion; mu, muscle; my, myofibril; sr, sarcoplasmic reticulum; tr, trachea.


mt
itr
my
C

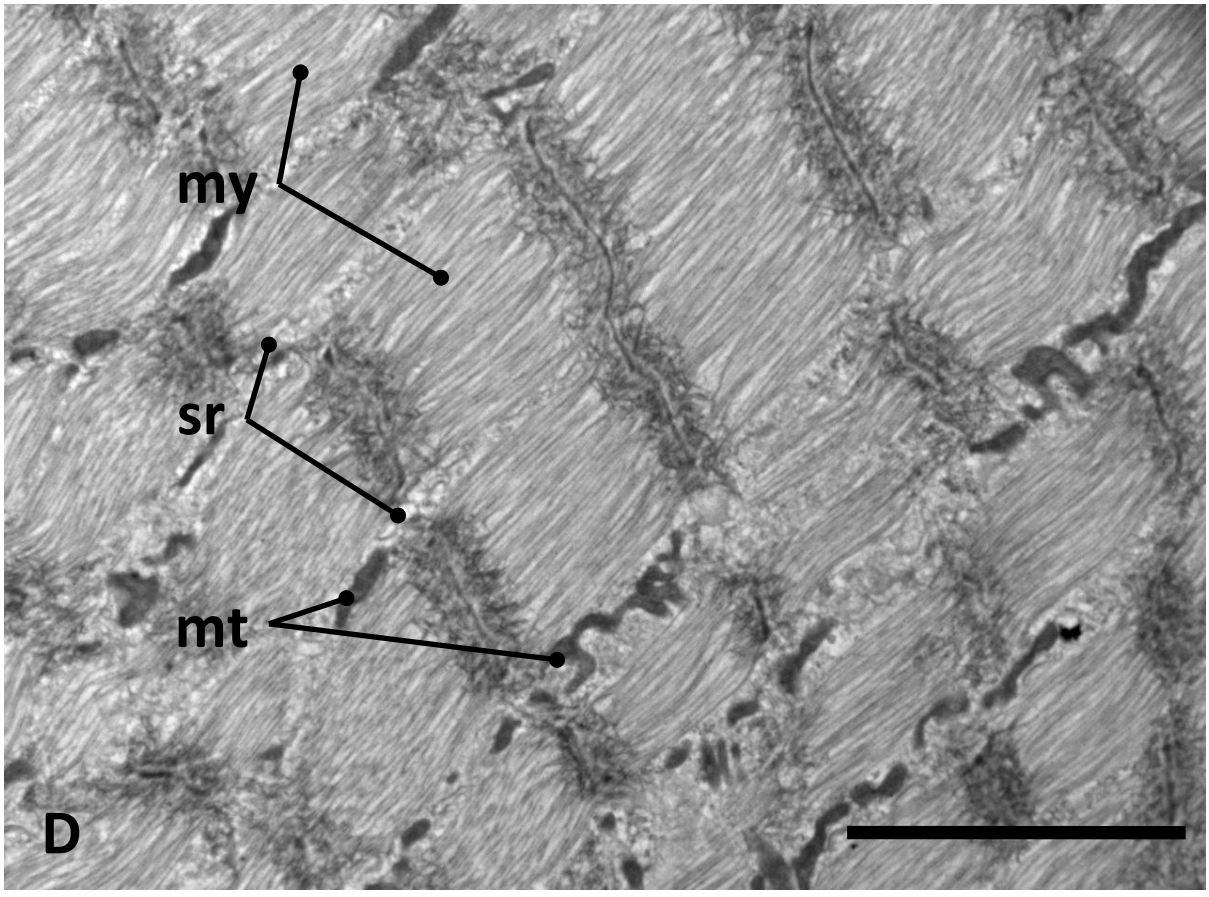
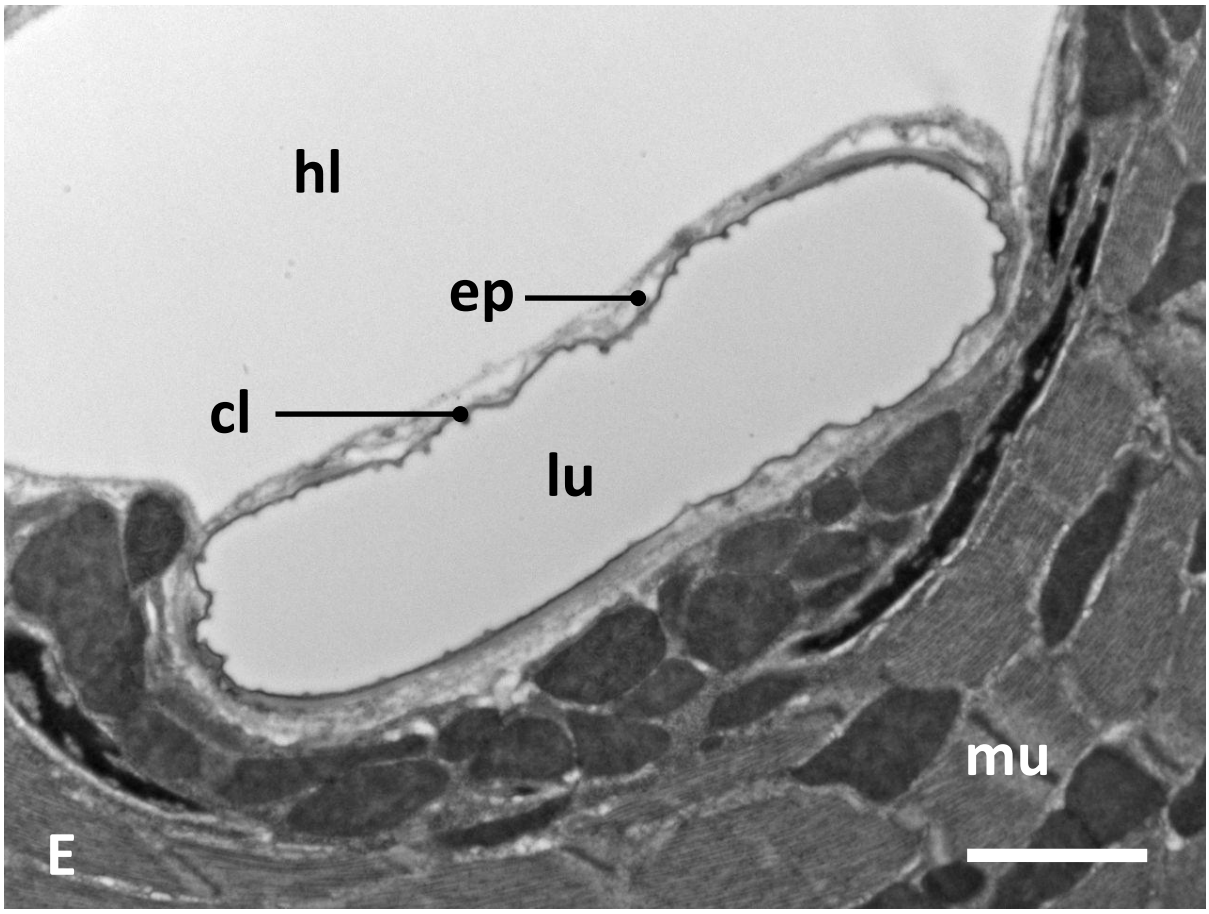

my
sr
mt
D

Fig. 1 (*continued*). C (scale bar = 5 μm) and D (scale bar = 5 μm) are high magnification micrographs showing the ultra-structure of a flight and hopping muscle cell, respectively, from which the volume fraction occupied by mitochondria and myofibril+sarcoplasmic reticulum organelles was calculated.


hl
ep
cl
lu
mu
E

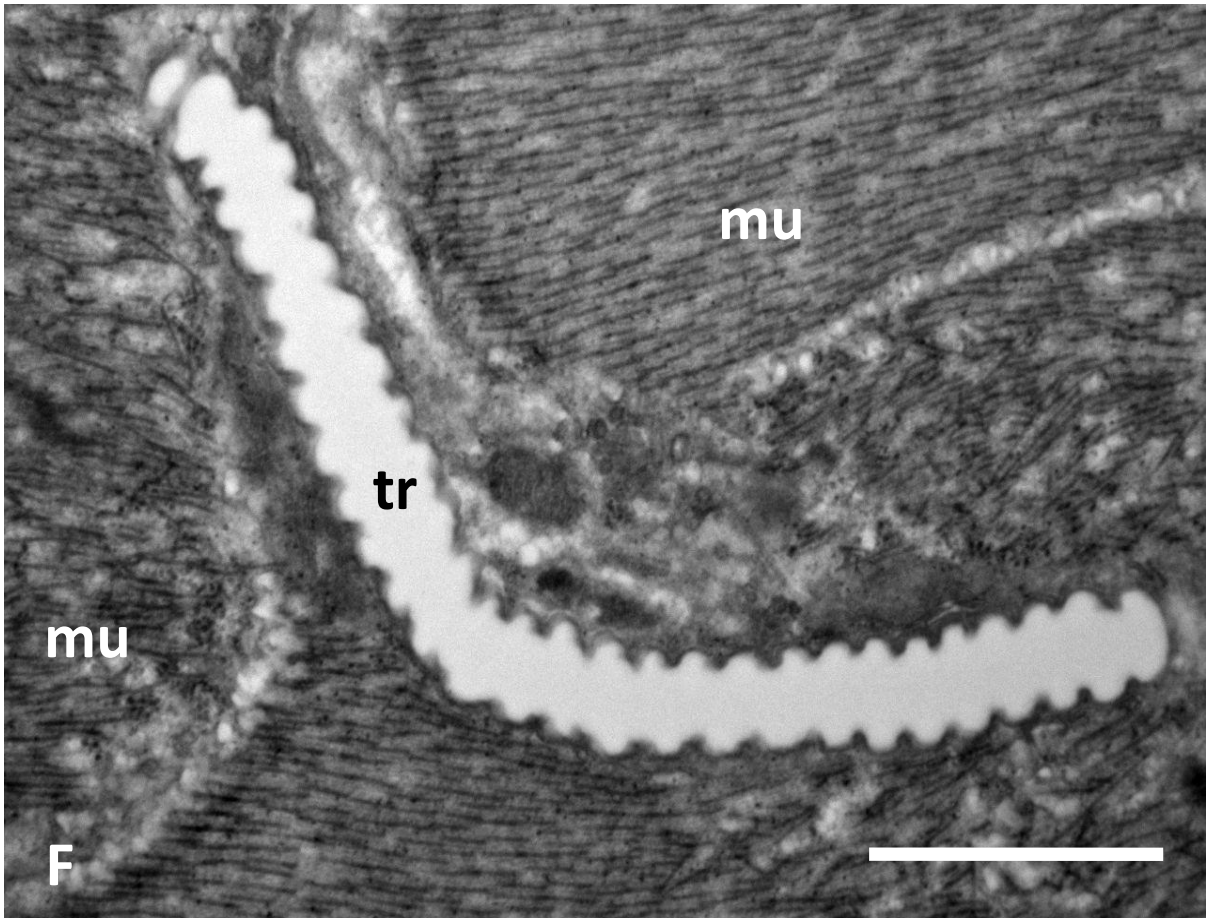

mu
tr
mu
F

Fig. 1 (*continued*). E (scale bar = 2 μm) is a micrograph of a trachea and F (scale bar = 1 μm) is of a tracheole in the flight muscle from which the surface area-to-volume ratio and harmonic mean barrier thickness of the cuticular intima and epidermal layer was calculated.

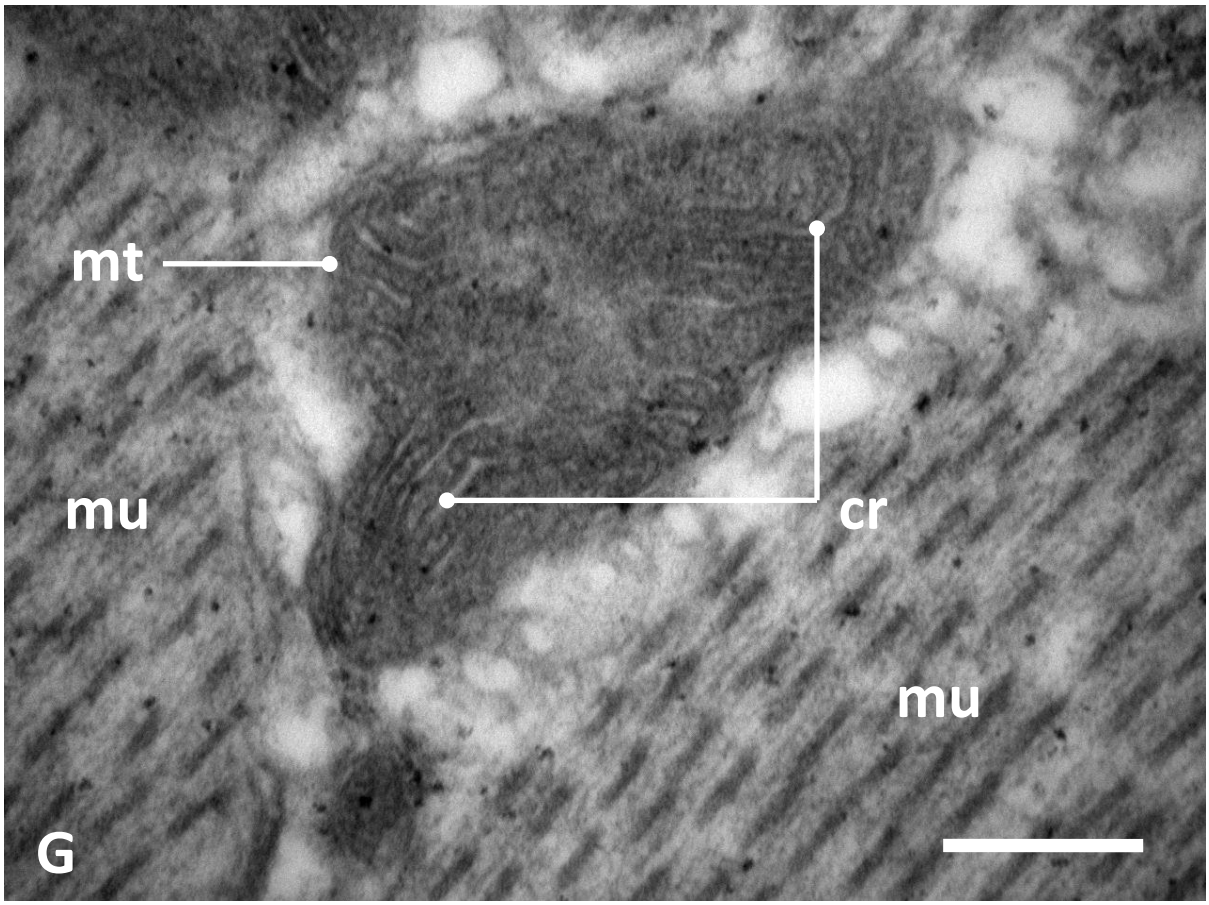


Fig. 1 (*continued*). G (scale bar = 0.2 μm) is a very high magnification image of a random mitochondrion in the flight muscle from which the surface area-to-volume ratio of the inner and outer mitochondrial membrane was calculated.

4.1. Body mass

Adult locusts used for flight muscle morphometry had a mean body mass of 0.935 ± 0.192 g, and adults used for hopping muscle morphometry had a statistically similar mean body mass of 0.816 ± 0.222 g (T-test, P=0.47). There was also no significant difference between the body mass of adult locusts used in the current study and those used in earlier respirometry experiments (ANOVA, P=0.21; and Tukey's post-hoc, P>0.05) (Chapters Two & Three). Nevertheless, body mass-specific values are presented (except for volume density, surface density, and thickness estimates).

4.2. Morphometry

4.2.1. Muscle volume

The flight muscle (Fig. 1A) has a volume of $1.6\times10^{11} \pm 2.1\times10^{10}$ μm^3 g^{-1} body mass, whereas the hopping muscle (Fig. 1B) has a much smaller volume of $5.2\times10^{10} \pm 3.1\times10^{9}$ μm^3 g^{-1}. Assuming a muscle density of 0.94 ml g^{-1} (Mendez and Keys 1960), the mass of the flight muscle is 0.171 ± 0.022 g g^{-1} body mass (17% of body mass), whereas the mass of the hopping muscle is 0.055 ± 0.003 g g^{-1} (6% of body mass). Therefore, the volume (mass) of the flight muscle is 3.1-fold higher than the volume of the hopping muscle (T-test, P<0.05).

4.2.2. Tracheal dimensions

The volume of the tracheal system in the flight muscle is $1.1\times10^{10} \pm 9.7\times10^{8}$ μm^3 g^{-1} body mass, and in the hopping muscle it is $6.0\times10^{9} \pm 1.7\times10^{9}$ μm^3 g^{-1} (Table 2). The outer epidermal layer of the tracheal system in the flight muscle covers an area of $6.9\times10^{9} \pm 1.9\times10^{9}$ μm^2 g^{-1} body mass, and in the hopping muscle the outer epidermal surface area is $2.4\times10^{9} \pm 4.5\times10^{8}$ μm^2 g^{-1}. The inner cuticle layer of the tracheal system covers a smaller area; in the flight muscle it is $6.3\times10^{9} \pm 1.0\times10^{9}$ μm^2 g^{-1} body mass, and in the hopping muscle it is $1.9\times10^{9} \pm 4.3\times10^{8}$ μm^2 g^{-1} (Table 2). Therefore, the volume of the tracheal system is 1.8-fold larger in the flight muscle (T-test, P<0.05), the outer epidermal surface area is 2.9-fold higher in the flight muscle (T-test, P<0.05), and the inner cuticle surface area is 3.4-fold higher in the flight muscle compared to the hopping muscle (T-test, P<0.05).

Class I tracheae (tracheoles) constitute about 7.5% of tracheal system volume in both hopping and flight muscle (Table 2). The percentage of tracheoles internalised within the fibres of the flight muscle is 37 ± 8%, and in the hopping muscle it is 30 ± 16%, which are statistically indistinguishable from each other (Mann Whitney U-test, P=0.10). The volume density of tracheoles in the flight muscle is 0.63 ± 0.07%, and in the hopping muscle it is 0.67

± 0.19%, although the volume density of tracheole lumen in the flight muscle is 0.21 ± 0.05%, and in the hopping muscle it is just 0.10 ± 0.03% (Table 2). So even though the density of tracheoles in the flight muscle is statistically indistinguishable from that of the hopping muscle (T-test, P=0.36), the 2.0-fold higher tracheole lumen density in the flight muscle is statistically significant (T-test, P<0.05).

The total volume of tracheoles in the flight muscle is $1.0\times10^{9} \pm 2.3\times10^{8}$ μm^3 g^{-1} body mass, whereas in the hopping muscle it is $3.4\times10^{8} \pm 8.4\times10^{7}$ μm^3 g^{-1}. However, the tracheole lumen volume is much less; in the flight muscle it is $3.5\times10^{8} \pm 1.2\times10^{8}$ μm^3 g^{-1} body mass, and in the hopping muscle it is just $5.5\times10^{7} \pm 1.8\times10^{7}$ μm^3 g^{-1} (Table 2). Therefore, the total tracheole volume is 2.9-fold higher in the flight muscle compared to the hopping muscle (T-test, P<0.05), whereas the tracheole lumen volume is 6.4-fold higher in the flight muscle compared to the hopping muscle (Mann Whitney U-test, P<0.05).

The tracheole outer epidermal layer covers an area of $4.8\times10^{9} \pm 1.1\times10^{9}$ μm^2 g^{-1} body mass in the flight muscle and $1.6\times10^{9} \pm 3.9\times10^{8}$ μm^2 g^{-1} in the hopping muscle (Table 2). The tracheole inner cuticle layer covers a smaller area; in the flight muscle it is $3.2\times10^{9} \pm 1.1\times10^{9}$ μm^2 g^{-1} body mass, and in the hopping muscle it is $5.0\times10^{8} \pm 1.7\times10^{8}$ μm^2 g^{-1}. Therefore, the surface area of the tracheole outer epidermal layer is 2.9-fold larger in the flight muscle than in the hopping muscle (T-test, P<0.05), whereas the inner cuticle surface area is 6.4-fold larger in the flight muscle compared to the hopping muscle (Mann Whitney U-test, P<0.05).

Class II tracheae represent just 4% of tracheal volume in both flight muscle and hopping muscle, and class III tracheae constitute 16% of tracheal volume in flight muscle and 6% in hopping muscle (Table 2). Most of the tracheal volume, therefore, is taken up by large class IV tracheae, which represent 70% of the tracheal system's volume in the flight muscle, and 84% in the hopping muscle. However, larger tracheae have thicker walls; the harmonic mean barrier thickness of the cuticle layer increases from approximately 0.032 ± 0.005 μm in class I tracheae to 0.39 ± 0.10 μm in class IV tracheae, and the harmonic thickness of the epidermal layer increases from approximately 0.070 ± 0.028 μm in class I tracheae to 0.46 ± 0.16 μm in class IV tracheae in both hopping and flight muscle (Table 3).

Table 2. Inner cuticle and outer epidermal surface area (μm^2 g^{-1} body mass, ± 95% CI) of class I tracheae (tracheoles), and of the entire tracheal system, within the flight muscle (N=3) and hopping muscle (N=3) of the adult locust (i.e. whole pterothorax and both metathoracic femurs). Also shown is the volume density (%, ± 95% CI) of class I tracheae, the volume (μm^3 g^{-1} body mass, ± 95% CI) of class I, II, III, and IV tracheae, and the volume of the entire tracheal system, in the flight and hopping muscle. ⋆Statistically significant.

	Flight muscle	Hopping muscle	Ratio
Class I tracheal inner cuticle surface area	$3.2\times10^{9} \pm 1.1\times10^{9}$	$5.0\times10^{8} \pm 1.7\times10^{8}$	6.4-fold⋆
Class I tracheal outer epidermal surface area	$4.8\times10^{9} \pm 1.1\times10^{9}$	$1.6\times10^{9} \pm 3.9\times10^{8}$	2.9-fold⋆
Total tracheal inner cuticle surface area	$6.3\times10^{9} \pm 1.0\times10^{9}$	$1.9\times10^{9} \pm 4.3\times10^{8}$	3.4-fold⋆
Total tracheal outer epidermal surface area	$6.9\times10^{9} \pm 1.9\times10^{9}$	$2.4\times10^{9} \pm 4.5\times10^{8}$	2.9-fold⋆
Class I tracheal volume density in muscle - lumen only	0.21 ± 0.05	0.10 ± 0.03	2.0-fold⋆
Class I tracheal volume density in muscle	0.63 ± 0.07	0.67 ± 0.19	0.9-fold
Class I tracheal volume - lumen only	$3.5\times10^{8} \pm 1.2\times10^{8}$	$5.5\times10^{7} \pm 1.8\times10^{7}$	6.4-fold⋆
Class I tracheal volume	$1.0\times10^{9} \pm 2.3\times10^{8}$	$3.4\times10^{8} \pm 8.4\times10^{7}$	2.9-fold⋆
Class II tracheal volume	$4.1\times10^{8} \pm 4.2\times10^{8}$	$2.4\times10^{8} \pm 1.5\times10^{8}$	1.7-fold
Class III tracheal volume	$1.8\times10^{9} \pm 8.7\times10^{8}$	$3.8\times10^{8} \pm 1.2\times10^{8}$	4.8-fold⋆
Class IV tracheal volume	$7.7\times10^{9} \pm 1.9\times10^{9}$	$5.0\times10^{9} \pm 1.6\times10^{9}$	1.5-fold
Total tracheal volume	$1.1\times10^{10} \pm 9.7\times10^{8}$	$6.0\times10^{9} \pm 1.7\times10^{9}$	1.8-fold⋆

Table 3. Harmonic mean barrier thickness (μm, ± 95% CI) of the inner cuticle and outer epidermal layer of class I, II, III, and IV tracheae within the flight muscle (N=3) and hopping muscle (N=3) of the adult locust. ⋆Statistically significant.

	Flight muscle	Hopping muscle	Ratio
Class I cuticle	0.034 ± 0.005	0.029 ± 0.002	1.2-fold
Class I epidermis	0.092 ± 0.034	0.047 ± 0.025	2.0-fold
Class II cuticle	0.061 ± 0.008	0.086 ± 0.021	0.7-fold⋆
Class II epidermis	0.187 ± 0.038	0.223 ± 0.116	0.8-fold
Class III cuticle	0.159 ± 0.045	0.143 ± 0.043	1.1-fold
Class III epidermis	0.273 ± 0.020	0.298 ± 0.096	0.9-fold
Class IV cuticle	0.315 ± 0.148	0.465 ± 0.043	0.7-fold
Class IV epidermis	0.463 ± 0.362	0.455 ± 0.064	1.0-fold

4.2.3. Tracheal diffusing capacity and tracheole service area

The anatomical lateral diffusing capacity (lateral conductance) of the entire tracheal system in the flight muscle is 385 ± 158 μmol O_2 kPa^{-1} h^{-1} g^{-1} body mass, and in the hopping muscle it is 82 ± 28 μmol O_2 kPa^{-1} h^{-1} g^{-1} (Table 4); the difference is 4.7-fold (T-test, P<0.05). Tracheoles provide around 80% of the tracheal system's lateral diffusing capacity for oxygen in both the flight muscle and hopping muscle. Therefore, the lateral diffusing capacity of the tracheoles in the flight muscle is 324 ± 144 μmol O_2 kPa^{-1} h^{-1} g^{-1} body mass, and in the hopping muscle it is 63 ± 25 μmol O_2 kPa^{-1} h^{-1} g^{-1} (Table 4); the difference is 5.1-fold (T-test, P<0.05).

The radial diffusing capacity (radial conductance) of the tracheoles is approximately one-third the lateral diffusing capacity (Table 4). In the flight muscle, the tracheole radial diffusing capacity is 113 ± 47 μmol O_2 kPa^{-1} h^{-1} g^{-1} body mass, and in the hopping muscle it is 16.7 ± 6.5 μmol O_2 kPa^{-1} h^{-1} g^{-1}; the difference is 6.8-fold (Mann Whitney U-test, P<0.05). Radial diffusing capacity is lower than lateral diffusing capacity primarily because Krogh's cylinder model for radial diffusion accounts for the extra resistance afforded by the muscle that surrounds each tracheole (Chapter Four), through which oxygen must diffuse. In the flight muscle, each tracheole services a mean transverse area of muscle that is approximately 119 ± 27 μm^2 (radius = 6.1 ± 0.7 μm), and in the hopping muscle the mean tracheole service area is 2-fold larger at approximately 246 ± 70 μm^2 (radius = 8.8 ± 1.3 μm) (T-test, P<0.05).

Table 4. Anatomical radial diffusing capacity (μmol O_2 kPa^{-1} h^{-1} g^{-1} body mass, ± 95% CI) of class I tracheae (tracheoles), and the anatomical lateral diffusing capacity (μmol O_2 kPa^{-1} h^{-1} g^{-1} body mass, ± 95% CI) of class I, II, III, and IV tracheae, and the entire tracheal system, within the flight muscle (N=3) and hopping muscle (N=3) of the adult locust. ⋆Statistically significant.

	Flight muscle	Hopping muscle	Ratio
Class I radial conductance	113 ± 47	16.7 ± 6.5	6.8-fold⋆
Class I lateral conductance	324 ± 144	63 ± 25	5.1-fold⋆
Class II lateral conductance	18 ± 29	5.0 ± 4.9	3.6-fold
Class III lateral conductance	21 ± 15	5.3 ± 3.8	4.0-fold
Class IV lateral conductance	22 ± 13	8.4 ± 4.6	2.6-fold
Total tracheal lateral conductance	385 ± 158	82 ± 28	4.7-fold⋆

4.2.4. Mitochondria

Mitochondria occupy 19.7 ± 0.3% of the flight muscle, and its total volume in the flight muscle is $3.2\times10^{10} \pm 3.9\times10^{9}$ μm^3 g^{-1} body mass (Table 5). In the hopping muscle, the mitochondrial volume density is just 3.1 ± 0.1%, and the total volume is $1.6\times10^{9} \pm 1.4\times10^{8}$ μm^3 g^{-1} body mass. This means that the mitochondrial volume density is 6.4-fold higher in the flight muscle than in the hopping muscle (T-test, $P<0.05$), and the total volume of mitochondria in the flight muscle is 19.8-fold higher compared to that of the hopping muscle (Mann Whitney U-test, $P<0.05$).

Flight muscle mitochondria have an average inner membrane surface density of 31.1 ± 2.3 μm^2 μm^{-3} mitochondria, which is not significantly different from the inner membrane surface density of mitochondria in the hopping muscle, which is 33.0 ± 1.0 μm^2 μm^{-3} (T-test, $P=0.11$) (Table 5). The total surface area of mitochondrial inner membrane in the flight muscle is $9.9\times10^{11} \pm 1.2\times10^{11}$ μm^2 g^{-1} body mass, and in the hopping muscle it is much less, $5.3\times10^{10} \pm 5.9\times10^{9}$ μm^2 g^{-1}. Therefore, the flight muscle has an 18.6-fold larger mitochondrial inner membrane surface area than the hopping muscle (Mann Whitney U-test, $P<0.05$).

The mean outer membrane surface density of mitochondria in the flight muscle is 5.1 ± 1.1 μm^2 μm^{-3} mitochondria, however, the smaller mitochondria of the hopping muscle have a significantly higher mean outer membrane surface density of 12.4 ± 2.2 μm^2 μm^{-3} (T-test, $P<0.05$) (Table 5). The total outer membrane surface area in the flight muscle is $1.6\times10^{11} \pm 4.2\times10^{10}$ μm^2 g^{-1} body mass, and in the hopping muscle it is $2.0\times10^{10} \pm 4.1\times10^{9}$ μm^2 g^{-1}, which represents an 8.2-fold difference (Mann Whitney U-test, $P<0.05$).

Table 5. Volume ($\mu m^3\ g^{-1}$ body mass, ± 95% CI) and volume density (%, ± 95% CI) of the myofibril+sarcoplasmic reticulum complex and mitochondria in the flight muscle (*N*=3) and hopping muscle (*N*=3) of the adult locust. Also shown is the mitochondrial inner and outer membrane surface area ($\mu m^2\ g^{-1}$ body mass, ± 95% CI) and surface density ($\mu m^2\ \mu m^{-3}$ mitochondria, ± 95% CI) in the flight and hopping muscle. ⋆Statistically significant.

	Flight muscle	Hopping muscle	Ratio
Myofibril + s/reticulum volume in muscle	$1.2\times10^{11} \pm 1.6\times10^{10}$	$4.9\times10^{10} \pm 3.0\times10^{9}$	2.5-fold⋆
Mitochondrial volume in muscle	$3.2\times10^{10} \pm 3.9\times10^{9}$	$1.6\times10^{9} \pm 1.4\times10^{8}$	19.8-fold⋆
Myofibril + s/reticulum volume density in muscle	77.2 ± 0.3	94.2 ± 0.2	0.8-fold⋆
Mitochondrial volume density in muscle	19.7 ± 0.3	3.1 ± 0.1	6.4-fold⋆
Mitochondrial inner membrane surface area	$9.9\times10^{11} \pm 1.2\times10^{11}$	$5.3\times10^{10} \pm 5.9\times10^{9}$	18.6-fold⋆
Mitochondrial inner membrane surface density	31.1 ± 2.3	33.0 ± 1.0	0.9-fold
Mitochondrial outer membrane surface area	$1.6\times10^{11} \pm 4.2\times10^{10}$	$2.0\times10^{10} \pm 4.1\times10^{9}$	8.2-fold⋆
Mitochondrial outer membrane surface density	5.1 ± 1.1	12.4 ± 2.2	0.4-fold⋆

5. Discussion

The flight muscle of the adult locust consumes 6.1-fold more oxygen during flight than the hopping muscle consumes during jumping exercise (Chapters Two & Three). However, the 6.1-fold higher metabolic input required for flight is not associated with a proportionately larger muscle volume. Instead, the flight muscle is only 3.1-times larger than the hopping muscle (Fig. 1A,B). This means that during strenuous exercise, 1 ml of flight muscle consumes around twice the amount of oxygen, per unit time, as 1 ml of hopping muscle. From these results, we can predict that if the insect respiratory system complies with the economic design principles of symmorphosis, then the total investment made into structures responsible for the delivery (tracheal system) and consumption (mitochondria) of oxygen should be around 6.1-fold higher in the flight muscle compared to the hopping muscle, and that the density of these respiratory components should be around 2.0-fold higher in the flight muscle compared to the hopping muscle (Weibel et al., 1991; Weibel et al., 1987c).

5.1. Tracheal system and oxygen delivery

The volume of the tracheal system in the flight muscle is around 2-fold larger compared to that of the hopping muscle (Table 2). Likewise, the inner cuticle and outer epidermal surface of the tracheal system both cover an area that is approximately 3-fold larger in the flight muscle than in the hopping muscle (Table 2). The larger dimensions of the tracheal system associated with the flight muscle is consistent with the greater oxygen requirements for flight, although the magnitude of difference falls somewhat short of the 6.1-fold predicted by symmorphosis.

Interestingly, much of the tracheal volume can be attributed to large class IV tracheae and air sacs, which function to ventilate the tracheal system (Westneat et al., 2003; Maina 1989; Weis-Fogh 1967). The absolute volume of class IV tracheae in the flight muscle is just 1.5-fold larger compared to that of the hopping muscle (Table 2). The smaller volume of large class IV tracheae in the flight muscle, relative to aerobic capacity, could be due to the efficiency at which the tracheal system in the flight muscle is auto-ventilated at wing-stroke frequency (Weis-Fogh 1967; Weis-Fogh 1964c). However, this result should also be treated with some caution because the volume of class IV tracheae is likely to decrease appreciably within a given life stage as other tissues grow and compress existing tracheae (Greenlee and Harrison 2004b).

While large class IV tracheae and air sacs are responsible for ventilation, small terminal class I tracheae (tracheoles) function to transfer oxygen from the tracheal system to

the tissue (Chapter Four; Hartung et al., 2004; Schmitz and Perry 2002a; Schmitz and Perry 1999). It is therefore reasonable to suspect that strong selective pressures should influence the design of the tracheoles in such a way that their functional capacity to deliver oxygen is congruent with the maximum oxygen needs of the tissue they service. The results of the present study seem to confirm this, as a close symmorphotic match is evident between the 6.1-fold difference in the aerobic capacity of hopping and flight muscle and the 6.4-fold difference in tracheole lumen volume (Table 2). Physiologically, it is the tracheole lumen volume that is of greatest importance because oxygen delivery along the tracheoles occurs in the gas-phase.

Although the tracheole lumen plays a key role in oxygen delivery, the capacity of the tracheal system to deliver oxygen will also depend upon the dimensions of the tracheole walls, across which oxygen must diffuse. Because tracheoles are more-or-less shaped like a cylinder, the inner cuticle surface covers a smaller area than the outer epidermal surface (Table 2). Logically, it would seem that the inner cuticle layer would therefore have the strongest influence over the maximum oxygen delivery capabilities of the tracheoles, given the capacity of a wall to transmit a gas will be limited by the side of the wall with the smaller surface area. Interestingly, the total tracheole inner cuticle surface area in the flight muscle is 6.4-times larger than in the hopping muscle, and is therefore well matched to the different aerobic capacities of the two muscles (Table 2).

Of course, the thickness of the tracheole walls will also influence the rate at which oxygen can diffuse into the muscle: thicker walls will lead to slower rates of diffusion. The harmonic mean barrier thickness of the tracheole cuticle layer in the hopping muscle is statistically indistinguishable from that of the flight muscle, and likewise, the tracheole epidermal thickness is also similar in both muscles (Table 3). Given the similar thickness of the walls, the anatomical lateral diffusing capacity of the tracheoles to transfer oxygen from one side of the wall, to the other side of the wall, will be largely influenced by the inner cuticle surface area, which is factored into the calculation for lateral conductance (Chapter Four). Accordingly, the lateral diffusing capacity of tracheoles in the flight muscle is 5.1-fold higher than in the hopping muscle, which is roughly congruent with the 6.1-fold difference in the muscle's aerobic capacity during strenuous exercise (Table 4). This provides good evidence for symmorphotic design of the insect tracheal system, since it appears no more tracheole structure exists than is necessary to meet the maximum oxygen requirements of the muscle.

However, the model used to calculate the lateral diffusing capacity for oxygen across the tracheole walls does not account for the extra journey oxygen must take as it diffuses into the muscle surrounding the tracheoles. It is also relevant to consider that the diffusion of oxygen into the surrounding muscle does not occur laterally, but instead follows a radial path, just as oxygen diffuses radially from a capillary source in vertebrate animals. Krogh's cylinder model for radial diffusion therefore offers a more appropriate model on which to estimate the true anatomical diffusing capacity of the tracheoles (Chapter Four; Kreuzer 1982; Krogh 1919). According to this model, each tracheole in the hopping muscle services a 240 μm^2 mean cross-sectional area of muscle (radius of 8.8 μm), whereas in the flight muscle, the mean cross-sectional service area is 120 μm^2 (radius of 6.1 μm). Impressively, nearly 50 years ago Weis-Fogh estimated that in locust flight muscle the maximum radial diffusion distance for oxygen out of a 1 μm diameter tracheole would be around 5.4 μm (Weis-Fogh 1964b). The two-fold larger tracheole service area in the hopping muscle is congruent with the fact that the volume-specific aerobic capacity of hopping muscle is half that of the flight muscle. Therefore, the total anatomical radial diffusing capacity of the tracheoles is 6.8-fold higher in the flight muscle compared to the hopping muscle, and this is well matched to the 6.1-fold difference in the muscle's functional aerobic capacity (Table 4).

The congruency that exists between the muscle's functional aerobic capacity and its tracheole lumen volume, tracheole inner cuticle surface area, and tracheole lateral and radial diffusing capacity, is consistent with the economical design principles of symmorphosis. This finding adds weight to an earlier allometric assessment of the insect tracheal system, where it was established that the increase in the maximum oxygen consumption rate of hopping muscle during juvenile locust development is associated with a proportional increase in the oxygen delivery capabilities of the tracheal system supplying the hopping muscle (Chapter Four). The results of the present study also complement an earlier ontogenetic study on American locusts *Schistocerca americana*, where the convective capacity of large tracheae located between the spiracles and the digestive tract was found to match the metabolic rate of locusts shortly after feeding (Harrison et al., 2005).

5.2. Mitochondria as oxygen sinks

While the function of the tracheal system is to deliver oxygen, the function of mitochondria at the end of the respiratory cascade is to use the oxygen to produce ATP. Mitochondria in the flight muscle tend to be much larger in size than mitochondria in the hopping muscle (Fig. 1C,D), but despite this, their inner membrane surface densities are both approximately 32 μm^2

μm^{-3} (Table 5). Because mitochondrial inner membrane surface densities are similar in hopping and flight muscle, enzyme concentrations within the mitochondria are also likely to be similar, since the protein complexes required for oxidative phosphorylation are embedded in the inner membrane (Suarez 1996).

Given that differences in mitochondrial enzyme concentration are unlikely to contribute towards the difference in aerobic capacity between the flight and hopping muscle, attention can focus on differences in mitochondrial volume between the two muscles. The volume density of mitochondria in the hopping muscle is 3.1%, whereas in the flight muscle, mitochondria occupy 19.7% of muscle volume (Table 5). The 6.4-fold higher mitochondrial volume density in the flight muscle, combined with a 3.1-fold larger muscle mass, leads to a total mitochondrial volume that is 19.8-fold higher in the flight muscle compared to the hopping muscle. Clearly, a 19.8-fold higher mitochondrial volume is disproportionate to the 6.1-fold higher aerobic capacity of the flight muscle, and suggests that the flight muscle is over-supplied with mitochondria by a factor of 3-fold. Therefore, the principles of symmorphosis must be rejected at this final step of the oxygen cascade unless an explanation can be found.

The apparent mismatch between the muscle's functional aerobic capacity and its mitochondrial volume is inconsistent with the results of an earlier allometric study on locusts, where it was shown that the hopping muscle's maximum oxygen consumption rate scales in proportion with the hopping muscle's mitochondrial volume throughout juvenile development (Chapter Four). It is also inconsistent with several studies on mammals, where aerobic capacity appears to be completely dependent on the volume of mitochondria in the skeletal muscles (Weibel et al., 2004; Schwerzmann et al., 1989; Hoppeler et al., 1987; Else and Hulbert 1985; Mathieu et al., 1981).

The lack of congruence between aerobic capacity and mitochondrial volume in the present study demands that all relevant data be closely scrutinised. It seems quite unlikely that either flight or hopping respirometry estimates could be wrong by a factor of 300%, given they correspond well with other published data, and also considering that additional steps were taken to maximise the work rate of the locomotory muscles through the attachment of weights to exercising locusts (Chapters Two & Three). Likewise, it also seems unlikely that Cavalieri calculations for muscle volume could be wrong by 300%. To confirm its accuracy, if the Cavalieri-derived flight muscle volume is converted to a mass estimate assuming a density of 0.94 ml g^{-1} (Mendez and Keys 1960), it is evident that flight muscles represent around 17% of body mass, which aligns well with 18% estimated for the adult desert locust

Schistocerca gregaria (Weis-Fogh 1952). The only other source of potential error is in the calculation of mitochondrial volume density; however this too seems unlikely given that the 19.7% mitochondrial density estimated for flight muscle in the present study is consistent with the 20-25% density estimated for flight muscle in the adult gray bird grasshopper *S. nitens* (Mizisin and Ready 1986). Likewise, the 3% mitochondrial density estimated for hopping muscle in the present study is consistent with the 4% density estimated for hopping muscle in the adult American locust (Hartung et al., 2004). Given that both respirometry and morphometry data align closely with other reports in the literature, the lack of symmorphotic congruence between aerobic capacity and mitochondrial volume appears to be a genuine phenomenon.

Explanations for this apparent over-investment in mitochondria are speculative at this stage. One possibility is that the disproportionately high volume density of mitochondria in the flight muscle could serve to reduce mean diffusion distances for ATP, ADP and inorganic phosphate (Pi), which cycle between mitochondria and the myofibril-sarcoplasmic reticulum complex during exercise (Suarez 2003; Ellington 2001; Suarez 1996). The hopping muscle, on the other hand, might function with relatively smaller and sparsely distributed mitochondria due to the presence of arginine kinase, since maximum activity levels of this enzyme are 3.5-fold higher in locust hopping muscle than flight muscle (Newsholme et al., 1978). During exercise, arginine kinase is thought to increase the overall flux of high-energy phosphate in muscle cells via a process of facilitated diffusion whereby both ATP and phosphoarginine diffuse out of the mitochondria towards the myofibrils and sarcoplasmic reticulum (Kinsey et al., 2011; Ellington 2001; Schneider et al., 1989). Potentially, this process could be facilitated by the high outer membrane surface density of mitochondria in the hopping muscle (Table 5). If this hypothesis is correct, then arginine kinase in the hopping muscle is responsible for increasing the volume-specific output of the mitochondria, and it allows the hopping muscle to function with relatively less mitochondria and longer average diffusion distances for ATP, ADP, and Pi. Certainly, muscles that are built for peak force production, such as those used to power hopping, would benefit from a low mitochondrial volume density because it increases space available for myofibril contractile machinery, whereas muscles that require a reliable, constant, and long-term source of ATP, such as flight muscle, might instead benefit from a high volume density of mitochondria.

5.3. Summary

This study has demonstrated that the difference in aerobic capacity between the hopping and flight muscle of locusts is matched by a proportional difference in tracheole lumen volume, tracheole inner cuticle surface area, and tracheole lateral and radial diffusing capacity. This suggests that no more tracheal structure exists than is necessary to meet the maximum oxygen needs of the muscle, and therefore, provides strong evidence that the insect tracheal system conforms to the economic design principles of symmorphosis. This conclusion is in agreement with our earlier allometric ontogenetic assessment of the locust tracheal system (Chapter Four).

However, this study has also found that the difference in aerobic capacity between the hopping and flight muscle is not matched by an equivalent difference in the volume of mitochondria in the two muscles. In fact, the flight muscle appears to be over-supplied with mitochondria by a factor of 3-fold. Although our earlier allometric examination found good matching between the volume of mitochondria and its functional capacity in the locust hopping muscle (Chapter Four), the results of the present study suggest that symmorphosis should be rejected at this final step of the oxygen cascade unless an explanation can be found. Potentially, the high concentration of arginine kinase in locust hopping muscle could maximise the mitochondria's functional output, thereby allowing the hopping muscle to function despite having relatively small and sparsely distributed mitochondria.

Finally, it should be recognised that while the present study searches for simple proportional relationships between structural investment and functional capacity as a means to test for symmorphosis in the insect respiratory system, it would be instructive to complement such research with additional measurements that search for hidden excess capacities by manipulating ambient oxygen partial pressure on exercising locusts. If maximum oxygen uptake increased significantly under hyperoxia then it would suggest an over-supply of mitochondria, and if maximum oxygen uptake was maintained under moderate hypoxia then it would suggest an over-investment in the tracheal system. The results of this type of study would provide a direct test of whether or not the maximum functional capacity of mitochondria to consume oxygen is matched by the maximum functional capacity of the tracheal system to deliver it. Potentially, the apparent 3-fold excess aerobic capacity of mitochondria in the locust flight muscle might be functionally realised during flight under an ambient oxygen partial pressure of 63 kPa.

6. Acknowledgements

This research was supported by the Australian Research Council, project no. DP0879605. Mr Kerry Gascoigne and Dr Mike Teo of Flinders Microscopy and Ms Ruth Williams and Ms Lyn Waterhouse of Adelaide Microscopy shared their expertise in the field of electron microscopy, which was greatly appreciated.

Chapter Six: Discussion

Symmorphosis and the insect respiratory system

Insects achieve higher mass-specific aerobic metabolic rates than any other animal, yet there is still significant variation that exists between individuals, which can be attributed to allometric variation due to the influence of body mass and locomotor variation due to the different energy requirements for flight versus terrestrial locomotion. Throughout the lifecycle of the locust, both sources of variation are evident, since maximum oxygen consumption rate of the hopping muscle increases significantly throughout ontogeny, and upon reaching adulthood, the development of highly aerobic flight muscles provides a metabolic contrast with the hopping muscle. The aim of this thesis was to determine whether the locust respiratory system conforms to Taylor and Weibel's theory of symmorphosis, such that variation in the aerobic capacity of locust hopping and flight muscle is associated with equal variation in tracheal volume, tracheal surface area, tracheal diffusing capacity, mitochondrial volume, and mitochondrial inner membrane surface area in the two muscles (Weibel et al., 1998; Weibel et al., 1991).

Measuring maximum oxygen flux through the insect respiratory system

To determine whether the locust respiratory system conforms to the principles of symmorphosis, it was first necessary to measure the maximum oxygen consumption rate of the hopping and flight muscles. In other animals, the aerobic limit is determined as the point at which further increases in exercise intensity are met entirely by anaerobic respiration, which is evident by a rise in lactic acid levels (Taylor et al., 1987a; Seeherman et al., 1981). The maximum oxygen consumption rate of insects is a little more difficult to establish because there is often minimal reliance on anaerobic metabolism owing to the effectiveness at which the tracheal system supplies oxygen. In locusts for example, although lactate is produced during the initial 2 min of hopping, thereafter it is apparently a predominantly aerobic process (Kirkton et al., 2005; Harrison et al., 1991), and flight is thought to be entirely aerobic (Beenakkers et al., 1981; Worm and Beenakkers 1980).

The capacity of the tracheal system to deliver oxygen requires that additional steps are taken to ensure near maximum rates of aerobic respiration are achieved. In this thesis, gas exchange was measured in locusts at selected developmental stages while they performed intense hopping exercise, and then the experiments were repeated on a second cohort of locusts that had a weight affixed to the prothorax (Chapter Two). It was reasoned that the additional energy required to carry the weight might induce an increase in oxygen uptake.

However, locusts forced to hop with a weight had similar maximum oxygen consumption rates as those exercised without a weight, which suggests that both weighted and unweighted individuals were probably operating at or near their aerobic limits during exercise, and if weights did induce an increase in overall energy expenditure, then it was likely achieved using anaerobic pathways. Any number of factors could set the functional aerobic metabolic limit of the jumping muscles, including the capacity to deliver and utilise oxygen and metabolic substrate, or even the mechanical limits of the myofibril machinery or associated nervous system. If a single factor is responsible for limiting hopping metabolic rate, then it follows that all other components of the jumping system are present in excess. Alternatively, symmorphosis predicts that all structures involved in hopping are quantitatively matched to the functional capacity of the entire system, such that no single component limits maximum oxygen consumption rate (Weibel et al., 1998; Weibel et al., 1991).

Ascertaining the maximum oxygen consumption rate of locusts during flight presents its own set of unique challenges. Previous estimates of locust flight metabolism are relatively modest compared to other insect groups. For instance, a 1 g locust might typically consume around 1000 μmol O_2 g^{-1} h^{-1} during flight, whereas a similar sized bee or moth often exceeds 2000 to 3000 μmol O_2 g^{-1} h^{-1} (Casey et al., 1985; Bartholomew and Casey 1978). Potentially, this might be an artefact of the need to tether locusts for flight measurements, as this is known to interrupt sensory feedback loops and induce unnatural flight behaviour (Kutsch et al., 1999; Preiss and Gewecke 1991; Dudley and Ellington 1990; Zarnack and Wortmann 1989). To test this, gas exchange was measured in adult locusts as they performed tethered flight exercise, and then the experiments were repeated on individuals with a small weight affixed to each wing (Chapter Three). Similar to the reasoning behind attaching weights to hopping locusts, the extra effort required per wing-stroke might reveal untapped metabolic potential. However, the addition of weights once again failed to induce an increase in maximum oxygen consumption rate, and gas exchange rates were generally in agreement with measurements from earlier studies (Rascon and Harrison 2005; Armstrong and Mordue 1985; Weis-Fogh 1967), which suggest that locusts were probably flying near their aerobic limits.

To further explore whether locusts were physically exerting themselves during tethered-flight, lift and wing-stroke frequency was measured in a third cohort of locusts (Chapter Three). On average, locusts produced enough lift to support 90% of body mass, and the confidence interval for this measurement overlaps with 100%, which equates to level flight. Furthermore, the study recorded an average wing-stroke frequency of 24 Hz and this aligns well with estimates from free-flying locusts, which are around 23 Hz (Baker et al.,

1981). Given the similarity in lift and wing-stroke frequency between tethered locusts in the current study and free-flying locusts, and also the fact that weights failed to increase oxygen uptake during flight, it seems likely that locusts were exerting themselves to the extent that near-maximum aerobic metabolic rates were attained. This confirms initial observations that locusts appear to consume less energy during flight compared to other insects. Previous authors have linked low flight metabolic rates with low wing-stroke frequency (Harrison et al., 1996; Casey et al., 1985; Casey et al., 1981; Curtsinger and Laurie-Ahlberg 1981; Bartholomew and Casey 1978) and low wing-loading (May 1981; Casey 1976; Bartholomew and Heinrich 1973; Heinrich 1971), both of which apply to locusts. However, it is also reasonable to suspect that the energetics of insect flight, together with wing-loading and wing-stroke frequency, might also correlate with the size and efficiency of the insect flight motor. Interestingly, locust flight muscle represents just 17% of body mass (Chapter Five), which compared to other insects is at the low end of a range that spans 17-56% (Marden 1987). Small flight muscles are of course less expensive to build and maintain than comparatively larger flight muscles, and this could free-up energy for other requirements, particularly reproduction. However, the trade-off of having a small flight motor is reduced flight performance evident by locusts' apparent inability, or need, to lift heavy loads, hover in still air, compete in aerial mating challenges, initiate flight solely under the power of the flight muscles, or overcome low muscle temperatures (Marden 2000).

Design of the insect tracheal system

With the functional aerobic limits of the hopping and flight muscle established, it was then asked whether the amount of respiratory structure involved in the delivery and consumption of oxygen occur in proportional quantities, as predicted by symmorphosis. For most terrestrial vertebrates, the lung represents the interface between the environment and the internal components of the respiratory system, and it has been demonstrated that mammals appear to have more lung structure than required to satisfy maximum oxygen demands during exercise (Canals et al., 2010; Hsia et al., 1992; Gehr et al., 1981). This excess lung structure seems to be more pronounced with increasing body size, which could be an adaptation to counter a lower oxygen pressure head for diffusion across the alveoli wall in larger mammals (Gehr et al., 1981; Weibel et al., 1981b). A similar problem with oxygen delivery down long tracheal tubing is also thought to occur in large insects (Kaiser et al., 2007). In fact, oxygen diffusion limitation in large insects is central to the idea that prehistoric insect gigantism was facilitated by hyperoxic atmospheres that occurred during the late Palaeozoic (Dudley 1998;

Graham et al., 1995). Therefore, analogous to what occurs in mammals, there might be a disproportionate investment in tracheal structure with increasing insect body size in order to counter a lower oxygen pressure head for diffusion across the tracheal walls.

To determine whether there is a relative over-supply of tracheae with increasing insect body mass, or whether the tracheal system is designed to match the maximum aerobic needs of the muscle, as predicted by symmorphosis, the dimensions of the tracheal system within the locust hopping femur were quantified throughout juvenile development and then analysed allometrically (Chapter Four). Interestingly, the results lend support to the idea that larger insects might face additional challenges in delivering oxygen. While the aerobic capacity of the hopping muscle scales with an exponent of $M_b^{1.02}$, the volume of the tracheal system servicing the hopping muscle scales with a significantly steeper exponent of $M_b^{1.12}$, which means that larger locusts have disproportionately more tracheae. Furthermore, the volume of air sacs and other large tracheae thought to function in tracheal ventilation (Westneat et al., 2003; Maina 1989; Weis-Fogh 1967), scale with an even higher exponent of $M_b^{1.16}$, which further suggest that larger locusts encounter limitations with oxygen diffusion.

However, the transfer of oxygen from the tracheal system to the muscle occurs almost entirely at the terminal tracheoles. Importantly, it was shown that the total lumen volume of the tracheoles increases with body mass with an exponent of $M_b^{0.99}$, which is congruent with the scaling of aerobic capacity. In fact, the total inner surface area of the tracheoles, the lateral diffusing capacity of the tracheoles, and the radial diffusing capacity of the tracheoles, all scale in parallel ($M_b^{0.99}$) with the hopping muscle's maximum oxygen consumption rate. This suggests that the increasing oxygen requirements of the hopping muscle throughout development are satisfied by a proportional amount of tracheole structure, which provides strong evidence that the tracheal system is designed according to the principles of symmorphosis.

Exploiting the increase in hopping muscle aerobic capacity throughout development is one way to test for symmorphosis, the other way is to take advantage of the vast difference in energy expenditure of adult flight muscle compared to adult hopping muscle. If the insect tracheal system conforms to symmorphosis then the difference in aerobic capacity between the flight and hopping muscle should be matched by a similar difference in the amount of tracheal structure in the two muscles. In mammals, it has been shown that nonathletic species have more lung structure than athletic species, relative to maximum aerobic needs (Weibel et al., 1987a), and that all mammals appear to have more lung and pulmonary capillary structure than they require to saturate the blood with oxygen (Karas et al., 1987a). Potentially, the

oversupply of lung tissue could represent a safety factor that allows mammals to tolerate hypoxia, as would occur at high altitudes (Taylor et al., 1987b). In this respect, a similar phenomenon could occur in insects, in that locust flight muscle might be relatively over-supplied with tracheoles given it is more likely to operate at higher altitudes than hopping muscle.

To determine whether the flight muscle is relatively over-supplied with tracheoles, or whether the abundance of tracheoles matches the muscle's maximum oxygen requirements, as predicted by symmorphosis, the morphology of the tracheal system was quantified within the flight and hopping muscle of adult locusts (Chapter Five). It was shown that the tracheal system is almost perfectly matched to the muscle's maximum oxygen needs, such that the 6.1-fold higher aerobic capacity of the flight muscle is associated with a 6.4-fold higher tracheole lumen volume, a 6.4-fold higher tracheole inner surface area, a 5.1-fold higher tracheole lateral diffusing capacity, and a 6.8-fold higher tracheole radial diffusing capacity. The matching between structure and function suggests that both the hopping and flight muscle have enough, but not too much, tracheal structure. Therefore, both the allometric analysis and the comparison between flight and hopping muscle suggest that the tracheal system adheres to the economic design principles of symmorphosis.

Design of the insect mitochondrial sink

Once oxygen is delivered to the muscle by the tracheal system, it is used and ultimately consumed by mitochondria in the synthesis of ATP via oxidative phosphorylation. According to symmorphosis, the amount of mitochondria present within the muscle should relate directly to the aerobic capacity of the muscle. Indeed, this has been well documented in mammals, where mitochondrial volume is strictly proportional to maximum oxygen consumption rate, such that oxygen uptake per unit volume of mitochondria is highly conserved across body mass and athletic ability (Weibel et al., 2004; Weibel et al., 1992; Weibel et al., 1991; Hoppeler et al., 1987; Mathieu et al., 1981).

To test whether a similar relationship between mitochondria and aerobic capacity occurs in insects, an allometric analysis was performed on the dimensions of the mitochondrial sink in the hopping muscle of locusts throughout juvenile development (Chapter Four). The results of this study found that the total volume of mitochondria in the hopping muscle increases with body mass with an exponent of $M_b^{1.02}$, and the total surface area of inner mitochondrial membrane increases with an exponent of $M_b^{0.99}$, both of which are in direct proportion to the scaling of the hopping muscle's maximum oxygen consumption

rate, $M_b^{1.02}$. This suggests that the amount of mitochondria in the hopping muscle is matched to the muscle's aerobic capacity, and therefore provides strong evidence that symmorphosis has acted upon the evolutionary design of the mitochondrial sink.

The final test for symmorphosis was to determine whether the highly aerobic locust flight muscle is complemented with proportionately more mitochondria. To make this assessment, the volume and inner membrane surface area of mitochondria was quantified in the hopping and flight muscle of adult locusts (Chapter Five). Surprisingly, the 6.1-fold higher maximum oxygen consumption rate of the flight muscle is associated with a 19.8-fold higher volume of mitochondria, and an 18.6-fold larger inner membrane surface area. Clearly, there is a mismatch between the amount of mitochondria in the muscle and the aerobic capacity of the muscle. In fact, every microlitre of mitochondria in the flight muscle operates at around one-third the maximum functional capacity as every microlitre of mitochondria in the hopping muscle. Therefore, symmorphosis must be rejected at this final step of the oxygen cascade unless a satisfactory reason can be found.

At this stage, explanations for this apparent mismatch between structural investment and functional capacity remain speculative. However, it seems possible that the disproportionate volume of mitochondria in the flight muscle might serve to reduce the mean diffusion distance for ATP, ADP and inorganic phosphate (Pi) (Suarez 2003; Ellington 2001; Suarez 1996). Short diffusion distances might allow these molecules to flux at a high rate between the mitochondria and the myofibrils and sarcoplasmic reticulum during flight. However, if hopping muscle can function with a relatively low mitochondrial volume density, then why can't flight muscle? A possible answer to this question could lie in the different biochemistries of the two muscles. It has been established that the enzyme, arginine kinase, is 3.5-fold more active in locust hopping muscle than in locust flight muscle (Newsholme et al., 1978). This is of significant interest because arginine kinase is thought to maintain and facilitate the availability of ATP in muscle by shuttling high-energy phosphate out of the mitochondria in the form of ATP and in the form of phosphoarginine (Kinsey et al., 2011; Ellington 2001; Schneider et al., 1989; Newsholme et al., 1978). Potentially, this process of facilitated diffusion could in turn make available more ADP and Pi at the site of the mitochondria, which could increase rates of oxidative phosphorylation, and therefore increase rates of oxygen consumption. If this is correct, then it might explain how mitochondria in the hopping muscle are able to achieve volume-specific rates of oxygen consumption that are 3-fold higher than mitochondria in the flight muscle.

Conclusion

The principles of symmorphosis are upheld with respect to the design of the tracheal system on two fronts – in response to the growing oxygen needs of the locust hopping muscle throughout development, and in response to the vastly different oxygen requirements of the flight muscle compared to the hopping muscle. Symmorphosis is also upheld with respect to the amount of mitochondria in the hopping muscle throughout development, such that mitochondrial volume is strictly proportional to the hopping muscle's maximum oxygen needs. However, the finding that mitochondria in the flight muscle operate at around one-third the maximum functional capacity of mitochondria in the hopping muscle, suggest that the flight muscle is over-supplied with mitochondria by a factor of 3-fold. Therefore, symmorphosis must be rejected at this final step of the oxygen cascade. Potentially, the high volume density of mitochondria in the flight muscle might function to reduce the ATP, ADP and Pi diffusion distances in response to a lack of arginine kinase, which in the hopping muscle, is thought to increase the overall diffusive flux of high energy phosphates from the mitochondria to the myofibrils and sarcoplasmic reticulum during exercise.

Appendix: Moulting of insect tracheae captured by light and electron-microscopy in the metathoracic femur of a third instar locust *Locusta migratoria*

Preamble

The following appendix forms the basis of a published co-authored manuscript* and is reproduced with permission from the *Journal of Insect Physiology*. Snelling fixed the tissue, collected the images and wrote the manuscript. Seymour provided valuable advice and helped synthesise ideas discussed in the paper, and Runciman provided assistance with tissue fixation techniques and electron microscopy. They both give permission** for the inclusion of the manuscript in the thesis.

*Snelling EP, Seymour RS, Runciman S (2011) Moulting of insect tracheae captured by light and electron-microscopy in the metathoracic femur of a third instar locust *Locusta migratoria*. *Journal of Insect Physiology* **57**, 1312-1316.

**Signatures of co-authors:

Roger Seymour

Sue Runciman

1. Abstract

The insect tracheal system is an air-filled branching network of internal tubes that functions to exchange respiratory gases between the tissues and the environment. The light and electron-micrographs presented in this study show tracheae in the process of moulting, captured from the metathoracic hopping femur of a juvenile third instar locust *Locusta migratoria*. The images provide evidence for the detachment of the cuticular intima from the tracheal epithelial cells, the presence of moulting fluid between the new and old cuticle layers, and the withdrawal of the shed cuticular lining through larger upstream regions of the tracheal system during moulting. The micrographs also reveal that the cuticular intima of the fine terminal branches of the tracheal system is cast at ecdysis. Therefore, the hypothesis that tracheoles retain their cuticle lining at each moult may not apply to all insect species or developmental stages.

2. Introduction

The insect tracheal system functions to exchange respiratory gases between the atmosphere and the tissue (Wigglesworth 1965). The pathway for oxygen begins with its diffusion into the spiracle openings, where it is then delivered in the gas-phase along an internal system of successively smaller tracheal tubes (Fig. 1), the terminal branches of which are commonly referred to as tracheoles. Oxygen diffuses across the tracheole walls and into the surrounding tissue where it is consumed by mitochondria during aerobic respiration (Wigglesworth 1983; Whitten 1972; Wigglesworth 1965).

The maximum rate that oxygen can be delivered along the tracheal system is at least equal to the maximum rate it is required for aerobic metabolism, because even during heavy exercise there is little accumulation of anaerobic products (Beenakkers et al., 1981; Worm and Beenakkers 1980; Sacktor 1976). The tracheal system also keeps pace with increasing oxygen demands of the insect throughout ontogeny, and we now have a good understanding of the developmental processes involved. The basic plan of the tracheal system is laid out during embryogenesis when major tracheae arise from epithelial sacs composed of tracheal precursor cells (Ghabrial et al., 2003; Manning and Krasnow 1993). In *Drosophila* at least, the embryonic growth of major tracheae occurs solely by cell migration and elongation (Samakovlis et al., 1996), and it is not until egg hatching that the terminal tracheoles really begin to develop in the juvenile instar (Ghabrial et al., 2003; Manning and Krasnow 1993). Impressively, the tracheoles react and grow towards signals produced by oxygen-starved cells (Jarecki et al., 1999; Guillemin et al., 1996; Wigglesworth 1954). Experiments performed mostly on *Rhodnius* have shown that when a major trachea is severed, or if a metabolically active organ is implanted into the insect body, nearby tracheoles are pulled by epidermal filaments to service the hypoxic tissue, and if the insect is then given the opportunity to moult, the intrusion and proliferation of tracheoles is even more extensive (Manning and Krasnow 1993; Wigglesworth 1977; Wigglesworth 1959; Locke 1958a; Wigglesworth 1954; Wigglesworth 1953).

The growth and proliferation of hypoxic-seeking tracheoles is not the only mechanism insects use to enhance oxygen delivery capacities during development. Insects also significantly increase the size of the tracheal system with each moult. This is achieved through the synthesis of new tracheal tubes that are cemented onto the system, and by a substantial increase in the volume of existing tracheae (Manning and Krasnow 1993; Wigglesworth 1981; Wigglesworth 1973; Locke 1958b; Wigglesworth 1954; Keister 1948). Existing tracheae increase in size as the epithelial cells divide and multiply (Wigglesworth

1981; Ryerse and Locke 1978), although in *Drosophila* larvae it might solely be due to changes in cell shape and size (Manning and Krasnow 1993; Madhavan and Schneiderman 1977). Either way, the diameter of the tracheal wall increases, and as this occurs the cuticular intima becomes detached from the epithelial layer in a process known as apolysis (Wigglesworth 1973). The exuvial space between the new wall and the shed cuticular intima fills with moulting fluid (Jungreis 1974; Passonneau and Williams 1953), and a new cuticle begins to line the new and larger tracheae (Ryerse and Locke 1978). The old cuticular intima is then withdrawn through the tracheal system towards the spiracles where it is shed along with the rest of the exuviae at ecdysis. To complete the moulting process, moulting fluid is resorbed by the epithelial layer (Lensky and Rakover 1972) and the lumen of the new and more extensive tracheal system fills with air (Wigglesworth 1981; Ryerse and Locke 1978; Locke 1958b; Keister 1948).

Although the process of tracheal apolysis and ecdysis is fairly well established, there is confusion over whether or not the cuticular intima of the tracheoles is shed along with the rest of the tracheal system at moulting. Apparently, tracheoles in *Rhodnius* remain unchanged throughout their lifecycle (Wigglesworth 1973), and in *Bombyx*, the tracheoles also appear to retain their cuticle with each moult, at least in the first three larval stages (Matsuura and Tashiro 1976). However, earlier studies on *Sciara* (Keister 1948) and *Drosophila* (Whitten 1957) using phase-contrast optical microscopy found that the cuticular intima of tracheoles is shed in the early larval stages, but not in the final larval or pupal moults. Keister (1948) suggested that partial moulting might take place in complex tracheal systems, especially when tracheoles penetrate the surface of other cells, and complete moulting might only occur in insects with relatively simple tracheal systems.

High magnification electron micrographs of tracheoles in the process of moulting have never been captured and published, and so the early claims made by Keister (1948) and Whitten (1957), that in some insects at least, the tracheoles do in fact shed their cuticular lining remain unsubstantiated. The purpose of the current paper is to present a series of light and electron-micrographs captured from the metathoracic femur of a third instar migratory locust *Locusta migratoria* that provide unequivocal evidence that some tracheoles shed their cuticle lining at moulting.

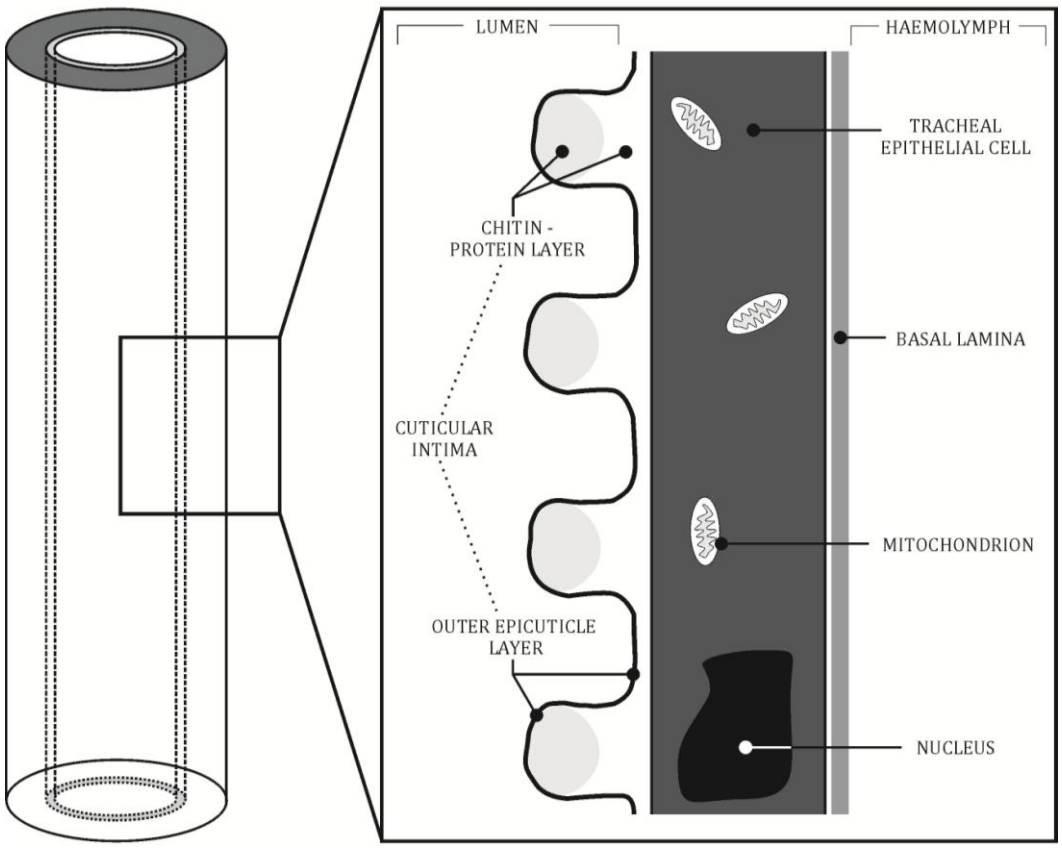


Fig. 1. Diagram of an insect trachea showing the outer epicuticle layer, the chitin-protein matrix layer, the epithelial layer, and the basal lamina (after Wigglesworth 1965; Locke 1957). In smaller tracheae, the thickness of the respective layers is much reduced, and the chitin-protein complex is often absent. In very small terminal tracheae (tracheoles) the epithelial layer may also be absent.

3. Methods

The locust reported in the current study was a single third instar gregarious-phase nymph, three to four days post-moult, of the species *Locusta migratoria*. It was sourced from a breeding colony at the University of Adelaide, Australia, where locusts were reared in a large terrarium at 33 ± 1°C, with a relative humidity of ~30%, under a 12:12 h light-dark cycle, with *ad libitum* access to seedling wheatgrass and wheat germ. When the locust was taken from the colony, it displayed no apparent visual indication that it was in the initial stages of moulting, and was simply part of a much larger cohort of approximately 20 locusts processed for electron microscopy.

The procedure used to dissect and fix locust tissue was modified based on the methods of previous electron microscopy studies of insects and spiders (Biserova and Pfluger 2004; Hartung et al., 2004; Kohnert et al., 2004; Schmitz and Perry 2002a; Schmitz and Perry 2002b). Initially, the locust was fasted for 6-10 h, before it was cold anaesthetised for 20 min in a refrigerator at 4°C. Both metathoracic femurs were carefully removed with angled spring

scissors and then a razor was used to slice each femur along the transverse plane into six equal length tissue pieces. The femur pieces were immediately immersed into a chemical fixative solution of 2.5% glutaraldehyde and 2% formaldehyde in 0.2 M phosphate buffer with pH 7.4, and left overnight in a refrigerator at 4°C. On the second day, each piece was given a series of buffer rinses; the first rinse was 20 min followed by four, 60-min rinses. Then there were three, 20-min distilled water rinses and then the tissue was placed into a 1% aqueous solution of osmium tetroxide for secondary fixation and left overnight at room temperature. On the third day, each piece was given five, 20-min rinses in distilled water and then placed into a 2% aqueous solution of uranyl acetate and left overnight at room temperature. On the fourth day, the pieces were given four, 20-min rinses in distilled water and then dehydrated in ethyl alcohol in 10% incremental steps starting from 50% to 80%, each for 20 min. The tissue was then further dehydrated in consecutive, 20-min immersions in 90% ethanol (×2), 100% ethanol (×2), and finally pure propylene oxide (×2). Following dehydration, the samples were incrementally infiltrated with embedding resin (Durcupan, Fluka, Buchs, Switzerland) at ratios of 3:1, 2:2, 1:3 (propylene oxide : resin) each for a duration of 60 min, and then left overnight at room temperature in pure resin. On the fifth day, each piece was aligned longitudinally and in a proximal to distal orientation in individually labelled embedding moulds where they were covered with pure embedding resin and left to polymerise in a 70°C oven for 48 h.

One metathoracic femur was then randomly selected for light microscopy analysis. Twelve parallel, transverse and equidistant, 1-µm thick sections were cut proximally to distally along the leg using 8 mm glass knives and an ultramicrotome (EM UC6, Leica Microsystems, Wetzlar, Germany). The sections were placed onto glass slides, stained with toluidine blue, rinsed with distilled water, and air-dried. Each section was viewed under an optical microscope (BX51, Olympus, Hamburg, Germany) and tracheae were photographed with a mounted digital colour camera (ColorView III, Soft Imaging System, Olympus, Germany) which generated 24-bit 2576 × 1932 pixel resolution images. The remaining femur was used for transmission electron microscopy. Six equidistant 70-nm vertical sections were cut proximally to distally along the leg at systematically random angles around the vertical plane using a diamond knife (Diatome, Biel, Switzerland) and ultramicrotome. Sections were placed onto 3 mm copper mesh grids, stained with lead citrate, and viewed with a transmission electron microscope (CM 100, Philips, Eindhoven, The Netherlands) where 16-bit 1280 × 1024 pixel resolution images of tracheae were captured with a mounted digital camera (MegaView II, Soft Imaging System, Olympus, Germany).

4. Results and discussion

4.1. Description of moulting tracheae

The moulting of the tracheal system begins with the formation of a new and larger tracheal wall around the existing wall (Fig. 2A), and the detachment of the old cuticular intima from the epithelial layer (Fig. 2B) (Ryerse and Locke 1978; Wigglesworth 1973). The large trachea depicted in Fig. 2A for instance, appears to have increased nearly 2-fold in diameter, while the smaller tracheae (tracheoles) in Fig. 3 also appear to have increased in size as the fourth instar tracheal system establishes around the old third instar system. However, it is difficult to establish how much of this apparent increase in size is due to the enlargement of the tracheal walls, and how much is actually a result of smaller distal tracheae being pulled up through larger upstream tracheae. Clearly though, even a modest increase in the size of tracheae and tracheoles during apolysis would facilitate a much easier withdrawal of the shed cuticular intima through the tracheal system during ecdysis.

The next step of the tracheal moulting process probably overlaps somewhat with the previous, and involves the secretion of moulting fluid in the space between the new tracheal wall and the shed cuticular intima (Figs 3, 4) (Wigglesworth 1981; Ryerse and Locke 1978). Apparently, the fluid contains chitinase and protease enzymes that partially breakdown the old cuticle (Jungreis 1974; Passonneau and Williams 1953). It is also speculated that the fluid might facilitate the smooth withdrawal of the shed cuticular intima through the lateral regions of the tracheal system during ecdysis (Keister 1948).

The process by which the old cuticle is withdrawn through larger upstream regions of the tracheal system is captured in the micrographs. In Fig. 4B for instance, the shed cuticular intima of nine smaller tracheoles is in the process of being withdrawn through the fluid-filled lumen of a single large trachea. After the old cuticular lining has retracted from the tracheae, the moulting fluid along with the enzymatic digestion products of the old cuticle is apparently resorbed by the epithelial layer (Lensky and Rakover 1972), and the tracheal system once again fills with air (Fig. 5) (Manning and Krasnow 1993; Wigglesworth 1981; Keister 1948).

4.2. Shedding of the cuticular intima

It is clear from the micrographs that when the tracheal system moults only the cuticular intima is cast, while the epidermal layer remains. In large tracheae, apolysis of the cuticular intima includes the detachment of both the outer epicuticle and the chitin-protein layers (Fig. 2B). Smaller tracheae, on the other hand, tend to lack a prominent chitin-protein complex, and so only the outer epicuticle layer detaches from the tracheal wall during apolysis (Fig. 3). In

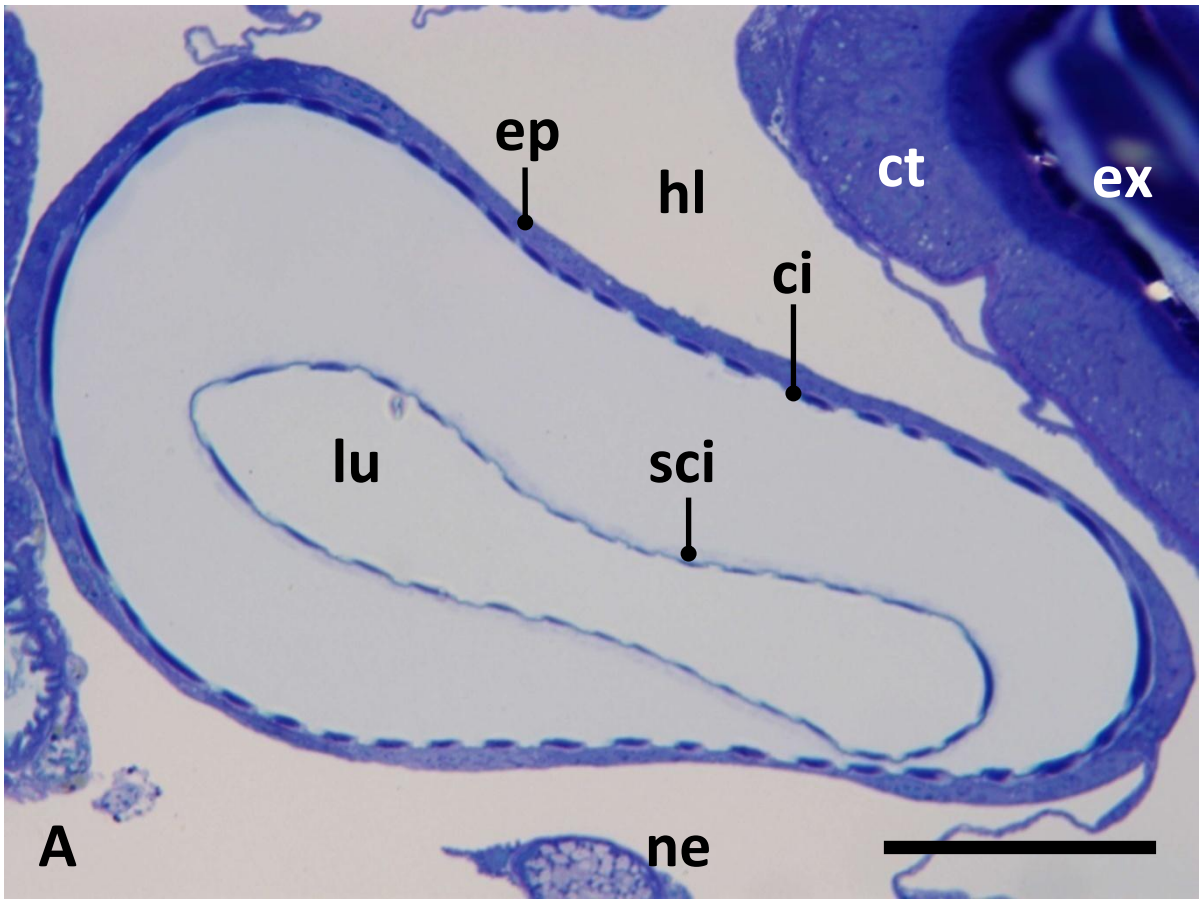
fact, it is apparent that the cuticular intima of even the smallest tracheal tubes are shed and withdrawn during the moulting process. For example, some of the tracheae depicted in Figs 3, 4 are close to 0.3 µm in diameter. Tracheae this small are generally referred to as tracheoles (Chapman 1998; Wigglesworth and Lee 1982; Wigglesworth 1965). Indeed, 0.3 µm seems to represent the lower limit for tracheole diameter not only in locust hopping muscle (Chapter Four), but in a variety of insect tissue (Pickard 1974). This is an interesting finding because the cuticular intima of the terminal tracheoles in *Rhodnius* is apparently never shed (Wigglesworth 1973), whereas studies on *Sciara* and *Drosophila* have found that the tracheole cuticular lining is shed in the early larval stages, but not in the final larval or pupal moults (Whitten 1957; Keister 1948). Therefore, it would appear that the retention of the inner cuticle lining during moulting should not be considered a defining characteristic of all tracheoles.

4.3. Difference between a trachea and a tracheole

In the past tracheoles have been distinguished from tracheae based on the belief that they never shed their cuticular intima at ecdysis; however the results of the current study (Figs 3, 4), as well as earlier studies on *Sciara* and *Drosophila* (Whitten 1957; Keister 1948), cast doubt on the usefulness of this distinction. Tracheae and tracheoles have also been differentiated on the grounds that the latter appear to be smooth-walled and lack the taenidia that larger tracheae possess (Fig. 2B); however, with the development of electron microscopy it has been revealed that the fine terminal branches of the tracheal system do indeed possess micro-taenidia (Fig. 3E) (Buck 1962). It has also been established that while many tracheoles invaginate the surface of other cells to become functionally intracellular, this is certainly not a defining characteristic of all tracheoles (Whitten 1972), including those found in locust hopping muscle (Chapter Four). Therefore, this too cannot be used to clearly differentiate tracheoles from larger tracheae.

The ambiguity surrounding the definition of a tracheole was first noted around 50 years ago (Buck 1962). However, in recent years our understanding of the development and ultrastructure of the tracheal system's fine terminal branches has improved (Ghabrial et al., 2003; Manning and Krasnow 1993), and we also now have a greater appreciation of the different physiological roles of tracheae and smaller tracheoles (Schmitz and Perry 1999). This gives us the opportunity to distinguish tracheoles from larger tracheae irrespective of whether the tracheal tube's cuticular intima is cast at each moult, whether it has micro-taenidia, or whether it penetrates the surface of other cells. Tracheoles can be defined as the

terminal blind-ending branches of the insect tracheal system, usually with an inner diameter less than 2 μm, that arise as long cytoplasmic extensions from a terminal tracheolar cell (Samakovlis et al., 1996), lacking the mestracheon (seam) of larger tracheae (Manning and Krasnow 1993), and providing the primary site for gas exchange between the tissues and the tracheal system (Schmitz and Perry 1999).


ep
hl
ct
ex
ci
lu
sci
A
ne

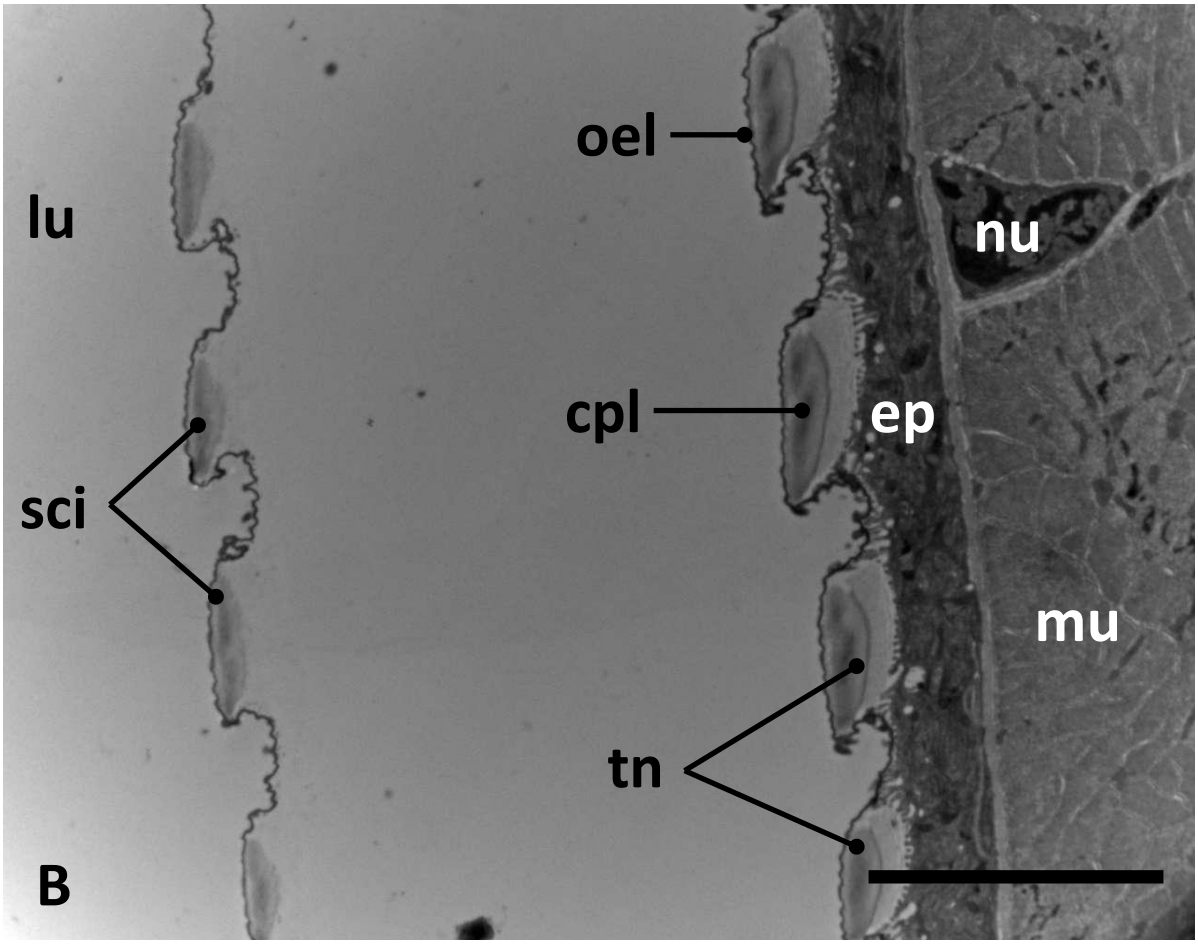

oel
lu
nu
cpl
ep
sci
mu
tn
B

Fig. 2. Tracheae in the metathoracic femur of a third instar locust in the process of shedding its cuticular lining, while larger fourth instar tracheae establish around the old system. A (scale bar = 40 μm) is a low magnification light micrograph of a large trachea where the old cuticular intima has detached from the tracheal wall. B (scale bar = 10 μm) is a high magnification electron micrograph of the wall of a large trachea, showing the detached outer epicuticle and chitin-protein layers of the old cuticular intima. Abbreviations; ci, cuticular intima; cpl, chitin-protein layer; ct, connective tissue; ep, epithelial layer; ex, exoskeleton; fl, moulting fluid; hl, haemolymph; lu, lumen; mt, mitochondria; mu, muscle; my, myofibril; ne, nerve; nu, nucleus; oel, outer epicuticle layer; sci, shed cuticular intima; tn, taenidia.

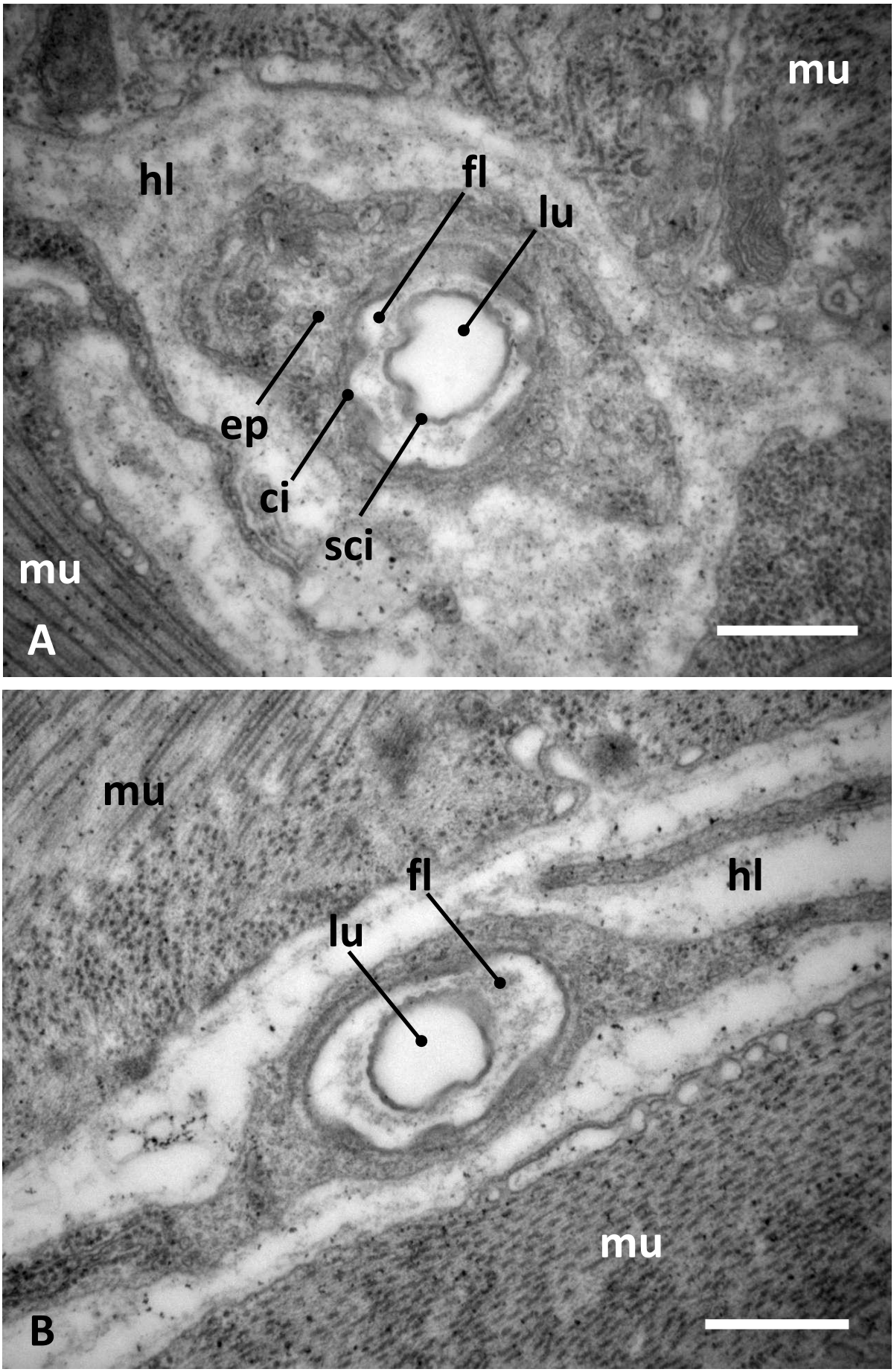
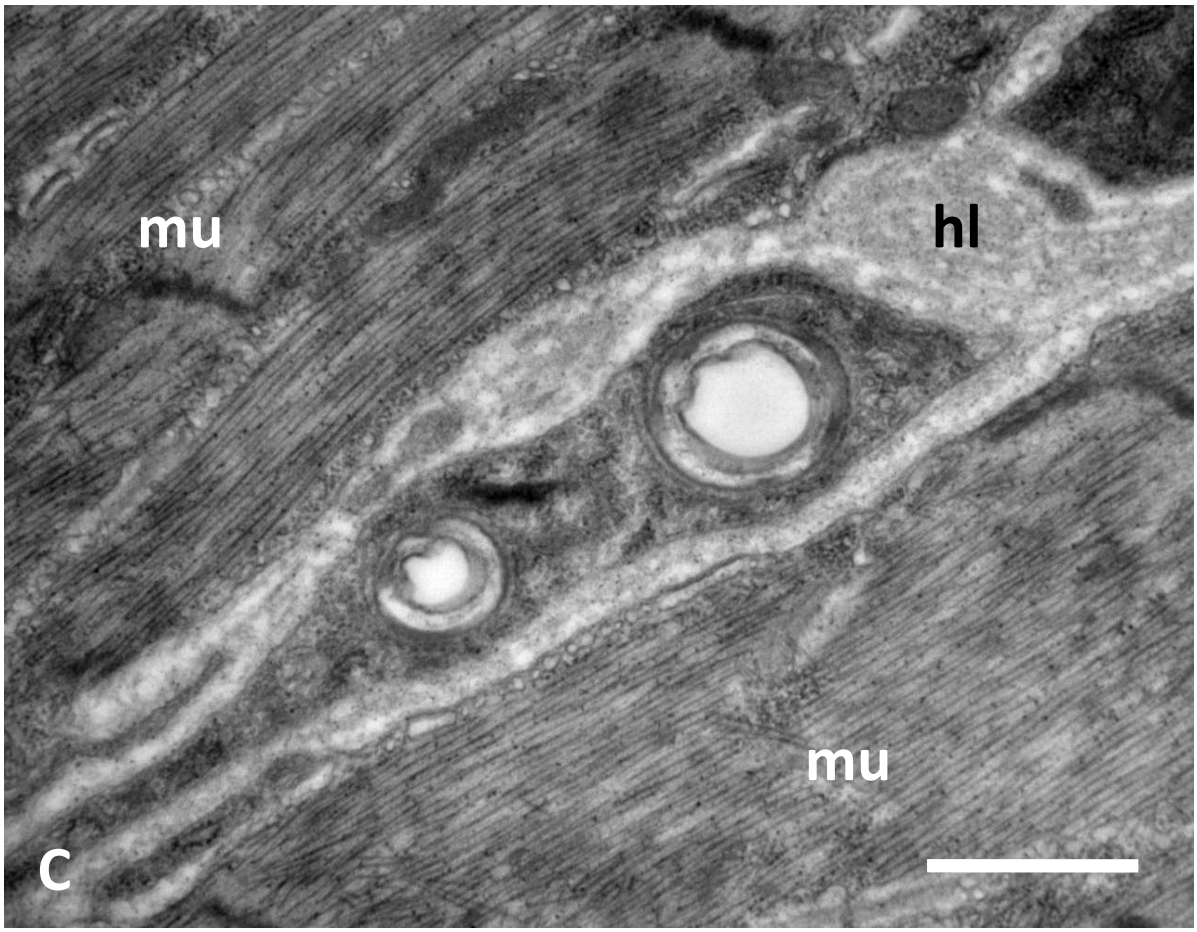

mu
hl
fl
lu
ep
ci
sci
mu
A
mu
fl
hl
lu
mu
B

Fig. 3. Small terminal tracheae (tracheoles) in the process of moulting. A (scale bar = 0.5 μm) and B (scale bar = 0.5 μm) are high magnification electron micrographs sectioned across the tracheole's transverse plane that show the old cuticular intima detached from the tracheole wall and moulting fluid in the exuvial space between the new and shed cuticular intima. See Fig. 2 for abbreviations.


mu
hl
mu
C

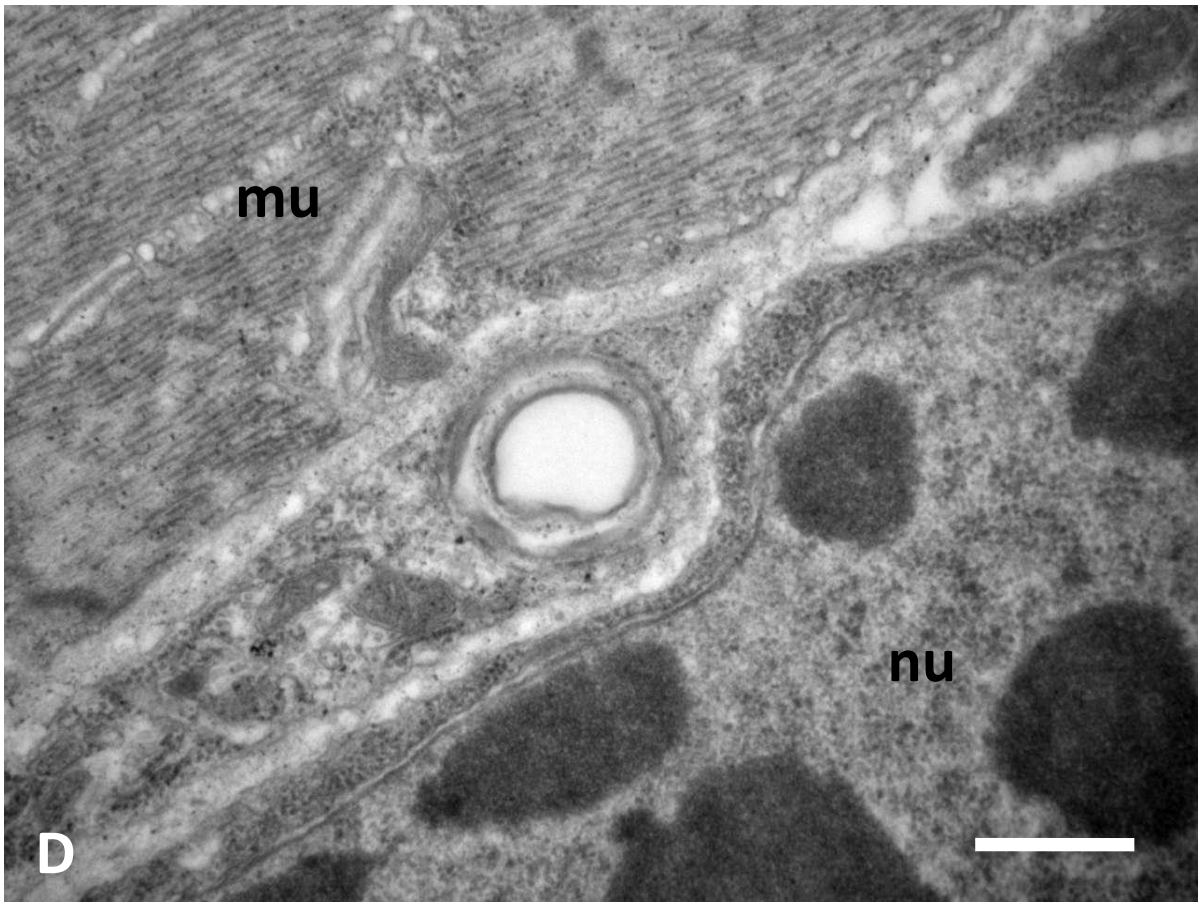

mu
nu
D

Fig. 3 (*continued*). C (scale bar = 1 μm) and D (scale bar = 1 μm) are high magnification electron micrographs sectioned across the tracheole's transverse plane that show the old cuticular intima detached from the tracheole wall and moulting fluid in the exuvial space between the new and shed cuticular intima. See Fig. 2 for abbreviations.

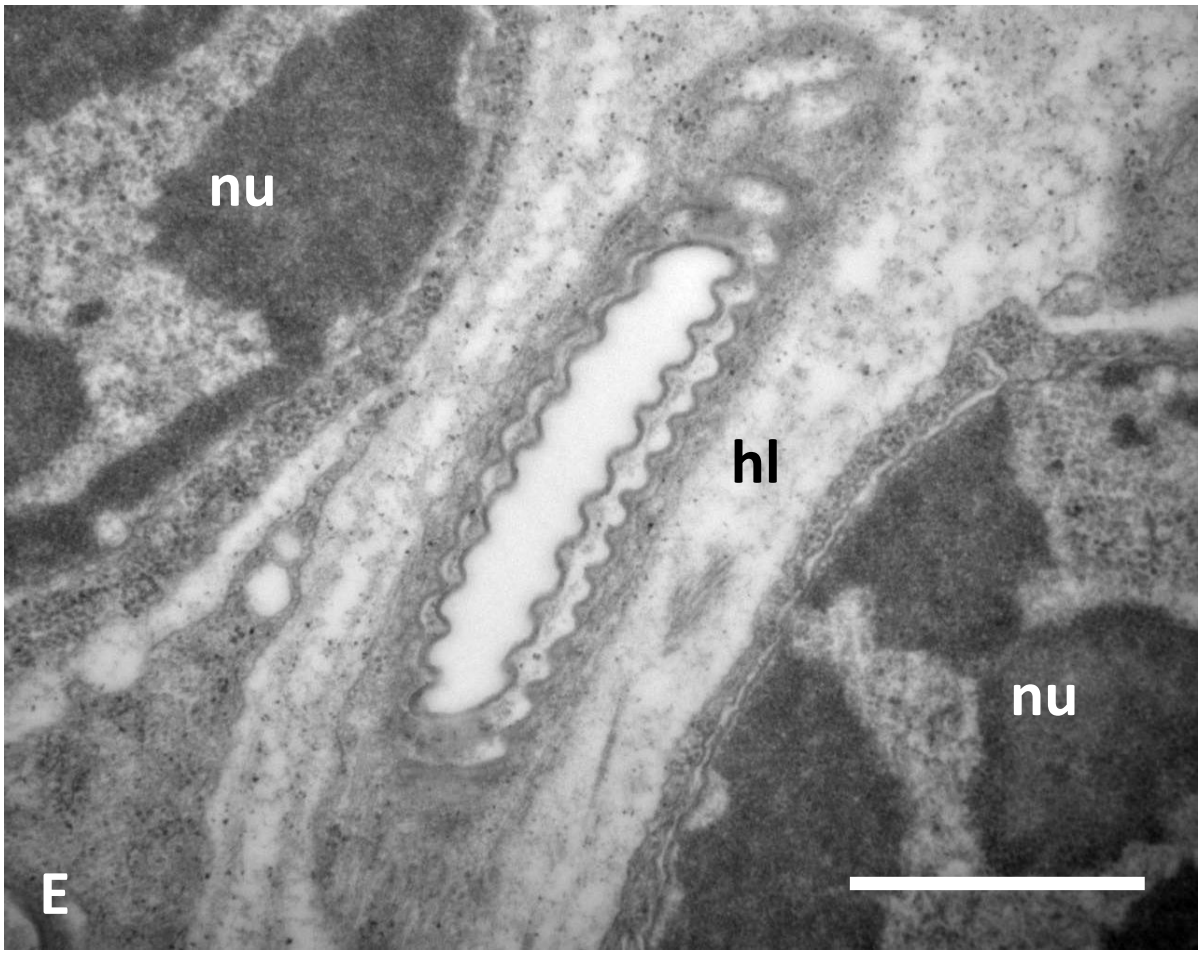
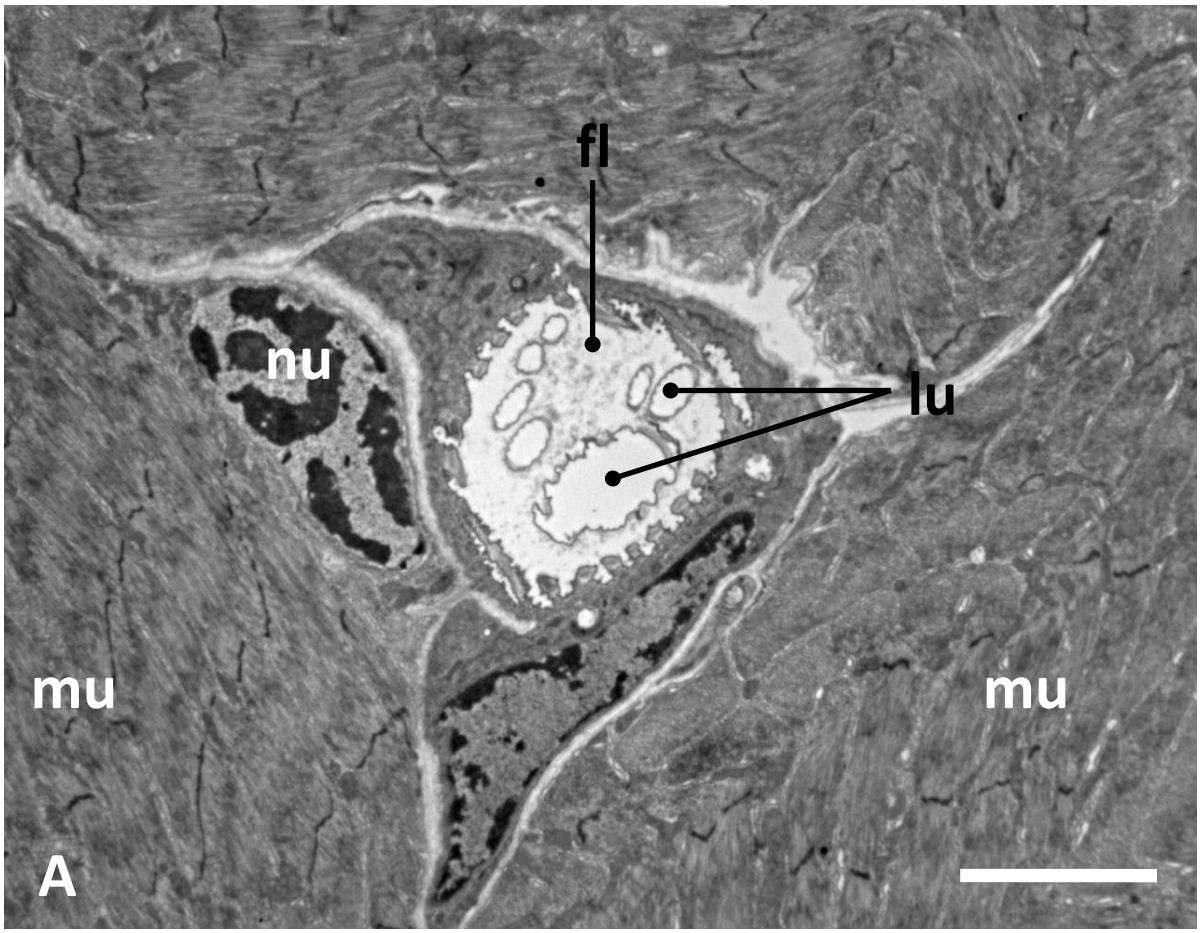


Fig. 3 (*continued*). E (scale bar = 1 μm) is a high magnification electron micrograph sectioned along the tracheole's longitudinal plane that shows the old cuticular intima detached from the tracheole wall and moulting fluid in the exuvial space between the new and shed cuticular intima. See Fig. 2 for abbreviations.


fl
nu
lu
mu
mu
A

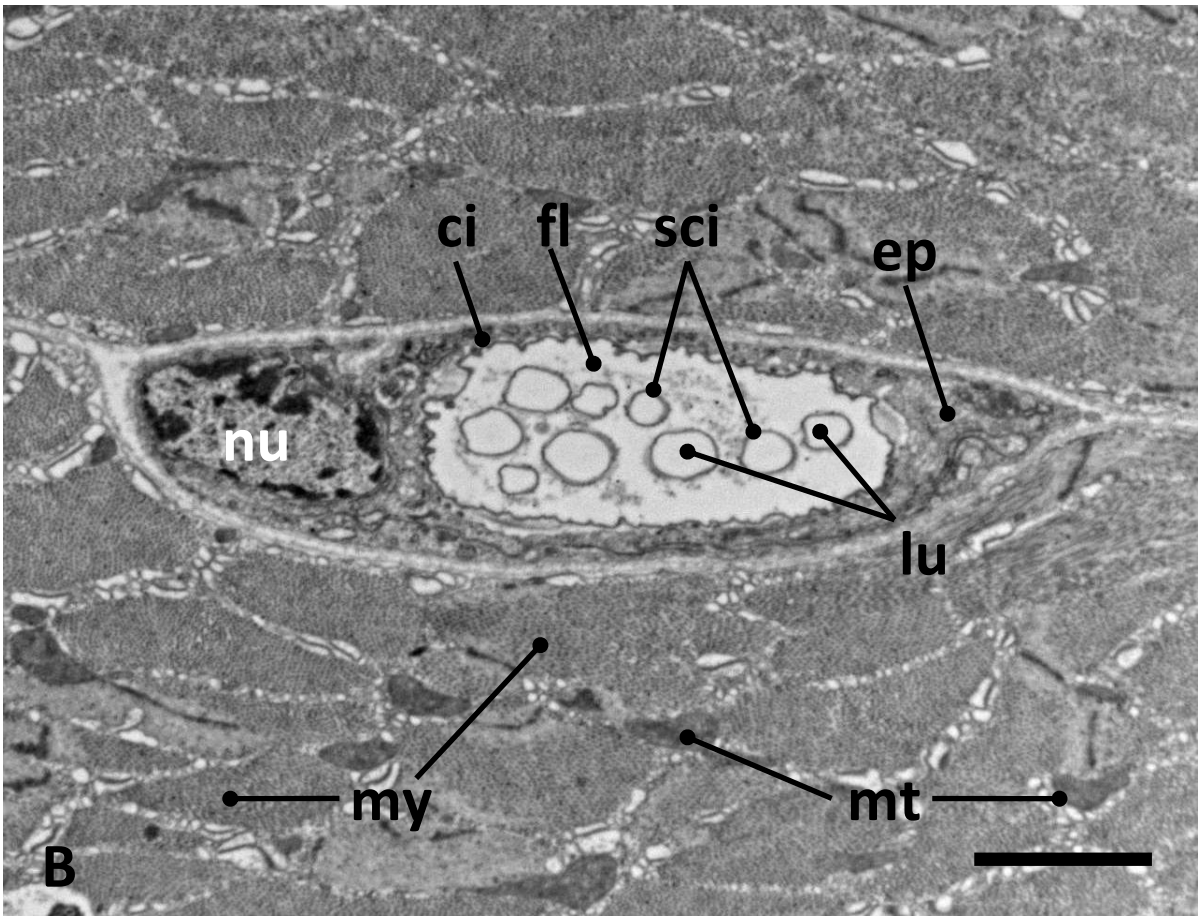

ci
fl
sci
ep
nu
lu
my
mt
B

Fig. 4. Tracheae and small terminal tracheae (tracheoles) in the process of moulting. A (scale bar = 5 μm) and B (scale bar = 2 μm) are electron micrographs that capture the shed cuticular intima of a number of 'downstream' tracheoles being withdrawn through larger 'upstream' tracheae with moulting fluid in the exuvial space between the new and old cuticular intima. See Fig. 2 for abbreviations.

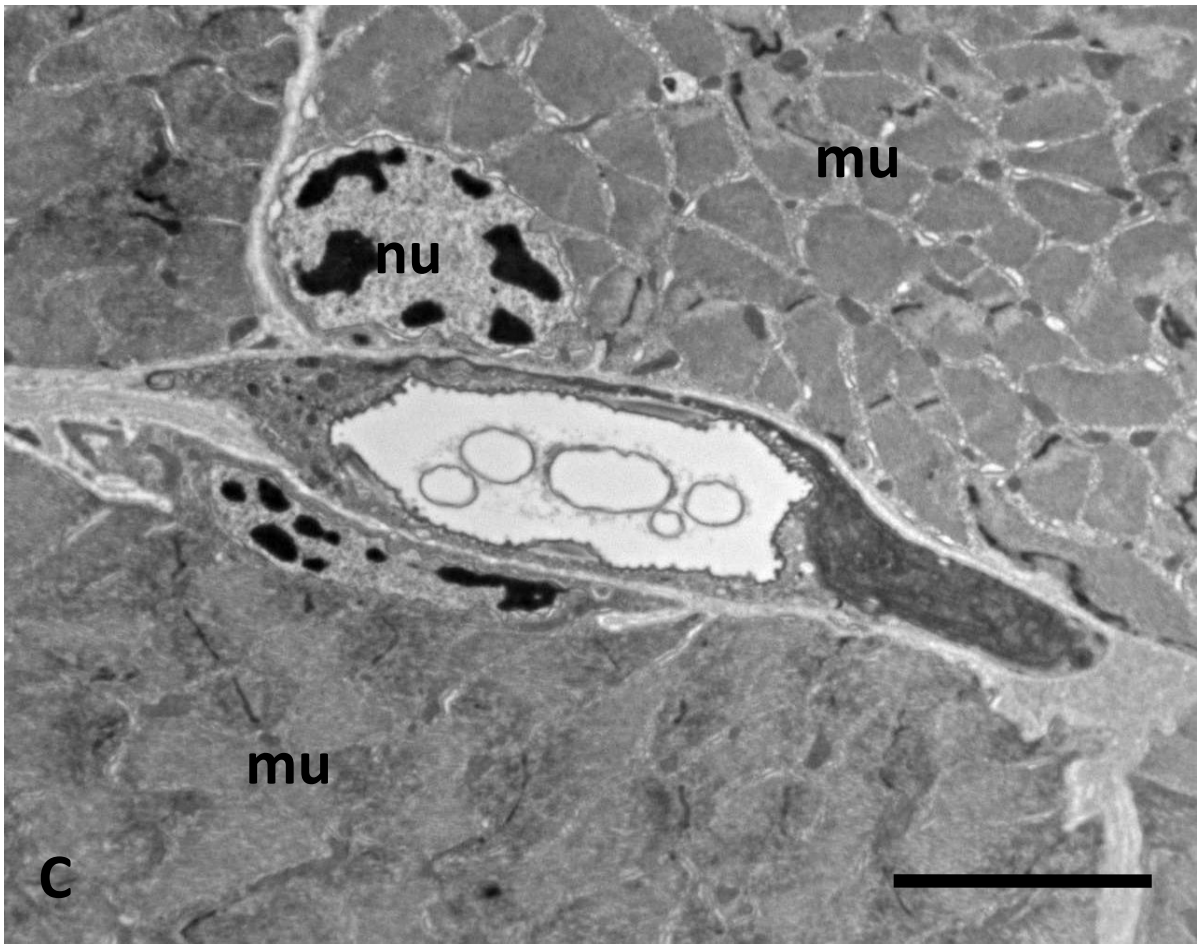


Fig. 4 (*continued*). C (scale bar = 5 μm) is an electron micrograph that also captures the shed cuticular intima of tracheoles being withdrawn through larger tracheae with moulting fluid in the exuvial space between the new and old cuticular intima. See Fig. 2 for abbreviations.

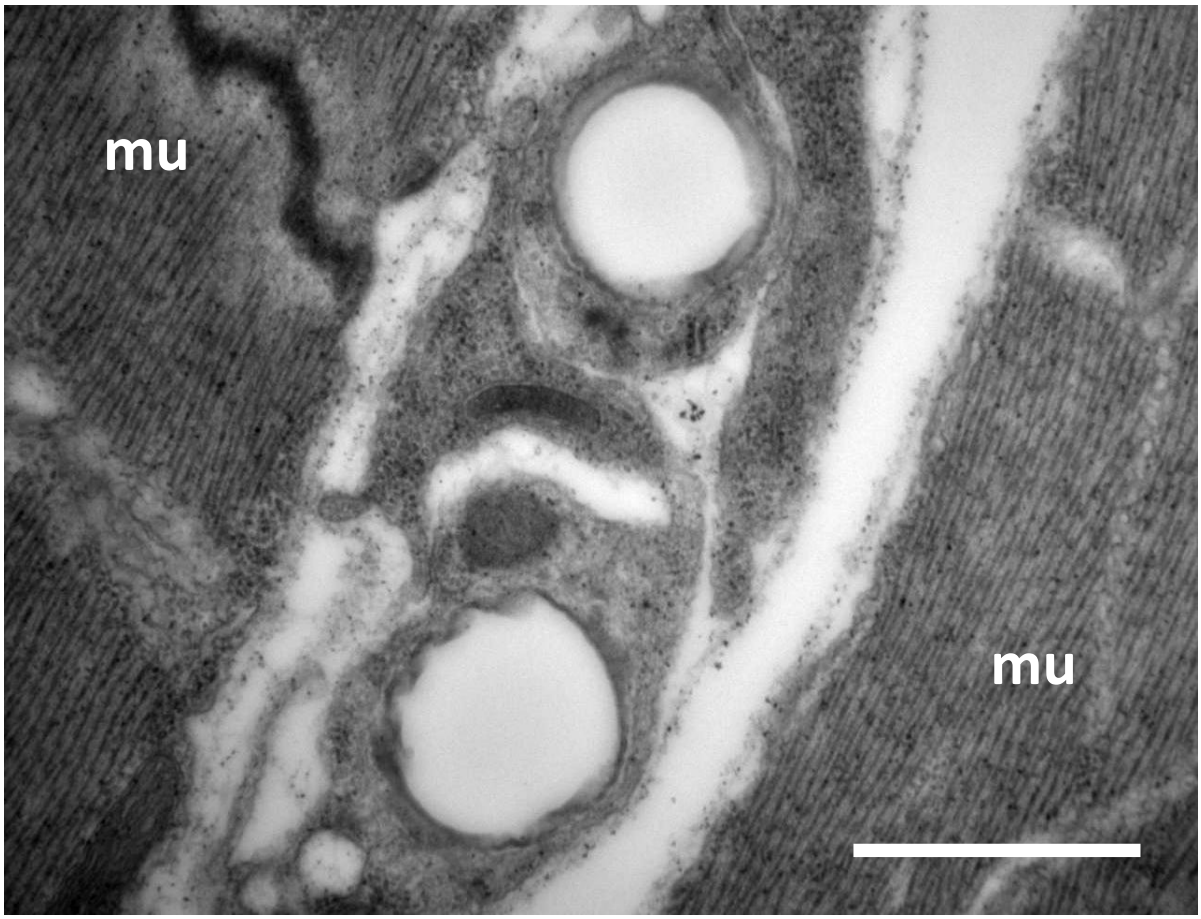


Fig. 5. Small terminal tracheae (tracheoles) in the metathoracic hopping femur of a third instar locust not in the process of moulting (presented here for comparison). The electron micrograph (scale bar = 1 μm) shows the cuticular intima is closely apposed to the epithelial layer, there is no moulting fluid, and the lumen is filled with air. See Fig. 2 for abbreviations.

5. Acknowledgements

This research was supported by the Australian Research Council, project no. DP0879605. Mr Kerry Gascoigne and Dr Mike Teo of Flinders Microscopy and Ms Ruth Williams and Ms Lyn Waterhouse of Adelaide Microscopy shared their expertise in the field of electron microscopy, which was greatly appreciated. Professor Jon Harrison and one anonymous reviewer provided comments that improved an earlier version of this manuscript.

References

Addo-Bediako A, Chown SL, Gaston KJ (2002) Metabolic cold adaptation in insects: a large-scale perspective. *Functional Ecology* **16**, 332-338.

Albrecht FO (1953) 'The Anatomy of the Migratory Locust.' (Athlone Press: London)

Armstrong G, Mordue W (1985) Oxygen consumption of flying locusts. *Physiological Entomology* **10**, 353-358.

Auerswald L, Schneider P, Gade G (1998) Proline powers pre-flight warm-up in the African fruit beetle *Pachnoda sinuata* (Cetoniinae). *Journal of Experimental Biology* **201**, 1651-1657.

Baddeley AJ, Gundersen HJG, Cruz-Orive LM (1986) Estimation of surface area from vertical sections. *Journal of Microscopy* **142**, 259-276.

Bailey CG, Riegert PW (1973) Energy dynamics of *Encoptolophus sordidus costalis* (Scudder) (Orthoptera: Acrididae) in a grassland ecosystem. *Canadian Journal of Zoology* **51**, 91-100.

Baker PS (1979) The wing movements of flying locusts during steering behaviour. *Journal of Comparative Physiology* **131**, 49-58.

Baker PS, Gewecke M, Cooter RJ (1981) The natural flight of the migratory locust, *Locusta migratoria* L. III: wing-beat frequency, flight speed and attitude. *Journal of Comparative Physiology* **141**, 233-237.

Balderrama NM, Almeida DLO, Nunez JA (1992) Metabolic rate during foraging in the honeybee. *Journal of Comparative Physiology. B, Biochemical, Systemic, and Environmental Physiology* **162**, 440-447.

Banavar JR, Damuth J, Maritan A, Rinaldo A (2002) Supply-demand balance and metabolic scaling. *Proceedings of the National Academy of Sciences of the United States of America* **99**, 10506-10509.

Banavar JR, Moses ME, Brown JH, Damuth J, Rinaldo A, Sibly RM, Maritan A (2010) A general basis for quarter-power scaling in animals. *Proceedings of the National Academy of Sciences of the United States of America* **107**, 15816-15820.

Barbosa LA, Garcia GJM, da Silva JKL (2006) The scaling of maximum and basal metabolic rates of mammals and birds. *Physica A: Statistical Mechanics and its Applications* **359**, 547-554.

Bartels H (1971) Diffusion coefficients and Krogh's diffusion constants. In 'Respiration and Circulation'. (Eds PL Altman and DS Dittmer) pp. 21-22. (Federation of American Societies for Experimental Biology: Bethesda, Maryland)

Bartholomew GA, Casey TM (1978) Oxygen consumption of moths during rest, pre-flight warm-up, and flight in relation to body size and wing morphology. *Journal of Experimental Biology* **76**, 11-25.

Bartholomew GA, Heinrich B (1973) A field study of flight temperatures in moths in relation to body weight and wing loading. *Journal of Experimental Biology* **58**, 123-135.

Bartholomew GA, Lighton JRB, Feener DH (1988) Energetics of trail running, load carriage, and emigration in the column-raiding army ant *Eciton hamatum*. *Physiological Zoology* **61**, 57-68.

Bartholomew GA, Lighton JRB, Louw GN (1985) Energetics of locomotion and patterns of respiration in tenebrionid beetles from the Namib Desert. *Journal of Comparative Physiology. B, Biochemical, Systemic, and Environmental Physiology* **155**, 155-162.

Beenakkers AMT, Vanderhorst DJ, Vanmarrewijk WJA (1981) Metabolism during locust flight. *Comparative Biochemistry and Physiology. Part B, Comparative Biochemistry* **69**, 315-321.

Beenakkers AMT, Vanderhorst DJ, Vanmarrewijk WJA (1984) Insect flight muscle metabolism. *Insect Biochemistry* **14**, 243-260.

Bennet-Clark HC (1975) The energetics of the jump of the locust *Schistocerca gregaria*. *Journal of Experimental Biology* **63**, 53-83.

Biserova NM, Pfluger HJ (2004) The ultrastructure of locust pleuroaxillary "steering" muscles in comparison to other skeletal muscles. *Zoology* **107**, 229-242.

Bishop CM (1999) The maximum oxygen consumption and aerobic scope of birds and mammals: getting to the heart of the matter. *Proceedings of the Royal Society of London. Series B: Biological Sciences* **266**, 2275-2281.

Bridges CR, Scheid P (1982) Buffering and CO_2 dissociation of body fluids in the pupa of the silkworm moth, *Hyalophora cecropia*. *Respiration Physiology* **48**, 183-197.

Brown JH, West GB, Enquist BJ (2005) Yes, West, Brown and Enquist's model of allometric scaling is both mathematically correct and biologically relevant. *Functional Ecology* **19**, 735-738.

Buck J (1962) Some physical aspects of insect respiration. *Annual Review of Entomology* **7**, 27-56.

Canals M, Figueroa DP, Sabat P (2010) Symmorphosis in the proximal pathway for oxygen in the leaf-eared mouse *Phyllotis darwini*. *Biological Research* **43**, 75-81.

Canals M, Martinez BB, Figueroa D, Sabat P (2011) Adjustments of the oxygen diffusing capacity to energetic demands during the development of the quail (*Coturnix coturnix japonica*). *Comparative Biochemistry and Physiology. Part A, Molecular and Integrative Physiology* **159**, 339-345.

Casey TM (1976) Flight energetics of sphinx moths: power input during hovering flight. *Journal of Experimental Biology* **64**, 529-543.

Casey TM, Hegel JR, Buser CS (1981) Physiology and energetics of pre-flight warm-up in the eastern tent caterpillar moth *Malacosoma americanum*. *Journal of Experimental Biology* **94**, 119-135.

Casey TM, May ML, Morgan KR (1985) Flight energetics of euglossine bees in relation to morphology and wing stroke frequency. *Journal of Experimental Biology* **116**, 271-289.

Chapman RF (1998) 'The Insects: Structure and Function.' (Cambridge University Press: Cambridge)

Chappell MA, Bailey NW, Redak RA, Antolin M, Zuk M (2009) Metabolic similarity despite striking behavioral divergence: aerobic performance in low- and high-density forms of the Mormon cricket. *Physiological and Biochemical Zoology* **82**, 405-418.

Chown SL, Gibbs AG, Hetz SK, Klok CJ, Lighton JRB, Marais E (2006) Discontinuous gas exchange in insects: a clarification of hypotheses and approaches. *Physiological and Biochemical Zoology* **79**, 333-343.

Chown SL, Marais E, Terblanche JS, Klok CJ, Lighton JRB, Blackburn TM (2007) Scaling of insect metabolic rate is inconsistent with the nutrient supply network model. *Functional Ecology* **21**, 282-290.

Cloupeau M, Devillers JF, Devezeaux D (1979) Direct measurements of instantaneous lift in desert locust: comparison with Jensen's experiments on detached wings. *Journal of Experimental Biology* **80**, 1-15.

Conley KE, Kayar SR, Rosler K, Hoppeler H, Weibel ER, Taylor CR (1987) Adaptive variation in the mammalian respiratory system in relation to energetic demand IV: capillaries and their relationship to oxidative capacity. *Respiration Physiology* **69**, 47-64.

Contreras HL, Bradley TJ (2009) Metabolic rate controls respiratory pattern in insects. *Journal of Experimental Biology* **212**, 424-428.

Cruz-Orive LM, Weibel ER (1990) Recent stereological methods for cell biology: a brief survey. *American Journal of Physiology* **258**, 148-156.

Curtsinger JW, Laurie-Ahlberg CC (1981) Genetic variability of flight metabolism in *Drosophila melanogaster* I: characterization of power output during tethered flight. *Genetics* **98**, 549-564.

Darveau CA, Suarez RK, Andrews RD, Hochachka PW (2002) Allometric cascade as a unifying principle of body mass effects on metabolism. *Nature* **417**, 166-170.

Diamond J, Hammond K (1992) The matches achieved by natural selection between biological capacities and their natural loads. *Experientia* **48**, 551-557.

Diamond JM (1992) The red flag of optimality. *Nature* **355**, 204-206.

Diamond JM (1998) Evolution of biological safety factors: a cost/benefit analysis. In 'Principles of Animal Design: The Optimization and Symmorphosis Debate'. (Eds ER Weibel, CR Taylor and L Bolis) pp. 40-47. (Cambridge University Press: Cambridge)

Dingle H, Winchell R (1997) Juvenile hormone as a mediator of plasticity in insect life histories. *Archives of Insect Biochemistry and Physiology* **35**, 359-373.

Dudley R (1998) Atmospheric oxygen, giant Paleozoic insects and the evolution of aerial locomotor performance. *Journal of Experimental Biology* **201**, 1043-1050.

Dudley R, Ellington CP (1990) Mechanics of forward flight in bumblebees I: kinematics and morphology. *Journal of Experimental Biology* **148**, 19-52.

Dudley R, Gans C (1991) A critique of symmorphosis and optimality models in physiology. *Physiological Zoology* **64**, 627-637.

Ellington WR (2001) Evolution and physiological roles of phosphagen systems. *Annual Review of Physiology* **63**, 289-325.

Else PL, Hulbert AJ (1985) Mammals: an allometric study of metabolism at tissue and mitochondrial level. *American Journal of Physiology* **248**, R415-R421.

Gabriel JM (1985a) The development of the locust jumping mechanism I: allometric growth and its effect on jumping performance. *Journal of Experimental Biology* **118**, 313-326.

Gabriel JM (1985b) The development of the locust jumping mechanism II: energy storage and muscle mechanics. *Journal of Experimental Biology* **118**, 327-340.

Garland T (1998) Conceptual and methodological issues in testing the predictions of symmorphosis. In 'Principles of Animal Design: The Optimization and Symmorphosis Debate'. (Eds ER Weibel, CR Taylor and L Bolis) pp. 40-47. (Cambridge University Press: Cambridge)

Garland T, Huey RB (1987) Testing symmorphosis: does structure match functional requirements? *Evolution* **41**, 1404-1409.

Gebczynski AK, Konarzewski M (2011) Effects of oxygen availability on maximum aerobic performance in *Mus musculus* selected for basal metabolic rate or aerobic capacity. *Journal of Experimental Biology* **214**, 1714-1720.

Gee CE, Robertson RM (1998) Free-flight ability in locusts recovering from partial deafferentation. *Naturwissenschaften* **85**, 167-170.

Gehr P, Mwangi DK, Ammann A, Maloiy GMO, Taylor CR, Weibel ER (1981) Design of the mammalian respiratory system V: scaling morphometric pulmonary diffusing capacity to body mass: wild and domestic mammals. *Respiration Physiology* **44**, 61-86.

Gewecke M (1975) The influence of the air-current sense organs on the flight behaviour of *Locusta migratoria*. *Journal of Comparative Physiology* **103**, 79-95.

Gewecke M, Kutsch W (1979) Development of flight behavior in maturing adults of *Locusta migratoria* I: flight performance and wing-stroke parameters. *Journal of Insect Physiology* **25**, 249-253.

Ghabrial A, Luschnig S, Metzstein MM, Krasnow MA (2003) Branching morphogenesis of the *Drosophila* tracheal system. *Annual Review of Cell and Developmental Biology* **19**, 623-647.

Goldsworthy GJ, Coupland AJ (1974) The influence of the corpora cardiaca and substrate availability on flight speed and wing beat frequency in *Locusta*. *Journal of Comparative Physiology* **89**, 359-368.

Gouveia SM, Simpson SJ, Raubenheimer D, Zanotto FP (2000) Patterns of respiration in *Locusta migratoria* nymphs when feeding. *Physiological Entomology* **25**, 88-93.

Graham JB, Dudley R, Aguilar NM, Gans C (1995) Implications of the late Palaeozoic oxygen pulse for physiology and evolution. *Nature* **375**, 117-120.

Greenlee KJ, Harrison JF (2004a) Development of respiratory function in the American locust *Schistocerca americana* I: across-instar effects. *Journal of Experimental Biology* **207**, 497-508.

Greenlee KJ, Harrison JF (2004b) Development of respiratory function in the American locust *Schistocerca americana* II: within-instar effects. *Journal of Experimental Biology* **207**, 509-517.

Greenlee KJ, Henry JR, Kirkton SD, Westneat MW, Fezzaa K, Lee WK, Harrison JF (2009) Synchrotron imaging of the grasshopper tracheal system: morphological and physiological components of tracheal hypermetry. *American Journal of Physiology* **297**, 1343-1350.

Guillemin K, Groppe J, Ducker K, Treisman R, Hafen E, Affolter M, Krasnow MA (1996) The *pruned* gene encodes the *Drosophila* serum response factor and regulates cytoplasmic outgrowth during terminal branching of the tracheal system. *Development* **122**, 1353-1362.

Gulinson SL, Harrison JF (1996) Control of resting ventilation rate in grasshoppers. *Journal of Experimental Biology* **199**, 379-389.

Hadley NF, Quinlan MC (1993) Discontinuous carbon dioxide release in the eastern lubber grasshopper *Romalea guttata* and its effect on respiratory transpiration. *Journal of Experimental Biology* **177**, 169-180.

Harrison JF, Lafreniere JJ, Greenlee KJ (2005) Ontogeny of tracheal dimensions and gas exchange capacities in the grasshopper, *Schistocerca americana*. *Comparative Biochemistry and Physiology. Part A, Molecular and Integrative Physiology* **141**, 372-380.

Harrison JF, Lighton JRB (1998) Oxygen-sensitive flight metabolism in the dragonfly *Erythemis simplicicollis*. *Journal of Experimental Biology* **201**, 1739-1744.

Harrison JF, Nielsen DI, Page RE (1996) Malate dehydrogenase phenotype, temperature and colony effects on flight metabolic rate in the honey-bee, *Apis mellifera*. *Functional Ecology* **10**, 81-88.

Harrison JF, Phillips JE, Gleeson TT (1991) Activity physiology of the two-striped grasshopper, *Melanoplus bivittatus*: gas exchange, hemolymph acid-base status, lactate production, and the effect of temperature. *Physiological Zoology* **64**, 451-472.

Hartung DK, Kirkton SD, Harrison JF (2004) Ontogeny of tracheal system structure: a light and electron-microscopy study of the metathoracic femur of the American locust, *Schistocerca americana*. *Journal of Morphology* **262**, 800-812.

Heinrich B (1971) Temperature regulation of the sphinx moth, *Manduca sexta* I: flight energetics and body temperature during free and tethered flight. *Journal of Experimental Biology* **54**, 141-152.

Heinrich B (1975) Thermoregulation in bumblebees II: energetics of warm-up and free flight. *Journal of Comparative Physiology* **96**, 155-166.

Herreid CF, Full RJ (1984) Cockroaches on a treadmill: aerobic running. *Journal of Insect Physiology* **30**, 395-403.

Hetz SK, Bradley TJ (2005) Insects breathe discontinuously to avoid oxygen toxicity. *Nature* **433**, 516-519.

Hoppeler H, Kayar SR, Claasen H, Uhlmann E, Karas RH (1987) Adaptive variation in the mammalian respiratory system in relation to energetic demand III: skeletal muscles setting the demand for oxygen. *Respiration Physiology* **69**, 27-46.

Hoppeler H, Mathieu O, Krauer R, Claasen H, Armstrong RB, Weibel ER (1981a) Design of the mammalian respiratory system VI: distribution of mitochondria and capillaries in various muscles. *Respiration Physiology* **44**, 97-111.

Hoppeler H, Mathieu O, Weibel ER, Krauer R, Lindstedt SL, Taylor CR (1981b) Design of the mammalian respiratory system VIII: capillaries in skeletal muscles. *Respiration Physiology* **44**, 129-150.

Howard CV, Reed MG (1998) 'Unbiased Stereology: Three Dimensional Measurement in Microscopy.' (BIOS Scientific Publishers: Oxford)

Hsia CCW, Herazo LF, Johnson RL (1992) Cardiopulmonary adaptations to pneumonectomy in dogs I: maximal exercise performance. *Journal of Applied Physiology* **73**, 362-367.

Jarecki J, Johnson E, Krasnow MA (1999) Oxygen regulation of airway branching in *Drosophila* is mediated by branchless FGF. *Cell* **99**, 211-220.

Jensen M (1956) Biology and physics of locust flight III: the aerodynamics of locust flight. *Philosophical Transactions of the Royal Society of London. Series B: Biological Sciences* **239**, 511-552.

Jones JH, Lindstedt SL (1993) Limits to maximal performance. *Annual Review of Physiology* **55**, 547-569.

Jungreis AM (1974) Physiology and composition of molting fluid and midgut lumenal contents in the silkmoth *Hyalophora cecropia*. *Journal of Comparative Physiology* **88**, 113-127.

Kaiser A, Klok CJ, Socha JJ, Lee WK, Quinlan MC, Harrison JF (2007) Increase in tracheal investment with beetle size supports hypothesis of oxygen limitation on insect gigantism. *Proceedings of the National Academy of Sciences of the United States of America* **104**, 13198-13203.

Kammer AE, Heinrich B (1974) Metabolic rates related to muscle activity in bumblebees. *Journal of Experimental Biology* **61**, 219-227.

Kammer AE, Heinrich B (1978) Insect flight metabolism. In 'Advances in Insect Physiology'. (Eds JE Treherne, MJ Berridge and VB Wigglesworth) pp. 133-228. (Academic Press: London, New York)

Karas RH, Taylor CR, Jones JH, Lindstedt SL, Reeves RB, Weibel ER (1987a) Adaptive variation in the mammalian respiratory system in relation to energetic demand VII: flow of oxygen across the pulmonary gas exchanger. *Respiration Physiology* **69**, 101-115.

Karas RH, Taylor CR, Rösler K, Hoppeler H (1987b) Adaptive variation in the mammalian respiratory system in relation to energetic demand V: limits to oxygen transport by the circulation. *Respiration Physiology* **69**, 65-79.

Katz SL, Gosline JM (1993) Ontogenic scaling of jump performance in the African desert locust (*Schistocerca gregaria*). *Journal of Experimental Biology* **177**, 81-111.

Keister ML (1948) The morphogenesis of the tracheal system of *Sciara*. *Journal of Morphology* **83**, 373-424.

Kinsey ST, Locke BR, Dillaman RM (2011) Molecules in motion: influences of diffusion on metabolic structure and function in skeletal muscle. *Journal of Experimental Biology* **214**, 263-274.

Kirkton SD, Harrison JF (2006) Ontogeny of locomotory behaviour in the American locust, *Schistocerca americana*: from marathoner to broad jumper. *Animal Behaviour* **71**, 925-931.

Kirkton SD, Niska JA, Harrison JF (2005) Ontogenetic effects on aerobic and anaerobic metabolism during jumping in the American locust, *Schistocerca americana*. *Journal of Experimental Biology* **208**, 3003-3012.

Kohnert S, Perry SF, Schmitz A (2004) Morphometric analysis of the larval branchial chamber in the dragonfly *Aeshna cyanea* Muller (Insecta, Odonata, Anisoptera). *Journal of Morphology* **261**, 81-91.

Komai Y (1998) Augmented respiration in a flying insect. *Journal of Experimental Biology* **201**, 2359-2366.

Kozlowski J, Konarzewski M (2004) Is West, Brown and Enquist's model of allometric scaling mathematically correct and biologically relevant? *Functional Ecology* **18**, 283-289.

Kram R (1996) Inexpensive load carrying by rhinoceros beetles. *Journal of Experimental Biology* **199**, 609-612.

Kreuzer F (1982) Oxygen supply to tissues: the Krogh model and its assumptions. *Experientia* **38**, 1415-1426.

Krogh A (1919) The number and distribution of capillaries in muscles with calculations of the oxygen pressure head necessary for supplying the tissue. *Journal of Physiology* **52**, 409-415.

Krogh A, Weis-Fogh T (1951) The respiratory exchange of the desert locust (*Schistocerca gregaria*) before, during and after flight. *Journal of Experimental Biology* **28**, 344-357.

Kutsch W, Gewecke M (1979) Development of flight behavior in maturing adults of *Locusta migratoria* II: aerodynamic parameters. *Journal of Insect Physiology* **25**, 299-304.

Kutsch W, Stevenson P (1981) Time correlated flights of juvenile and mature locusts: a comparison between free and tethered animals. *Journal of Insect Physiology* **27**, 455-459.

Kutsch W, van der Wall M, Fischer H (1999) Analysis of free forward flight of *Schistocerca gregaria* employing telemetric transmission of muscle potentials. *Journal of Experimental Zoology* **284**, 119-129.

Lehmann FO, Dickinson MH (1997) The changes in power requirements and muscle efficiency during elevated force production in the fruit fly *Drosophila melanogaster*. *Journal of Experimental Biology* **200**, 1133-1143.

Lensky Y, Rakover Y (1972) Resorption of moulting fluid proteins during the ecdysis of the honey bee. *Comparative Biochemistry and Physiology. Part B, Comparative Biochemistry* **41**, 521-531.

Lighton JRB (1996) Discontinuous gas exchange in insects. *Annual Review of Entomology* **41**, 309-324.

Lighton JRB, Bartholomew GA, Feener DH (1987) Energetics of locomotion and load carriage and a model of the energy cost of foraging in the leaf-cutting ant *Atta columbica* Guer. *Physiological Zoology* **60**, 524-537.

Lighton JRB, Weier JA, Feener DH (1993) The energetics of locomotion and load carriage in the desert harvester ant *Pogonomyrmex rugosus*. *Journal of Experimental Biology* **181**, 49-61.

Locke M (1957) The structure of insect tracheae. *Quarterly Journal of Microscopical Science* **98**, 487-492.

Locke M (1958a) The co-ordination of growth in the tracheal system of insects. *Quarterly Journal of Microscopical Science* **99**, 373-391.

Locke M (1958b) The formation of tracheae and tracheoles in *Rhodnius prolixus*. *Quarterly Journal of Microscopical Science* **99**, 29-46.

Madhavan MM, Schneiderman HA (1977) Histological analysis of the dynamics of growth of imaginal discs and histoblast nests during the larval development of *Drosophila melanogaster*. *Wilhelm Roux's Archives of Developmental Biology* **183**, 269-305.

Maina JN (1989) Scanning and transmission electron microscopic study of the tracheal air sac system in a grasshopper *Chrotogonus senegalensis* (Kraus): Orthoptera: Acrididae: Pyrgomorphinae. *Anatomical Record* **223**, 393-405.

Manning G, Krasnow MA (1993) Development of the *Drosophila* tracheal system. In 'The Development of *Drosophila melanogaster*'. (Eds M Bate and A Martinez Arias) pp. 609-685. (Cold Spring Harbor Press: Cold Spring Harbor, New York)

Marden JH (1987) Maximum lift production during takeoff in flying animals. *Journal of Experimental Biology* **130**, 235-258.

Marden JH (2000) Variability in the size, composition, and function of insect flight muscles. *Annual Review of Physiology* **62**, 157-178.

Mathieu O, Krauer R, Hoppeler H, Gehr P, Lindstedt SL, Alexander RM, Taylor CR, Weibel ER (1981) Design of the mammalian respiratory system VII: scaling mitochondrial volume in skeletal muscle to body mass. *Respiration Physiology* **44**, 113-128.

Matsuura S, Tashiro Y (1976) Ultrastructural changes of posterior silk gland cells in early larval instars of silkworm, *Bombyx mori*. *Journal of Insect Physiology* **22**, 967-979.

May ML (1981) Wingstroke frequency of dragonflies (Odonata: Anisoptera) in relation of temperature and body size. *Journal of Comparative Physiology* **144**, 229-240.

Mayhew TM (1991) The new stereological methods for interpreting functional morphology from slices of cells and organs. *Experimental Physiology* **76**, 639-665.

Mendez J, Keys A (1960) Density and composition of mammalian muscle. *Metabolism: Clinical and Experimental* **9**, 184-188.

Mizisin AP, Ready NE (1986) Growth and development of flight muscle in the locust (*Schistocerca nitens*, Thunberg). *Journal of Experimental Zoology* **237**, 45-55.

Nespolo RF, Castaneda LE, Roff DA (2005) The effect of fasting on activity and resting metabolism in the sand cricket, *Gryllus firmus*: a multivariate approach. *Journal of Insect Physiology* **51**, 61-66.

Neville AC, Weis-Fogh T (1963) The effect of temperature on locust flight muscle. *Journal of Experimental Biology* **40**, 111-121.

Newsholme EA, Beis I, Leech AR, Zammit VA (1978) Role of creatine kinase and arginine kinase in muscle. *Biochemical Journal* **172**, 533-537.

Niven JE, Scharlemann JPW (2005) Do insect metabolic rates at rest and during flight scale with body mass? *Biology Letters* **1**, 346-349.

Pascoe JR, Ferraro GL, Cannon JH, Arthur RM, Wheat JD (1981) Exercise induced pulmonary hemorrhage in racing thoroughbreds: a preliminary study. *American Journal of Veterinary Research* **42**, 703-707.

Passonneau JV, Williams CM (1953) The moulting fluid of the *Cecropia* silkworm. *Journal of Experimental Biology* **30**, 545-560.

Pickard WF (1974) Transition regime diffusion and the structure of the insect tracheolar system. *Journal of Insect Physiology* **20**, 947-956.

Powers SK, Lawler J, Dempsey JA, Dodd S, Landry G (1989) Effects of incomplete pulmonary gas exchange on VO_2max. *Journal of Applied Physiology* **66**, 2491-2495.

Preiss R, Gewecke M (1991) Compensation of visually simulated wind drift in the swarming flight of the desert locust (*Schistocerca gregaria*). *Journal of Experimental Biology* **157**, 461-481.

Price CA, Enquist BJ, Savage VM (2007) A general model for allometric covariation in botanical form and function. *Proceedings of the National Academy of Sciences of the United States of America* **104**, 13204-13209.

Queathem E (1991) The ontogeny of grasshopper jumping performance. *Journal of Insect Physiology* **37**, 129-138.

Quinlan MC, Gibbs AG (2006) Discontinuous gas exchange in insects. *Respiratory Physiology and Neurobiology* **154**, 18-29.

Rascon B, Harrison JF (2005) Oxygen partial pressure effects on metabolic rate and behavior of tethered flying locusts. *Journal of Insect Physiology* **51**, 1193-1199.

Riveros AJ, Enquist BJ (2011) Metabolic scaling in insects supports the predictions of the WBE model. *Journal of Insect Physiology*, (in press).

Roberts SP, Harrison JF, Dudley R (2004) Allometry of kinematics and energetics in carpenter bees (*Xylocopa varipuncta*) hovering in variable-density gases. *Journal of Experimental Biology* **207**, 993-1004.

Robertson IC (1998) Flight muscle changes in male pine engraver beetles during reproduction: the effects of body size, mating status and breeding failure. *Physiological Entomology* **23**, 75-80.

Robertson RM, Johnson AG (1993) Collision avoidance of flying locusts: steering torques and behaviour. *Journal of Experimental Biology* **183**, 35-60.

Rogowitz GL, Chappell MA (2000) Energy metabolism of *Eucalyptus*-boring beetles at rest and during locomotion: gender makes a difference. *Journal of Experimental Biology* **203**, 1131-1139.

Runciman S, Seymour RS, Baudinette RV, Pearson JT (2005) An allometric study of lung morphology during development in the Australian pelican, *Pelicanus conspicillatus*, from embryo to adult. *Journal of Anatomy* **207**, 365-380.

Ryerse JS, Locke M (1978) Ecdysterone-mediated cuticle deposition and the control of growth in insect tracheae. *Journal of Insect Physiology* **24**, 541-550.

Sacktor B (1976) Biochemical adaptations for flight in the insect. *Biochemical Society Symposia* **41**, 111-131.

Samakovlis C, Hacohen N, Manning G, Sutherland DC, Guillemin K, Krasnow MA (1996) Development of the *Drosophila* tracheal system occurs by a series of morphologically distinct but genetically coupled branching events. *Development* **122**, 1395-1407.

Savage VM, Gillooly JF, Woodruff WH, West GB, Allen AP, Enquist BJ, Brown JH (2004) The predominance of quarter-power scaling in biology. *Functional Ecology* **18**, 257-282.

Schmitz A, Perry SF (1999) Stereological determination of tracheal volume and diffusing capacity of the tracheal walls in the stick insect *Carausius morosus* (Phasmatodea, Lonchodidae). *Physiological and Biochemical Zoology* **72**, 205-218.

Schmitz A, Perry SF (2001) Bimodal breathing in jumping spiders: morphometric partitioning of the lungs and tracheae in *Salticus scenicus* (Arachnida, Araneae, Salticidae). *Journal of Experimental Biology* **204**, 4321-4334.

Schmitz A, Perry SF (2002a) Morphometric analysis of the tracheal walls of the harvestmen *Nemastoma lugubre* (Arachnida, Opiliones, Nemastomatidae). *Arthropod Structure and Development* **30**, 229-241.

Schmitz A, Perry SF (2002b) Respiratory organs in wolf spiders: morphometric analysis of lungs and tracheae in *Pardosa lugubris* (L.) (Arachnida, Araneae, Lycosidae). *Arthropod Structure and Development* **31**, 217-230.

Schneider A, Wiesner RJ, Grieshaber MK (1989) On the role of arginine kinase in insect flight muscle. *Insect Biochemistry* **19**, 471-480.

Schwerzmann K, Hoppeler H, Kayar SR, Weibel ER (1989) Oxidative capacity of muscle and mitochondria: correlation of physiological, biochemical, and morphometric characteristics. *Proceedings of the National Academy of Sciences of the United States of America* **86**, 1583-1587.

Seeherman HJ, Taylor CR, Maloiy GMO, Armstrong RB (1981) Design of the mammalian respiratory system II: measuring maximum aerobic capacity. *Respiration Physiology* **44**, 11-23.

Seymour RS, Runciman S, Baudinette RV (2008) Development of maximum metabolic rate and pulmonary diffusing capacity in the superprecocial Australian Brush Turkey *Alectura lathami*: an allometric and morphometric study. *Comparative Biochemistry and Physiology. Part A, Molecular and Integrative Physiology* **150**, 169-175.

Seymour RS, Runciman S, Baudinette RV, Pearson JT (2004) Developmental allometry of pulmonary structure and function in the altricial Australian pelican *Pelecanus conspicillatus*. *Journal of Experimental Biology* **207**, 2663-2669.

Seymour RS, Withers PC, Weathers WW (1998) Energetics of burrowing, running, and free-living in the Namib Desert golden mole (*Eremitalpa namibensis*). *Journal of Zoology* **244**, 107-117.

Smith DS (1963) The structure of flight muscle sarcosomes in the blowfly *Calliphora erythrocephala* (Diptera). *Journal of Cell Biology* **19**, 115-138.

Smith JM (1978) Optimization theory in evolution. *Annual Review of Ecology and Systematics* **9**, 31-56.

Snodgrass RE (1929) The thoracic mechanism of a grasshopper and its antecedents. *Smithsonian Miscellaneous Collections* **82**, 1-111.

Strauss K, Reinhold K (2010) Scaling of metabolic rate in the lesser wax moth *Achroia grisella* does not fit the 3/4-power law and shows significant sex differences. *Physiological Entomology* **35**, 59-63.

Suarez RK (1996) Upper limits to mass-specific metabolic rates. *Annual Review of Physiology* **58**, 583-605.

Suarez RK (2000) Energy metabolism during insect flight: biochemical design and physiological performance. *Physiological and Biochemical Zoology* **73**, 765-771.

Suarez RK (2003) Shaken and stirred: muscle structure and metabolism. *Journal of Experimental Biology* **206**, 2021-2029.

Suarez RK, Darveau CA (2005) Multi-level regulation and metabolic scaling. *Journal of Experimental Biology* **208**, 1627-1634.

Suarez RK, Darveau CA, Welch KC, O'Brien DM, Roubik DW, Hochachka PW (2005) Energy metabolism in orchid bee flight muscles: carbohydrate fuels all. *Journal of Experimental Biology* **208**, 3573-3579.

Suarez RK, Lighton JRB, Brown GS, Mathieu-Costello O (1991) Mitochondrial respiration in hummingbird flight muscles. *Proceedings of the National Academy of Sciences of the United States of America* **88**, 4870-4873.

Taylor CR, Karas RH, Weibel ER, Hoppeler H (1987a) Adaptive variation in the mammalian respiratory system in relation to energetic demand II: reaching the limits to oxygen flow. *Respiration Physiology* **69**, 7-26.

Taylor CR, Maloiy GMO, Weibel ER, Langman VA, Kamau JMZ, Seeherman HJ, Heglund NC (1981) Design of the mammalian respiratory system III: scaling maximum aerobic capacity to body mass: wild and domestic mammals. *Respiration Physiology* **44**, 25-37.

Taylor CR, Weibel ER (1981a) Design of the mammalian respiratory system. *Respiration Physiology* **44**, 1-164.

Taylor CR, Weibel ER (1981b) Design of the mammalian respiratory system I: problem and strategy. *Respiration Physiology* **44**, 1-10.

Taylor CR, Weibel ER, Karas RH, Hoppeler H (1987b) Adaptive variation in the mammalian respiratory system in relation to energetic demand VIII: structural and functional design principles determining the limits to oxidative metabolism. *Respiration Physiology* **69**, 117-127.

Terblanche JS, Klok CJ, Chown SL (2004) Metabolic rate variation in *Glossina pallidipes* (Diptera : Glossinidae): gender, ageing and repeatability. *Journal of Insect Physiology* **50**, 419-428.

Weibel ER (1970) Morphometric estimation of pulmonary diffusion capacity I: model and method. *Respiration Physiology* **11**, 54-75.

Weibel ER, Bacigalupe LD, Schmitt B, Hoppeler H (2004) Allometric scaling of maximal metabolic rate in mammals: muscle aerobic capacity as determinant factor. *Respiratory Physiology and Neurobiology* **140**, 115-132.

Weibel ER, Gehr P, Cruz-Orive LM, Muller AE, Mwangi DK, Haussener V (1981a) Design of the mammalian respiratory system IV: morphometric estimation of pulmonary diffusing capacity: critical evaluation of a new sampling method. *Respiration Physiology* **44**, 39-59.

Weibel ER, Hoppeler H (2005) Exercise-induced maximal metabolic rate scales with muscle aerobic capacity. *Journal of Experimental Biology* **208**, 1635-1644.

Weibel ER, Knight BW (1964) A morphometric study on the thickness of the pulmonary air-blood barrier. *Journal of Cell Biology* **21**, 367-384.

Weibel ER, Marques LB, Constantinopol M, Doffey F, Gehr P, Taylor CR (1987a) Adaptive variation in the mammalian respiratory system in relation to energetic demand VI: the pulmonary gas exchanger. *Respiration Physiology* **69**, 81-100.

Weibel ER, Taylor CR, Bolis L (1998) 'Principles of Animal Design: The Optimization and Symmorphosis Debate.' (Cambridge University Press: Cambridge)

Weibel ER, Taylor CR, Gehr P, Hoppeler H, Mathieu O, Maloiy GMO (1981b) Design of the mammalian respiratory system IX: functional and structural limits for oxygen flow. *Respiration Physiology* **44**, 151-164.

Weibel ER, Taylor CR, Hoppeler H (1991) The concept of symmorphosis: a testable hypothesis of structure-function relationship. *Proceedings of the National Academy of Sciences of the United States of America* **88**, 10357-10361.

Weibel ER, Taylor CR, Hoppeler H (1992) Variations in function and design: testing symmorphosis in the respiratory system. *Respiration Physiology* **87**, 325-348.

Weibel ER, Taylor CR, Hoppeler H, Karas RH (1987b) Adaptive variation in the mammalian respiratory system in relation to energetic demand. *Respiration Physiology* **69**, 1-127.

Weibel ER, Taylor CR, Hoppeler H, Karas RH (1987c) Adaptive variation in the mammalian respiratory system in relation to energetic demand I: introduction to problem and strategy. *Respiration Physiology* **69**, 1-6.

Weis-Fogh T (1949) An aerodynamic sense organ stimulating and regulating flight in locusts. *Nature* **164**, 873-874.

Weis-Fogh T (1952) Fat combustion and metabolic rate of flying locusts. *Philosophical Transactions of the Royal Society of London. Series B: Biological Sciences* **237**, 1-36.

Weis-Fogh T (1956) Biology and physics of locust flight IV: notes on sensory mechanisms in locust flight. *Philosophical Transactions of the Royal Society of London. Series B: Biological Sciences* **239**, 553-584.

Weis-Fogh T (1964a) Biology and physics of locust flight VIII: lift and metabolic rate of flying locusts. *Journal of Experimental Biology* **41**, 257-271.

Weis-Fogh T (1964b) Diffusion in insect wing muscle, the most active tissue known. *Journal of Experimental Biology* **41**, 229-256.

Weis-Fogh T (1964c) Functional design of the tracheal system of flying insects as compared with the avian lung. *Journal of Experimental Biology* **41**, 207-227.

Weis-Fogh T (1967) Respiration and tracheal ventilation in locusts and other flying insects. *Journal of Experimental Biology* **47**, 561-587.

Weis-Fogh T, Jensen M (1956) Biology and physics of locust flight I: basic principles in insect flight: a critical review. *Philosophical Transactions of the Royal Society of London. Series B: Biological Sciences* **239**, 415-458.

West GB, Brown JH, Enquist BJ (1997) A general model for the origin of allometric scaling laws in biology. *Science* **276**, 122-126.

West GB, Brown JH, Enquist BJ (1999) The fourth dimension of life: fractal geometry and allometric scaling of organisms. *Science* **284**, 1677-1679.

West GB, Savage VM, Gillooly J, Enquist BJ, Woodruff WH, Brown JH (2003) Why does metabolic rate scale with body size? *Nature* **421**, 713-713.

Westneat MW, Betz O, Blob RW, Fezzaa K, Cooper WJ, Lee WK (2003) Tracheal respiration in insects visualized with synchrotron X-ray imaging. *Science* **299**, 558-560.

White CR, Matthews PGD, Seymour RS (2008) *In situ* measurement of calling metabolic rate in an Australian mole cricket, *Gryllotalpa monanka*. *Comparative Biochemistry and Physiology. Part A, Molecular and Integrative Physiology* **150**, 217-221.

White CR, Phillips NF, Seymour RS (2006) The scaling and temperature dependence of vertebrate metabolism. *Biology Letters* **2**, 125-127.

White CR, Seymour RS (2005) Allometric scaling of mammalian metabolism. *Journal of Experimental Biology* **208**, 1611-1619.

Whitten JM (1957) The post-embryonic development of the tracheal system in *Drosophila melanogaster*. *Quarterly Journal of Microscopical Science* **98**, 123-150.

Whitten JM (1972) Comparative anatomy of the tracheal system. *Annual Review of Entomology* **17**, 373-402.

Wigglesworth VB (1953) Motility of insect tracheoles. *Nature* **172**, 247-247.

Wigglesworth VB (1954) Growth and regeneration in the tracheal system of an insect, *Rhodnius prolixus* (Hemiptera). *Quarterly Journal of Microscopical Science* **95**, 115-137.

Wigglesworth VB (1959) The role of the epidermal cells in the 'migration' of tracheoles in *Rhodnius prolixus* (Hemiptera). *Journal of Experimental Biology* **36**, 632-640.

Wigglesworth VB (1965) 'The Principles of Insect Physiology.' (Methuen: London)

Wigglesworth VB (1973) The significance of 'apolysis' in moulting of insects. *Journal of Entomology. Series A: Physiology and Behaviour* **47**, 141-149.

Wigglesworth VB (1977) Structural changes in epidermal cells of *Rhodnius* during tracheole capture. *Journal of Cell Science* **26**, 161-174.

Wigglesworth VB (1981) The natural history of insect tracheoles. *Physiological Entomology* **6**, 121-128.

Wigglesworth VB (1983) The physiology of insect tracheoles. *Advances in Insect Physiology* **17**, 85-148.

Wigglesworth VB, Lee WM (1982) The supply of oxygen to the flight muscles of insects: a theory of tracheole physiology. *Tissue and Cell* **14**, 501-518.

Wilson DM (1962) Bifunctional muscles in the thorax of grasshoppers. *Journal of Experimental Biology* **39**, 669-677.

Withers PC (2001) Design, calibration and calculation for flow-through respirometry systems. *Australian Journal of Zoology* **49**, 445-461.

Wolf H (1993) The locust tegula: significance for flight rhythm generation, wing movement control and aerodynamic force production. *Journal of Experimental Biology* **182**, 229-253.

Wolf TJ, Schmid-Hempel P, Ellington CP, Stevenson RD (1989) Physiological correlates of foraging efforts in honeybees: oxygen consumption and nectar load. *Functional Ecology* **3**, 417-424.

Worm RAA, Beenakkers AMT (1980) Regulation of substrate utilization in the flight muscle of the locust, *Locusta migratoria*, during flight. *Insect Biochemistry* **10**, 53-59.

Zar JH (1998) 'Biostatistical Analysis.' (Prentice Hall: Englewood Cliffs, New Jersey)

Zarnack W, Wortmann M (1989) On the so-called constant-lift reaction of migratory locusts. *Journal of Experimental Biology* **147**, 111-124.

Zera AJ, Denno RF (1997) Physiology and ecology of dispersal polymorphism in insects. *Annual Review of Entomology* **42**, 207-230.